pmod wrc

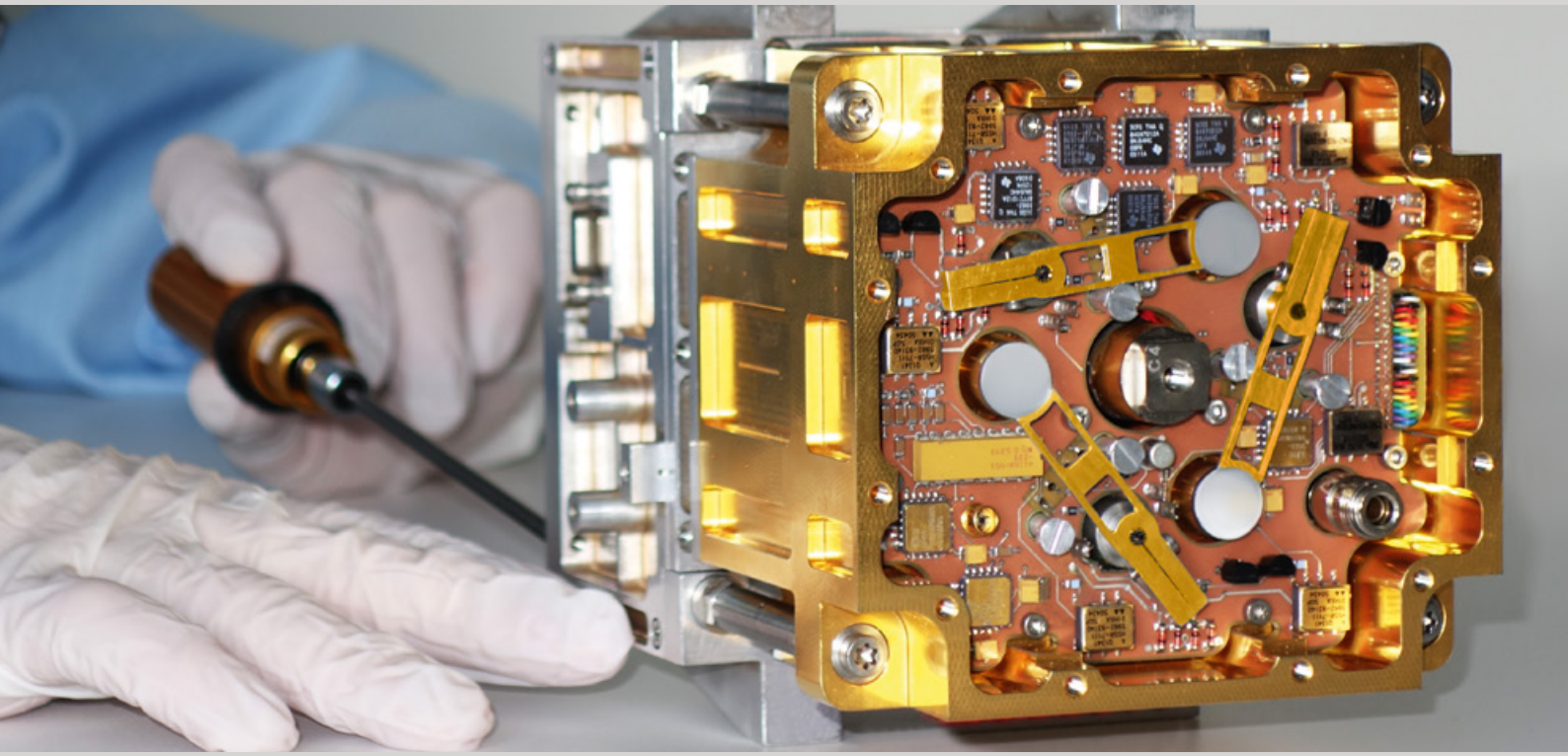

Annual Report
Jahresbericht 2016

Physikalisch-Meteorologisches Observatorium Davos und Weltstrahlungszentrum

Mission

Das PMOD/WRC

- dient als internationales Kalibrierzentrum für meteorologische Strahlungsmessinstrumente
- entwickelt Strahlungsmessinstrumente für den Einsatz am Boden und im Weltraum
- erforscht den Einfluss der Sonnenstrahlung auf das Erdklima.

Auftragerteilung

Das Physikalisch-Meteorologische Observatorium Davos (PMOD) beschäftigt sich seit seiner Gründung im Jahr 1907 mit Fragen des Einflusses der Sonnenstrahlung auf das Erdklima. Das Observatorium schloss sich 1926 dem Schweizerischen Forschungsinstitut für Hochgebirgsklima und Medizin Davos an und ist seither eine Abteilung dieser Stiftung. Auf Ersuchen der Weltmeteorologischen Organisation (WMO) beschloss der Bundesrat im Jahr 1970 die Finanzierung eines Kalibrierzentrums für Strahlungsmessung als Beitrag der Schweiz zum Weltwetterwacht-Programm der WMO. Nach diesem Beschluss wurde das PMOD beauftragt, das Weltstrahlungszentrum (World Radiation Center, WRC) zu errichten und zu betreiben.

Kerntätigkeiten

Das Weltstrahlungszentrum unterhält das Primärnormal für solare Bestrahlungsstärke bestehend aus einer Gruppe von hochpräzisen Absolut-Radiometern. Auf weitere Anfragen der WMO wurden 2004 das Kalibrierzentrum für Messinstrumente der atmosphärischen Langwellenstrahlung eingerichtet und 2008 das Kalibrierzentrum für spektrale Strahlungsmessungen zur Bestimmung der atmosphärischen Trübung. Seit 2013 wird auch das Europäische UV Kalibrierzentrum durch das Weltstrahlungszentrum betrieben. Das Weltstrahlungszentrum besteht heute aus vier Sektionen:

- Solare Radiometrie (WRC-SRS)
- Infrarot Radiometrie (WRC-IRS)
- Atmosphärische Trübungsmessungen (WRC-WORCC)
- UV Kalibrierzentrum (WRC-WCC-UV)

Die Kalibriertätigkeit ist in ein international anerkanntes Qualitätssystem eingebettet (ISO 17025) um eine zuverlässige und nachvollziehbare Einhaltung des Qualitätsstandards zu gewährleisten.

Das PMOD/WRC entwickelt und baut Radiometer, die zu den weltweit genauesten ihrer Art gehören und sowohl am Boden als auch im Weltraum eingesetzt werden. Diese Instrumente werden auch zum Kauf angeboten und kommen seit langem bei Meteorologischen Diensten weltweit zum Einsatz. Ein globales Netzwerk von Stationen zur Überwachung der atmosphärischen Trübung ist mit vom Institut entwickelten Präzisionsfilterradiometern ausgerüstet.

Im Weltraum und mittels Bodenmessungen gewonnene Daten werden in Forschungsprojekten zum Klimawandel und der Sonnenphysik analysiert. Diese Forschungstätigkeit ist in nationale, insbesondere mit der ETH Zürich, und internationale Zusammenarbeit eingebunden.

Das PMOD/WRC ist eine Abteilung der Stiftung
Schweizerisches Forschungsinstitut für
Hochgebirksklima und Medizin in Davos.

Physikalisch-Meteorologisches Observatorium Davos
und World Radiation Center (PMOD/WRC)
Dorfstrasse 33
7260 Davos Dorf
Schweiz

pmod wrc

Annual Report
Jahresbericht 2016

Table of Contents

Jahresbericht 2016

Werner Schmutz

Wissenschaft

Im März 2017 endete das Projekt Future and Past Solar Influence on the Terrestrial Climate (FUPSOL), das als Sinergia-Projekt vom Schweizerischen Nationalfonds finanziert wurde. Das FUPSOL Projekt war eine partnerschaftliche Multi-Instituts-Forschung, das nebst dem PMOD/WRC das Institut für Atmosphäre und Klima der ETH Zürich, die Abteilung Klima und Umweltphysik des Physikalischen Instituts der Universität Bern, das Oeschger-Zentrum für Klimaforschung der Universität Bern und die Abteilung Oberflächengewässer der EAWAG umfasste und über zwei mal drei Jahre lief. Insgesamt entstanden im Rahmen des Projekts 66 wissenschaftliche Publikationen, die von der Zitations- und Literaturdatenbank ISI Web of Science erfasst wurden und die bis April 2017 966-mal zitiert wurden. Von diesen war bei 55 Publikationen mindestens ein Koautor Mitarbeiter des PMOD/WRC und diese Arbeiten wurden 662-mal zitiert. Diese Zahlen sind meines Erachtens sehr eindrücklich und belegen mit trockener Statistik wie erfolgreich das FUPSOL Projekt war.

Anlässlich des letzten Projekttreffens der FUPSOL Partner Ende März in Davos hat der Nationalfonds eine Pressemitteilung veröffentlicht. Die Schlagzeile und der einführende Paragraph lauteten:

> *Einfluss der Sonne auf den Klimawandel erstmals beziffert.*
>
> *Modellrechnungen zeigen erstmals eine plausible Möglichkeit auf, wie Schwankungen der Sonnenaktivität einen spürbaren Effekt auf das Klima haben. Gemäss den vom Schweizerischen Nationalfonds geförderten Arbeiten könnte sich die menschgemachte Erderwärmung in den nächsten Jahrzehnten leicht verlangsamen: Eine schwächere Sonne wird voraussichtlich ein halbes Grad Abkühlung beitragen.*[1]

Als Wissenschaftler wünschte man sich eine etwas weniger reisserische Aufmachung bei Mitteilungen über Forschungsresultate, aber trotzdem war es erfreulich zu erleben, dass unsere Arbeiten bei den Medien auf erhebliches Interesse stiessen. Die Fernseh-Abendtagesschau berichtete in einem zweiminütigen Beitrag und die renommierte Radiosendung „Echo der Zeit“ brachte in einer vier Minuten dauernden Sendung eine ausgezeichnete Darstellung des Sachverhaltes. Wissenschaftlich betrachtet ist es ein wichtiges Resultat, dass natürliche Einflüsse gross genug sein könnten, um einen merklichen Einfluss auf den Klimawandel zu bewirken. Dabei geht es weniger um die Grössenordnung des Einflusses, der in jedem Fall, kleiner als die vom Menschen verursachte Erwärmung sein wird, auch wenn man die grossen Unsicherheiten des angegebenen halben Grades und der verschiedenen Szenarien des zukünftigen Verlaufs der Treibhausgasemissionen berücksichtig. Das wichtige Resultat ist das Verständnis, dass ein natürlicher Einfluss den Anstieg der Erwärmung dämpfen könnte und dass man diesen Einfluss berücksichtigen muss, wenn man den Verlauf der globalen Erwärmung beurteilt. Bei einer natürlich etwas gedämpfteren Klimaerwärmung könnte man bei einer Analyse des Temperaturverlaufs fälschlich auf einen weniger starken Einfluss des Menschen schliessen. Wenn in der Zukunft die Sonne sich tatsächlich abschwächen würde, und eine natürliche Beeinflussung eintreffen sollte, dann wird es wichtig sein, dass man schon vorher auf dieses Szenario hingewiesen hat, um dies dannzumal der Öffentlichkeit glaubwürdig darstellen zu können.

Dienstleistungsbetrieb Weltstrahlungszentrum

Das vergangene Jahr war das erste der Finanzierungsperiode 2016 – 2019 des Weltstrahlungszentrums. Nach dem ausserordentlichen Jahr 2015, in dem die 5-jährlichen Internationalen Pyrheliometer Vergleiche zu organisieren waren und das Institut durch ein externes Komitee auditiert wurde, kann man das Jahr 2016 als "normales Jahr" bezeichnen: Die vier Sektionen des Weltstrahlungszentrums arbeiteten effizient und problemlos.

Weltraumprojekte

Vor einem Jahr erwarteten wir die Inbetriebnahme unseres Radiometer-Weltraumexperiments Compact Lightweight Absolute Radiometer, CLARA. Das Instrument ist wissenschaftliche Nutzlast auf der norwegischen Mission NORSAT-1, die am 22. April 2016 von Kourou, Französisch-Guyana, mit einer Sojus-Rakete hätte gestartet werden sollen. Unglücklicherweise hat Arianespace buchstäblich in den letzten Tagen vor dem Start festgestellt, dass eine technische Inkompatibilität die Integration des Satelliten als sekundäre Nutzlast verunmöglicht. Die norwegische Weltraumorganisation arrangierte als nächste Startmöglichkeit den 14. Juli 2017 von Baikonur, Kasachstan, und wir hoffen, dass diesmal alles klappen wird.

Entwicklung und Bau von Instrumenten

Die Technik-Abteilung war durch die Konstruktionsphase von gleichzeitig vier Weltraumprojekten herausgefordert. Das Observatorium liefert Bestandteile für die zwei Experimente EUI und SPICE der Solar Orbiter Mission und entwickelt zwei eigene Experimente zur Messung der Gesamtstrahlung der Sonne. Das eine Experiment ist der Digital Absolute Radiometer, DARA, für ESA's PROBA 3 Mission und das andere ist der Joint Total Solar Irradiance Monitor, JTSIM, der auf der chinesischen FY-3E Erdbeobachtungsmission mitfliegen soll. Um die Arbeitslast in der Technik zu verringern, wurde der Bau von neuen PMO6-CC Instrumenten an die Firma Davos Instruments AG vergeben. Die Technik-Mitarbeiter haben sich mit Elan eingesetzt, und alle vier Projekte wurden plangemäss vorangebracht.

Personelles

Ich gratuliere unserm Elektronik-Lehrling Andri Morandi und den beiden Doktoranden Timofei Sukhodolov und Rinat Tagirov zu ihren erfolgreichen Abschlüssen. Herr Morandi blieb danach noch drei Monate bei uns und Dr. Sukhodolov wurde am Obs als Post-Doktorand für eines unserer vom Schweizerischen Nationalfonds geförderten Klimasimulations-Projekte angestellt. Dr. Tagirov bekam eine Post-Doktoranden-Stelle bei der Astrophysik Gruppe am Imperial College London. Dr. Cassandra Bolduc verliess uns per letzten September, da sie eine Wissenschaftler-Stelle im Dept. for Environment and Climate Change ihres Heimatlandes Kanada antreten konnte. Als neue Doktoranden kamen Alberto Remesal Oliva und Ioannis Panagiotis Raptis zu uns.

Die Technik-Abteilung wurde ab April 2016 mit Herrn Lloyd Beeler, einem Elektronikingenieur, verstärkt und im August hat Yanick Schoch seine Elektroniklehre angefangen. Eine weitere willkommene Unterstützung erhielten wir durch Herrn Nicholas Bresina, der als Elektronik-Praktikant vier Monate bei uns arbeitete, sowie von Jeanine Lehner, die seit August als Praktikantin in der Administration tätig ist. Dank unserer Zusammenarbeit mit dem chinesischen Changchun Institute of Optics, Fine Mechanics and Physics (CIOMP) im Rahmen des Weltraumprojekts JTSIM konnten wir Dr. Hongrui Wang als Projekt-Wissenschaftler anstellen. Seine Anwesenheit vor Ort erleichtert uns die Absprache technischer Fragen mit unseren Partnern wesentlich.

Dank

Ich bin froh, dass ich berichten kann, dass das PMOD/WRC finanziell, personell und organisatorisch gut aufgestellt ist. Damit dies intern so erreicht werden kann, braucht es Wohlwollen und Unterstützung von vielen Personen ausserhalb des Institutes. Wesentlicher Einsatz ist insbesondere von den Präsidenten der Stiftung und der Aufsichtskommission, Dr. Walter Ammann und Dr. Bertrand Calpini, gefordert. Weitere Personen mit einflussreichem Wirken im Hintergrund sind der ständige Delegierte der Schweiz bei der Meteorologischen Weltorganisation, Peter Binder, sowie Lukas Schumacher, Leiter der Finanzen und Logistik an der MeteoSchweiz. Diesen Personen danke ich im Namen des Observatoriums ganz herzlich. Weiter danke ich den Partnern in der Finanzierung des Weltstrahlungszentrums, Bund, Kanton Graubünden und Gemeinde Davos, die mit der Grundfinanzierung die Existenz des Observatoriums ermöglichen. Der Bau des Weltraumprojekts CLARA/NORSAT-1 hat mehr gekostet als im Budget vorgesehen war und deshalb haben wir eine Spende von Herrn Daniel Karbacher aus Küsnacht (ZH) eingesetzt um den Fehlbetrag zu decken. Ein spezielles Dankeschön geht an Herrn Karbacher für seinen grosszügigen Beitrag.

Den allerwichtigsten Beitrag leisten die Mitarbeiterinnen und Mitarbeiter, denen ich ganz herzlich für ihren grossartigen Einsatz zugunsten des Observatoriums danke.

PMOD/WRC staff on the instrument platform in front of the Institute building.

[1] Die Pressemitteilung vom 27.3.2017 ist über das News-Archiv des Schweizerischen Nationalfonds erhältlich: www.snf.ch/de/fokus-Forschung/newsroom/news-archiv/Seiten/default.aspx.

Introduction

Werner Schmutz

The past year was the first of the 2016–2019 funding period, which is covered by the current contract for funding of the World Radiation Center. After the special events in 2015, when the International Pyrheliometer Comparisons had to be organised and there was an external review of the institute, 2016 was what could be called "a normal year". This showed that the institute is on a solid financial and organisational basis. The operational services and all tasks in the Center's four sections are running effectively and smoothly.

Instrument development was dominated by numerous tasks involving space experiments. Currently, the PMOD/WRC is contributing to two experiments on the Solar Orbiter mission and we are developing two institute-led experiments to measure Total Solar Irradiance. One is the Digital Absolute Radiometer, or DARA, for the European Space Agency's (ESA) PROBA-3 space mission and the other is JTSIM, which is short for Joint Total Solar Irradiance Monitor, to fly on the Chinese FY-3 mission.

A year ago, we were expecting the transfer to space of the Compact Lightweight Absolute Radiometer, or CLARA, an experiment to measure the Total Solar Irradiance onboard the Norwegian space mission NORSAT-1, which was scheduled for a Soyuz launch from Kourou, French Guyana, on 22 April 2016 as a secondary payload. Unfortunately, this launch was cancelled by Arianespace due to a technical incompatibility of the structure fixing the satellite to the launcher. Now, NORSAT-1 is scheduled for launch from the space centre in Baikonur, Kazakhstan on 14 July 2017. Hopefully everything will go according to plan this time.

In conclusion, I am glad to be in a position to report that the institute is operating well and is prepared for the future, and I thank my staff for their dedication, which has made the institute's success possible. I acknowledge the continued, full support of the Board of Trustees and Supervisory Board, which is essential for the institute's existence.

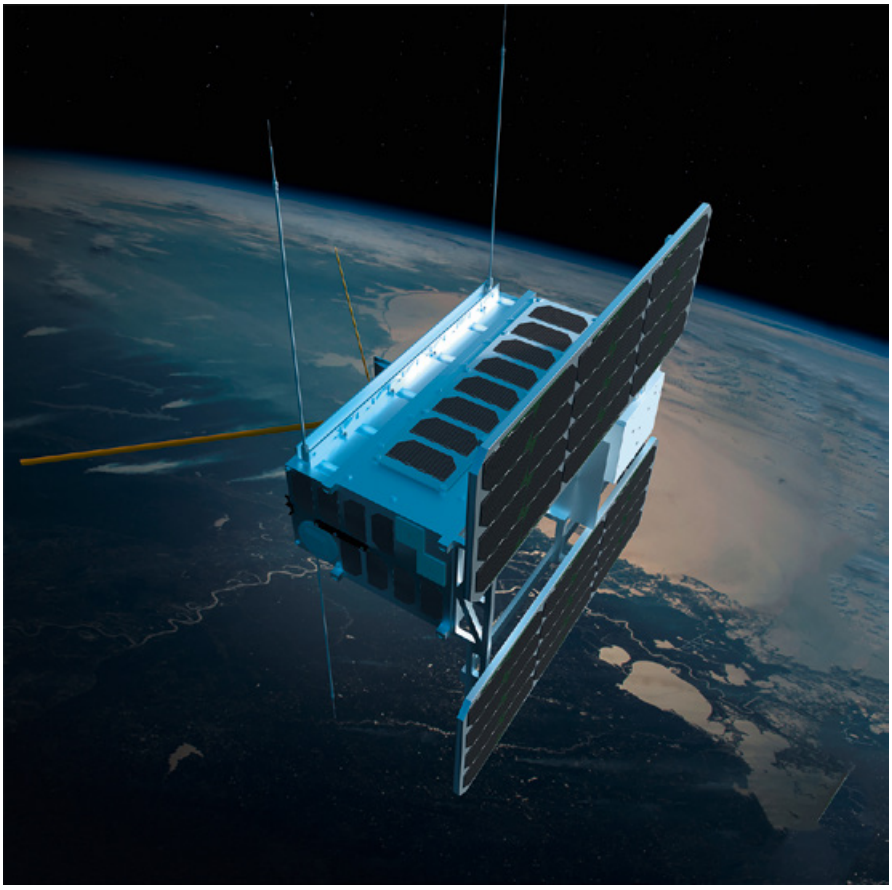

Artist's impression of NORSAT-1 in orbit.

Operational Services

Quality Management System, Calibration Services, and Instrument Sales

Quality Management System

Silvio Koller

PMOD/WRC QMS

The World Radation Center has six different Calibration and Measurement Capabilites (CMCs) listed in the KCDB of BIPM. These include:

- Responsivity, solar irradiance pyranometer (1)
- Responsivity, solar irradiance pyrheliometer (1)
- Responsivity, solar irradiance broadband detector (4)

Depending on the instruments wavelength range, the CMCs belong to different WRC calibration sections. No QM relevant changes occurred on the personnel side.

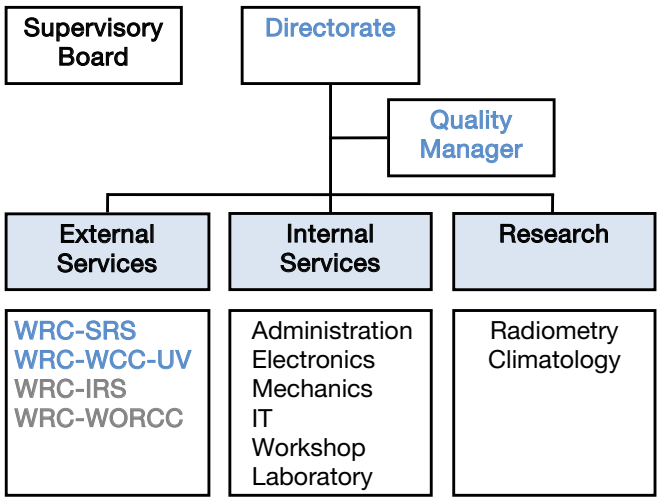

Figure 1. PMOD/WRC Quality Management System: Organisational chart. The WRC SRS and UV-WCC sections (in blue) perform calibrations according to the EN ISO/IEC standard 17025.

Quality Management System Activities

An overall revision of the QM documentation began in 2016, which should be completed and implemented in 2017. One major goal is the introduction of a common document structure and numbering system for all calibration sections, but also for the overall WRC-QM documents.

Three internal audits were conducted during this reporting period. All issues or non-conformities were resolved within the deadlines.

Calibration Services

Silvio Koller, Wolfgang Finsterle, and Julian Gröbner

The overall number of calibrations decreased slightly in 2016 (Figure 2) to similar values encountered before 2015. A larger number of calibrations occurred in 2015 as a result of the IPC-XII international comparison, held every five years at PMOD/WRC.

Solar Radiometry Section (WRC-SRS)

In 2016, the WRC-SRS section calibrated 13 pyrheliometers and 100 pyranometers. All certificates were issued with the "Comité International des Poids et Mesures" (CIPM) logo. Figure 3 shows the World Standard Group of pyrheliometers along with CSAR, MITRA and Customer instruments during calibration.

Infrared Radiometry Section (WRC-IRS)

The WRC-IRS section conducted 31 pyrgeometer calibrations in 2016.

Atmospheric Turbidity Section (WRC-WORCC)

The WRC-WORCC section calibrated 20 Precision Filter Radiometers (PFR) against the WORCC Triad standard. In addition, two precision solar spectroradiometers (PSR) were calibrated against a reference standard, traceable to the National Metrology Institute of Germany (PTB).

World Calibration Center for UV Section (WRC-WCC-UV)

Fourteen UVB broadband radiometers, five solar spectroradiometers and four lamps/diodes were calibrated by the WCC-UV section. These calibrations resulted in 18 certificates, of which three were issued with a CIPM logo. Figure 4 shows UV radiometers belonging to Customers being calibrated on the PMOD/WRC roof platform.

The WCC-UV section performed two quality assurance site audits of solar UV monitoring spectroradiometers at their respective field sites using the traveling reference spectroradiometer QASUME.

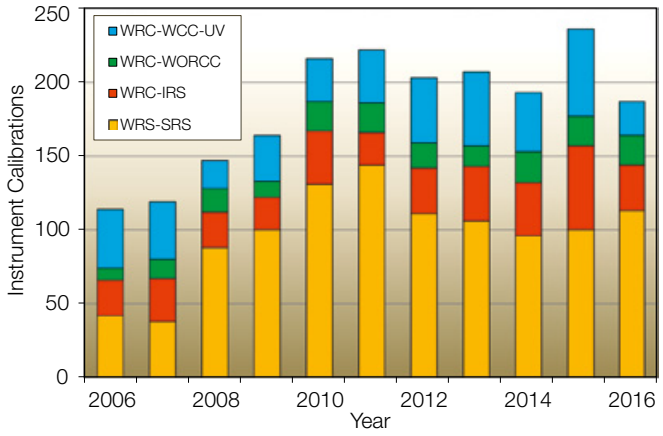

Figure 2. Statistics of instrument calibrations at PMOD/WRC for the 2006–2016 period.

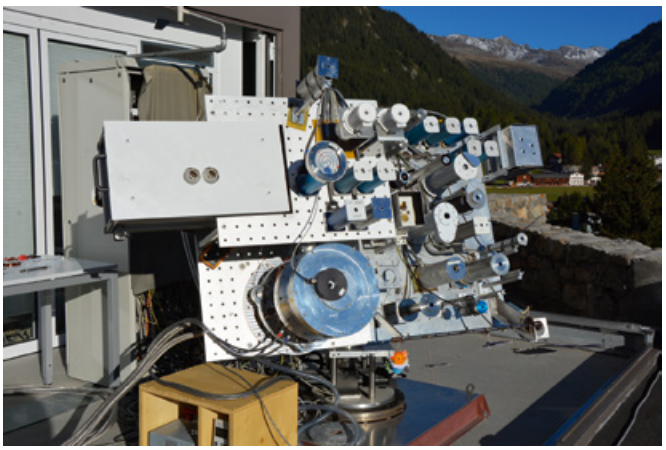

Figure 3. The World Standard Group.

Figure 4. Calibration of Customer UV broadband radiometers.

Instrument Sales

Daniel Pfiffner

In 2016, PMOD/WRC sold the following instruments:

- One PMO6-CC absolute radiometer to Black Photon, Germany.
- One Infrared Cloud Camera (IRCCAM) to the German Weather Service (DWD), Germany.
- Seven Ventilated Heating Systems (VHS) to ASIAQ, Greenland.

An overview of instrument sales statistics is shown in Figure 5 which compares the current year to previous years since 2008.The exceptionally good sales of PMO6-CC in 2015 was due to the IPC-XII pyrheliometer comparisons at Davos, so a lower number of sales in 2016 partially reflects the longer-term average of 2–3 instruments and partially the current production capacity.

In addition to the above instruments, an IRCCAM was sold for the first time. This research instrument allows the sky to be photographed and analysed at infrared wavelengths in order to determine the fractional cloud-cover.

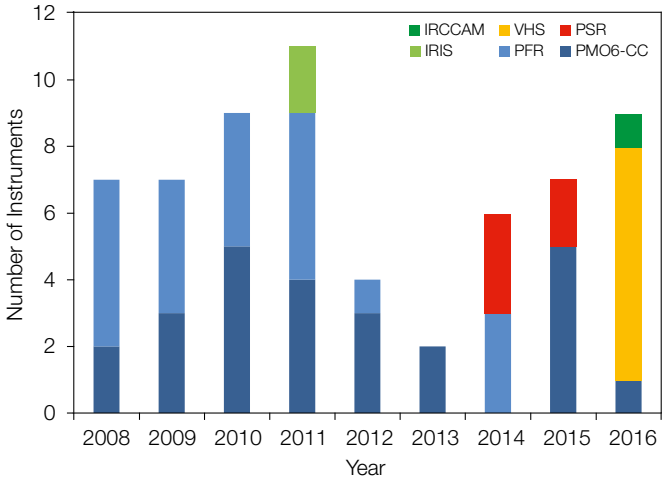

Figure 5. Number of PMOD/WRC instruments sold from 2008 up to and including 2016: i) IRCCAM = Infrared Cloud Camera, ii) VHS = Ventilated Heating Systems, iii) PSR = Precision Spectroradiometer, iv) IRIS = Infrared Integrating Sphere Radiometer, v) PFR = Precision Filter Radiometer, and vi) PMO6-CC = absolute cavity pyrheliometer.

Solar Radiometry Section (WRC-SRS)

Wolfgang Finsterle

The Solar Radiometry Section (SRS) of the WRC maintains and operates the World Standard Group (WSG) of Pyrheliometers which represents the World Radiometric Reference (WRR) for ground-based total solar irradiance measurements. The 2016 calibration season was successful with 113 issued calibration certificates. The start of a new research project on sensor cavity absorptance and participation in the NREL National Pyrheliometer Comparison, NPC-2016, were other highlights of the year.

In 2016, the SRS of the World Radiation Center calibrated 113 radiometers: These consisted of 100 pyranometers, 11 pyrheliometers with a thermopile sensor and two absolute cavity radiometers. The WSG was operated on 60 days, and the Cryogenic Solar Absolute Radiometer and Monitor for Integrated Transmittance (CSAR/MITRA) on 14 days (see article by Benjamin Walter).

On 14 June, the SRS calibration laboratory was audited by Julian Gröbner and Ricco Soder as part of PMOD's regular internal audit plan. The auditors concluded that the laboratory was generally in a good state and issued four recommendations, nine remarks, and five deviations, most of which were resolved by the end of the year.

On 1 June, the SRS welcomed Alberto Remesal Oliva, a new PhD student. Alberto Remesal Oliva is working on the SNF-sponsored research project "Understanding and improving the cavity absorptance and instrumental degradation of TSI radiometers". The project is a collaboration with the University of Zürich. It aims to drastically reduce the largest uncertainty component in present TSI space radiometers and has already produced promising results based on the optical analysis of two cavity sensors which had previously flown in space (see article by Albert Remesal Oliva).

The SRS participated in the National Pyrheliometer Comparison, NPC-2016, at NREL in Golden, Colorado (Figure 1) from 26 – 30 September. Two PMO6-CC and one AHF absolute cavity radiometer served as transfer standards in this comparison. The results of the NPC-2016 were published in the NREL technical report NREL/TP-3B10-67311, and clearly confirm that the WSG has been stable since the last IPC (see Table 1).

Table 1. The WRR correction factors for the three transfer standard pyrheliometers determined during NPC-2016 agree extremely well with the results from IPC-XII in 2015. The US standard group maintained by the National Renewable Energy Laboratory (NREL) served as the independent reference during NPC-2016. The observed relative changes are well below the significance threshold of the comparison and confirm the stability of the WSG.

	IPC-XII (2015)	NPC-2016	Relative change
PMO6-CC 0401	1.020799	1.02086	0.006%
PMO6-CC 0803	1.000335	1.00044	0.010%
AHF 32455	1.001380	1.00147	0.009%

The SRS is leading the revision process for the ISO 9060 international standard (Solar energy – Specification and classification of instruments for measuring hemispherical and direct solar radiation). Two committee meetings and several telephone conferences were held in 2016 before a new Draft International Standard (DIS) was published in December. The DIS introduces a new classification scheme for pyranometers and pyrheliometers based on application specific requirements, whereas the classification scheme employed in the previous international standard, which was published in 1990, is mainly based on instrument technology and is no longer appropriate to classify modern pyranometers and pyrheliometers in many cases.

Figure 1. This group photo was taken during the National Pyrheliometer Comparison, NPC-2016, at NREL in Golden, Colorado, USA. Christian Thomann represented the PMOD/WRC with a group of three transfer standard pyrheliometers. (Photo by Tom Stoffel).

Infrared Radiometry Section (WRC-IRS)

Julian Gröbner, Christian Thomann, and Stephan Nyeki

The Infrared Radiometry Section of the WRC maintains and operates the World Infrared Standard Group of pyrgeometers (WISG) which represents the world-wide reference for atmospheric long-wave irradiance measurements.

The WISG serves as the atmospheric long-wave irradiance reference for the calibration of pyrgeometers operated by institutes around the world. The WISG has been in continuous operation since 2004, and consists of four pyrgeometers which are installed on the PMOD/WRC roof platform.

The measurements of the individual WISG pyrgeometers with respect to their average are shown in Figure 1 for the period 2004 to the end of 2016. As can be seen, the internal consistency of the WISG is remarkable, with measurements from the four pyrgeometers agreeing to within ±1 Wm^{-2} over the whole time period. The WISG is currently seen as an interim transfer standard group with respect to its reference scale (WMO, 2006).

The traceability of the WISG to SI, and an eventual change of the WISG scale have been ongoing issues in recent years (e.g. Gröbner et al., 2014; Gröbner et al., 2015; Philipona, 2015). The evidence for a revision of the reference scale comes from concurrent operation of the WISG alongside the Infrared Integrating Sphere (IRIS) during night-time clear-sky conditions since 2008 which have yielded an underestimate of the WISG clear-sky long-wave irradiance by 2–6 Wm^{-2}, depending on the amount of integrated water vapour (IWV) (Gröbner et al., 2014). These results have been confirmed in three inter-comparison campaigns with the Absolute Cavity Pyrgeometer (ACP) developed by NREL (Reda et al., 2012) where the ACP and IRIS measurements were consistent to within ±1 Wm^{-2} during these campaigns (which is within the instrumental uncertainties of ±4 Wm^{-2} and ±2 Wm^{-2}, respectively). Figure 2 shows the difference in long-wave irradiance measured by the WISG and IRIS#2 during clear-sky nights at PMOD/WRC since 2012. A pronounced seasonal variability is observed, with the largest discrepancies between WISG and IRIS of up to 6 Wm^{-2} during summer. A more detailed analysis can be found in Gröbner et al. (2014) where a clear correlation with respect to integrated water vapour (grey line in Figure 2) was found.

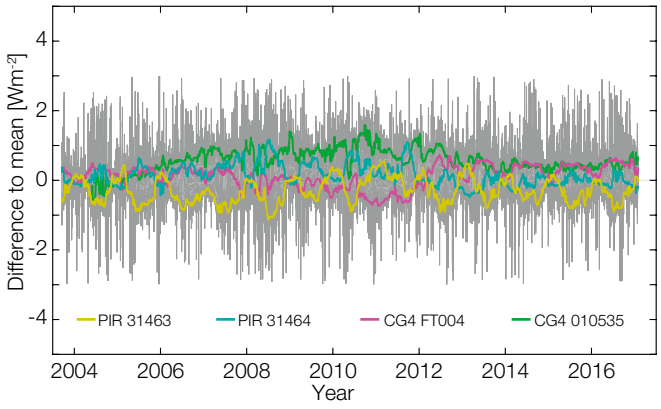

Figure 1. Night-time atmospheric long-wave measurements of the WISG pyrgeometers relative to their average. The coloured lines represent a 30-day running mean of each WISG pyrgeometer, while the grey shaded area represents the daily measurements.

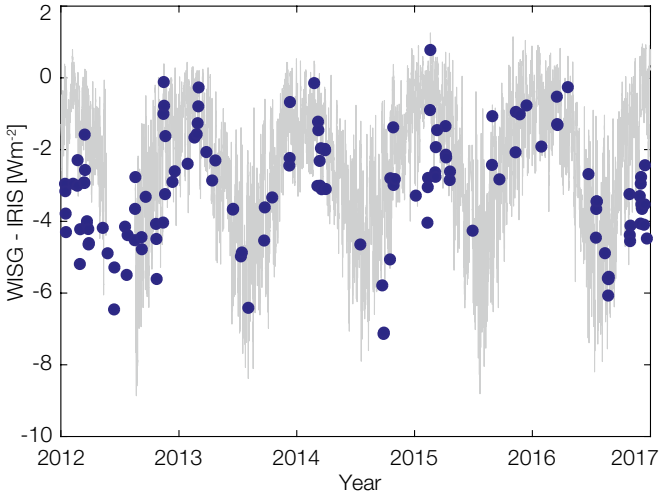

Figure 2. Daily average difference of night-time clear-sky long-wave irradiance measured by the WISG and IRIS#2 for the period 2012 to the end of 2016 (blue dots). The observed seasonal variability is inversely correlated to the integrated water vapour (grey line), drawn here in reverse mode.

These issues will be addressed in a number of ways. Firstly, in an international comparison organised by the Atmospheric Radiation Measurement program (ARM) at the Southern Great Plains test site (Oklahoma, US) in autumn 2017, where collocated measurements of ACP, IRIS and WISG traceable pyrgeometers will be performed. Secondly, the Metrology for Earth Observation and Climate (METEOC-3) project, partially funded by the European Metrology Programme for Innovation and Research (EMPIR), will aim to characterise and calibrate several IRIS radiometers with the aim of reaching an uncertainty of 2 Wm^{-2}. The tasks within the project will be performed by collaboration between PMOD/WRC, the Physikalisch-Technische Bundesanstalt (PTB) in Berlin, Germany, the National Physical Laboratory (NPL) in Teddington, GB and the Deutsche Wetterdienst in Lindenberg, Germany.

References:

Gröbner J. et al.: 2014, J. Geophys. Res. Atmos., 119, doi: 10.1002/2014JD021630.

Gröbner J. et al.: 2015, J. Geophys. Res. Atmos., 120, 6885–6886, doi: 10.1002/2015JD023345.

Philipona R.: 2015, J. Geophys. Res., 120, 6882–6884, doi: 10.1002/2014JD022990.

Reda, I. et al.: 2012, J. Atm. and Sol.-Terr. Phys. 77, 132–143, doi: 10.1016/j.jastp.2011.12.011.

WMO: 2006, CIMO-XIV, Activity Report, WMO No. 1019 (Part II), 7–14 December 2006.

Atmospheric Turbidity Section (WRC-WORCC)

Stelios Kazadzis, Natalia Kouremeti, and Julian Gröbner

The Atmospheric Turbidity Section of WRC maintains a standard group of three Precision Filter Radiometers that serve as a reference for Aerosol Optical Depth measurements within WMO. WORCC also operates the global GAW-PFR AOD network.

The PFR reference triad has been operating near continuously since the beginning of 2005. After the 2015 change of the triad instruments (N24 replaced N01), N24 continued measuring as part of the triad.

The instruments that are used for triad calibration transfer and checks, at Mauna Loa (USA) and Izaña (Spain), continued their measurements. An analysis of the PFR performance and Langley calibration-related uncertainties for five months of Langley measurements can be seen in Figure 1.

Annual quality assured data from five GAW-PFR stations were updated to 2016 and three for 2015, and submitted to WDCA. In 2016, eight instruments of the extended GAW-PFR network and 10 additional customer instruments were calibrated against the reference Triad at Davos. All calibrations were documented according to our Quality Management System.

The lunar PFR was deployed at Ny Ålesund from December 2015 to February 2016 and November 2016 to February 2017 for AOD monitoring during the Arctic winter, in collaboration with partners from NILU (Norway), ISAC/CNR (Italy), AWI (Germany), NOAA/CIRES (US), and IGF/PAS (Poland). A calibration of the lunar PFR

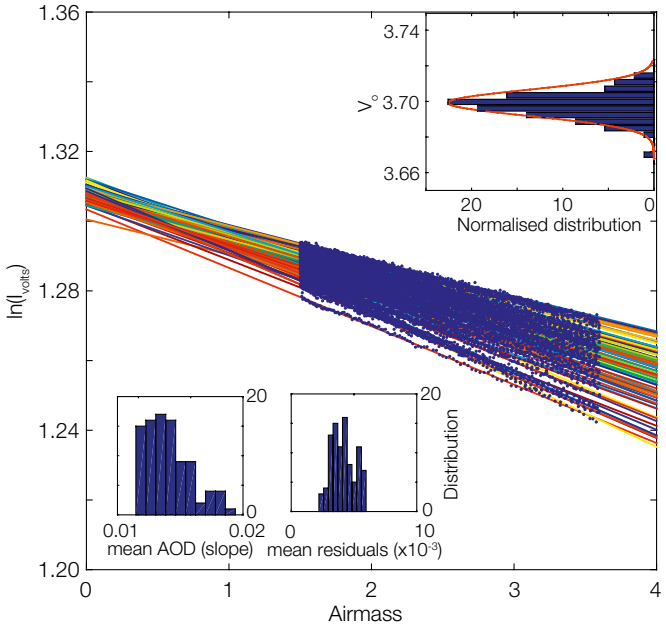

Figure 1. Langley plots at λ = 412 nm at Mauna Loa (ISA) from 17 November 2015 to 4 April 2016.

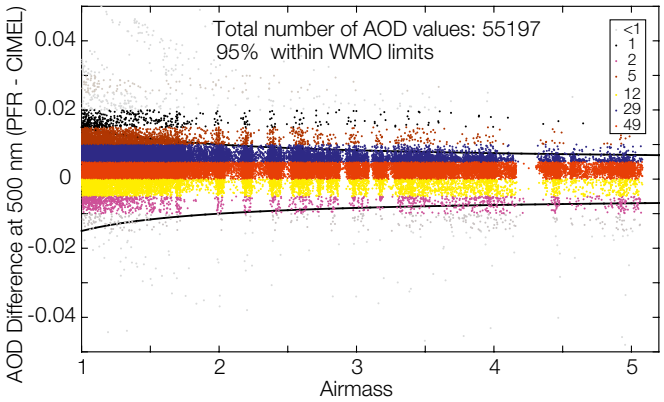

Figure 2. Six-year comparison (14 May 2009 – 31 Dec. 2014) of AOD at 500 nm from co-located PFR and CIMEL instruments at the Izaña Atmospheric Observatory on Tenerife (Spain).

was performed in Izaña, Spain, measuring one lunar cycle in October 2016, alongside the Triplet-Cimel belonging to AERONET.

WORCC has started a close collaboration with AERONET Europe and SKYNET Europe and Asia. Figure 2 shows for example a six-year comparison of co-located Aeronet Europe CIMEL and PFR radiometers at Izaña, Spain. In addition, two PFR instruments have been measuring alongside Skynet and AERONET instruments at Valencia, Spain and Chiba, Japan, for a year. A memorandum of understanding, including a 4-year collaboration plan, has been signed with CNR, Italy (representing Skynet Europe) for a close scientific collaboration on the traceability of SKYNET instruments, linked with the PFR triad. Similar agreements are planned with AERONET Europe.

Within the project "A travel standard for Aerosol Optical Depth in the UV", the UV version of the PFR (UV-PFR) has been tested as a reference instrument to calibrate Brewer spectrophotometers for AOD determinations. The UV-PFR participated in the Regional Brewer Calibration Center Europe campaign in 2015, followed by visits to Brewer monitoring stations in Madrid and Brussels.

Two Precision Spectroradiometers (PSR) have been re-calibrated and upgraded at PMOD/WRC. Three direct irradiance calibrations of PSR_006 (DWD) have been performed since production. The calibrations, spanning about 18 months, showed an agreement of 3% which is within the uncertainty of the calibration procedure, revealing the excellent stability of the instrument during the three years of continuous operation at DWD (MLO-RAO Lindenberg, Germany).

In addition, the stability of the PSR spectrometers has been verified by retrieving AOD from 2.5 years of direct irradiance measurements of both DWD instruments (PSR_004 and PSR_006) and by comparison to the collocated CIMEL -AERONET sun-photometer.

World Calibration Centre for UV (WRC-WCC-UV)

Julian Gröbner, Gregor Hülsen, and Luca Egli

The objective of the World Calibration Center for UV (WCC-UV) of WMO GAW is to assess the data quality of the Global GAW UV network and to harmonise the results from monitoring stations and programmes in order to ensure representative and consistent UV radiation data on a global scale.

A Quality Assurance site visit was organised at the National Institute of Water and Atmospheric Research (NIWA) at Lauder, New Zealand in January 2016. During two weeks, collocated measurements of global solar UV irradiance were performed by QASUME, the local monitoring instruments and a visiting instrument from the Australian Radiation Protection and Nuclear Safety Agency (ARPANSA). Figure 1 shows a view of the measurement site at Lauder. The campaign provided the first direct link between the WCC-UV and solar UV measurements performed at NIWA. The facilities provided by the local host were optimal for performing such an inter-comparison and together with excellent weather conditions a large number of measurements were obtained and analysed. A report describing the results of the campaign can be found on the QASUME web-site (see link at bottom of page).

The second main activity during 2016 was the organisation of an international campaign for measuring direct solar irradiance and total column ozone in the framework of the EMRP ENV59-ATMOZ project "Traceability for Atmospheric Total Column Ozone". The ATMOZ project aims to provide a framework of traceable ozone monitoring networks and to significantly enhance the reliability and reduce the uncertainty of total column ozone measurements with standard ozone monitoring instruments, such as Brewer, Dobson and new generations of array spectroradiometers. According to this objective, PMOD/WRC is coordinating an international consortium of national metrology institutes, national agencies, universities and industry. The newly developed devices and methods elaborated by the consortium partners were presented to the public and tested at the first ATMOZ measurement campaign.

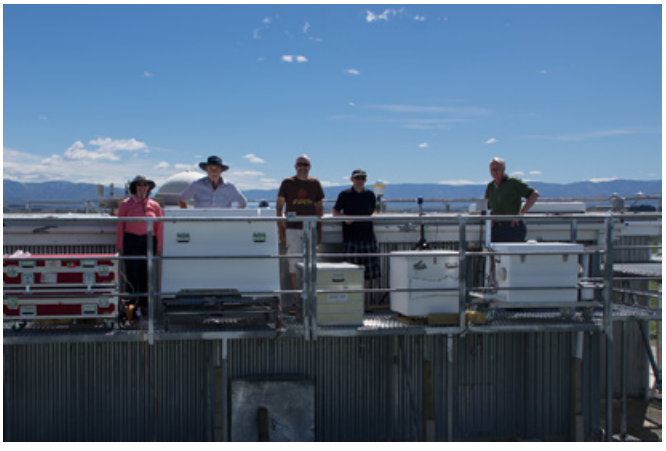

Figure 1. View of the measurement site at Lauder, New Zealand (photo courtesy of Kerryn King).

Figure 2. View of the measurement platform at Izaña Atmospheric Observatory.

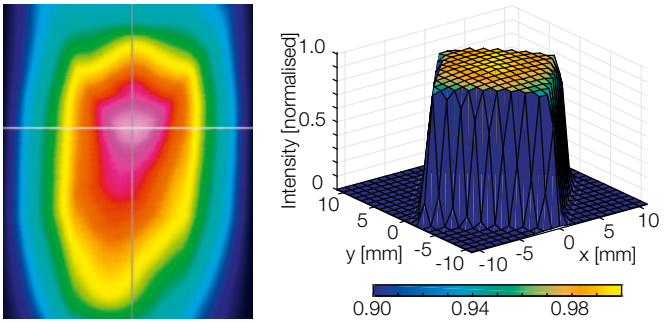

Figure 3. Left panel: Output field homogeneity of the SRF set-up before and after the insertion of the lens array. Right panel: Acton SRF output field at 400 nm (2 nm slit) on 13 January 2017.

The campaign was held at the Izaña Atmospheric Observatory (IZO) located on Tenerife (Canary Islands, Spain) from 12 – 25 September 2016. During two weeks, participants from the US, the Czech Republic, Germany, Greece, Spain and PMOD/WRC operated their spectroradiometers alongside the IZO reference instruments. Perfect weather conditions provided the opportunity to obtain a large amount of measurements in addition to extensive laboratory calibration and characterisation work. Figure 2 shows the measurement platform at IZO with several instruments which participated in the campaign.

The monochromatic light source used in the spectral response facility was improved by adding a micro-lens array (SUSS MicroOptics) to its exit slit. The radiance field used for illuminating devices under test (DUT) is now a well-defined square, flat, top field with an area of 12 x 12 mm^2 (see Figure 3). The homogeneity of the flat top is 1.6%, and is independent of wavelength. This improvement reduces measurement uncertainties due to positioning of the DUT. Measurement of the monitor diode, placed behind a beam splitter, was also improved by adding a lens which focusses the whole output field onto the sensitive area of the diode. QASUME site audits can be found at the WCC-UV website: www.pmodwrc.ch/wcc_uv/ wcc_uv.php?topic=qasume_audit.

The Cryogenic Solar Absolute Radiometer and the Window Transmittance Monitor

Benjamin Walter, Wolfgang Finsterle, and Nathan Mingard

The Cryogenic Solar Absolute Radiometer (CSAR) is expected to become the new World Radiometric Reference (WRR) for Direct Normal Irradiance (DNI) measurements, and will replace the currently used, less accurate World Standard Group (WSG) in the future. The Monitor to Measure the Integral Transmittance of Windows (MITRA) measures the spectrally integrated transmittance of a window identical to the entrance window of CSAR to correct the irradiance values for reflectance and absorption losses. Issues with the window cleanliness were resolved and the latest irradiance measurements performed with the CSAR/MITRA system in 2016 support previous findings of a ~0.3% difference between the International System of Units (SI) radiometric scale represented by CSAR and the currently used WRR scale. A defective motor on MITRA and an electrical defect on CSAR, due to a lightning event, were successfully resolved. However, it was not possible to perform irradiance measurements during the repair period from April to October 2016. A new improved MITRA-III instrument with four, instead of two, detectors was designed and partially built to further reduce the uncertainty of transmittance measurements and to allow different windows to be compared.

Direct Normal Irradiance (DNI) measurements are currently traceable back to the World Radiometric Reference (WRR) defined by the average irradiance reading of a group of six instruments called the World Standard Group (WSG) (Figure 1). A significant scale difference between this artefact based reference (WRR) and the International System of Units (SI) radiometric scale was observed, amongst others, by Fehlmann et al. (2012) to be 0.34% ± 0.09% (k = 1). In order to reduce the uncertainty of worldwide DNI measurements from the current value of 0.3% (WSG) towards the goal of 0.01%, and to provide a direct traceability of DNI measurements back to the SI scale, the Cryogenic Solar Absolute Radiometer (CSAR, Figure 1) was built by the National Physical Laboratory (NPL) and the PMOD/WRC (Winkler, 2012). The solar radiation is partly reflected and absorbed by the CSAR entrance window where the spectrally integrated window transmittance depends on the spectral composition of the

Figure 1. The CSAR and MITRA instruments next to the WSG on the sun tracking platform at PMOD/WRC measuring direct normal solar irradiance.

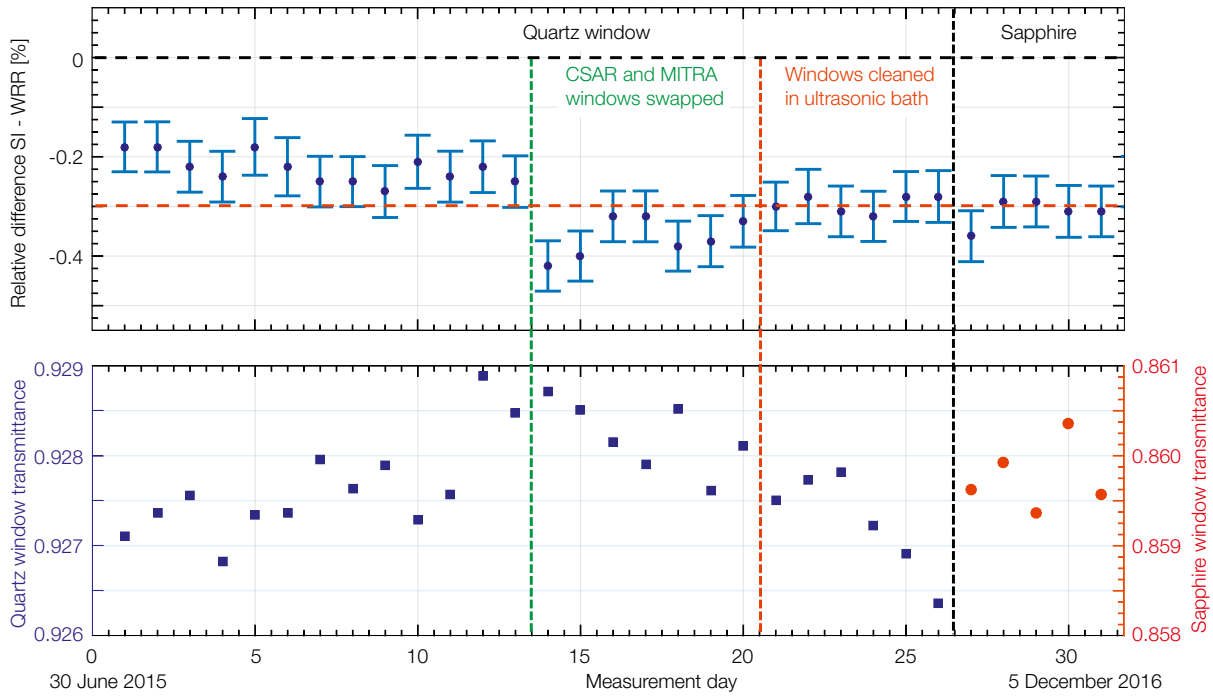

Figure 2. Top: Daily averages of 32 WRR to SI comparisons performed at PMOD/WRC with CSAR/MITRA since June 2015. Bottom: Corresponding daily averages of the spectrally integrated window transmittance as measured with MITRA.

solar irradiance and thus on the solar zenith angle and atmospheric conditions. Therefore, the effective transmittance is measured with the Monitor to Measure the Integral Transmittance of Windows (MITRA, Figure 1) in parallel with CSAR to correct its power readings for these losses.

Figure 2 provides a summary of the comparions of the SI scale represented by CSAR to the WRR performed from June 2015 to the end of 2016, together with daily averages of the respective MITRA transmittance measurements. The first 13 comparisons resulted in a difference of -0.22%, and was thus slightly less when compared to previous findings of a -0.3% difference. After swapping the windows, the difference increased to -0.36% on average, showing that the two windows were not as identical as expected. A different degree of contamination with microscopic particles (Walter et al., 2016) was found despite proper periodical cleaning of the windows with optical tissues and isopropanol. However, The average of these two measurement periods (-0.29%) agrees well with the previous findings of an approximate -0.3% difference. The average difference after cleaning the windows several times in an ultrasonic isopropanol bath and when using a different window material (sapphire) instead of the usual quartz windows was -0.3% (Figure 2). The consistent result for a different window material provides good proof of the general measurement concept and the reliability of the CSAR/MITRA instrument system.

The overall relative difference between the SI and the WRR radiometric scales determined with CSAR/MITRA is thus currently -0.3% ± 0.064%. Table 1 summarises the uncertainties for the scale comparisons which is currently dominated by the MITRA uncertainty. The scatter of the MITRA transmittance values (Figure 2) of about ±0.1% is partly a result of differences in the window cleanliness but mainly due to spectral changes of the solar irradiance resulting from different atmospheric conditions. For example, on measurement day 11 to 12 and 29 to 30, the transmittance of the window changed significantly by about 0.1% due to changes in the spectral composition of the irradiance, whereas the CSAR to WRR difference remained quite stable, changing only by 0.02%. This proves that spectral changes are well-corrected when applying the MITRA transmittance correction.

A new MITRA-III instrument is currently under construction with four instead of two detectors. This allows the transmittance of two windows to be compared, and thus allows window differences and cleanliness issues as mentioned above to be resolved. One of the four cavities will always be shaded and used to track parasitic heatflows between the cavities and the reference block resulting from instrument temperature drifts. Such parasitic heatflow effects are currently eliminated by performing periodical thermometer recalibrations. This procedure which introduces uncertainties can therefore be omitted in the new MITRA-III design.

Table 1. Summary of the SI to WRR scale comparison uncertainties (Walter et al., 2016).

Item	Uncertainty ($k=1$)
MITRA	0.036%
Window contamination	0.035%
CSAR	0.014%
Repeatability (statistical)	0.021%
WRR	0.030%
Overall SI-WRR intercomparison	**0.064%**

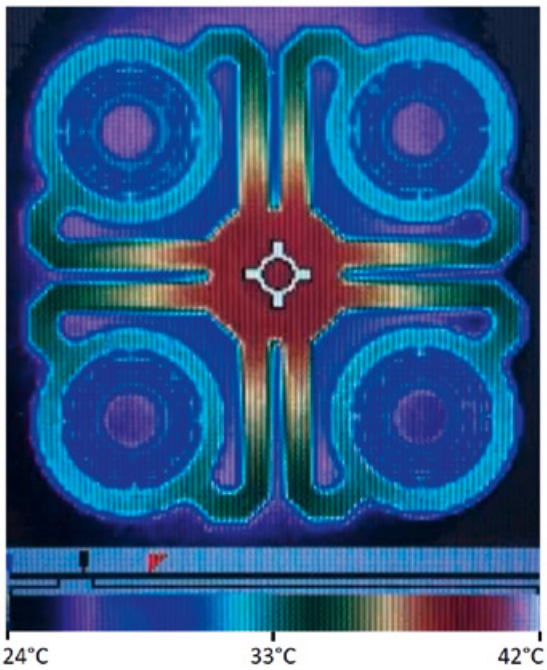

Figure 3. Thermal image of the new four-detector MITRA-III reference block showing a nearly perfect thermal symmetry for a constant heat input (50°C) in the centre. Cavity detectors are not mounted yet and the reference block was painted black to obtain a homogenous emissivity of $\varepsilon = 1$.

A new MITRA-III reference block has already been designed and produced in-house at PMOD/WRC. The thermal symmetry between the four detector branches of this novel reference block design is of crucial importance to accurately measure window transmittances. Figure 3 shows a thermal image taken with an infrared camera of the new reference block for a constant heat input at the center. A perfect thermal symmetry of the heatfluxes towards the detectors is obtained which guarantees an accurate performance of MITRA-III. The next steps will include the production of the electronics and the housing, and a new mechanism for moving the windows in front of the detectors will be designed and produced.

References:

Fehlmann A. et al.: 2012, Metrologia, 49, 34–38.

Walter B. et al.: 2014, Metrologia, 51, 344–349.

Walter B. et al.: 2016, IRS conference Auckland, special issue.

Winkler R.: 2012, PhD Thesis, University College, London.

Development of the ERMIS Spectroradiometer

Natalia Kouremeti, Julian Gröbner, Ricco Soder, Patrik Langer, and Pascal Schlatter

ERMIS is a new high resolution spectroradiometer for trace gas retrievals in the UV/VIS spectral region. The key feature of the spectroradiometer is the combination of a Czerny-Turner design with a rotating grating and a CCD detector, resulting in a resolution of 0.25 nm over the 295 – 660 nm spectral range.

A new high resolution spectroradiometer (ERMIS, Figure 1) has been developed in the framework of the EMRP joint research project, ATMOZ "Traceability for total column ozone". The primary objective of ERMIS is the retrieval of the total column ozone amount using measurements of direct solar irradiance in combination with a retrieval model based on the Beer-Lambert law and a DOAS technique.

ERMIS was designed with the objective of allowing not only the retrieval of total column ozone, but to be versatile enough to also retrieve other trace gas concentrations such as nitrogen dioxide (NO_2), oxygen dimer (O4) and water vapour (H_2O) in the 400 – 670 nm visible range. Therefore, a nominal resolution of < 0.3 nm, defined as the full-width-at-half-maximum (FWHM) was chosen.

To achieve the required resolution, a Czerny-Turner design was selected with a rotating grating (Figure 2). To reduce the aberrations in the system, a parabolic mirror is used as a collimating mirror, while a custom-made spherical mirror is used as the focusing mirror. The high resolution and large oversampling of the detector is obtained by using a diffraction grating with 1800 lines.mm^{-1}, dispersing a wavelength range of ~95 to 65 nm across the detector (Hamamatsu-S101411108) depending on the grating position.

In order to minimise the noise level, the detector is cooled down to -20°C using a three-stage cooling system. The spectroradiometer is filled with N_2 and pressurised to 1.5 bar to avoid condensation

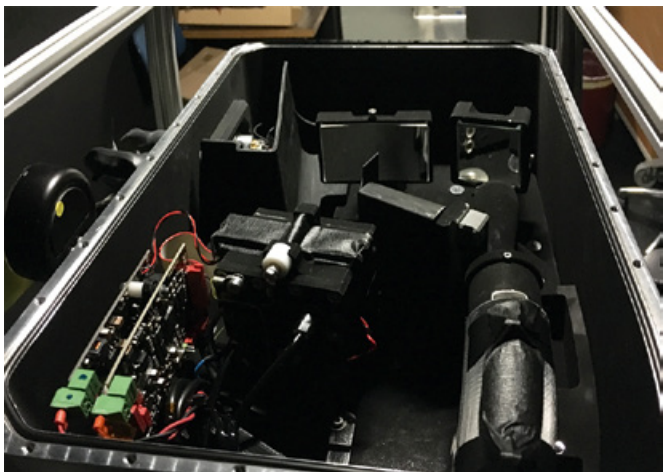

Figure 1. The ERMIS spectroradiometer.

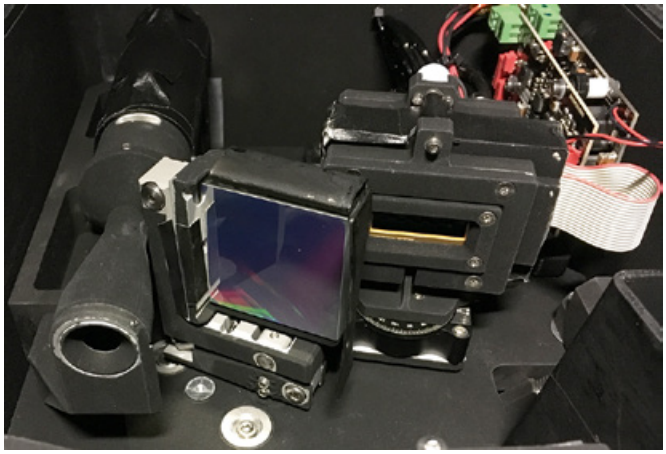

Figure 2. Close-up view of ERMIS.

on the detector and deterioration of the optical components. The solar radiation is collected through a telescope with a 1° field-of-view which images the radiation onto an optical fibre. The radiation exiting the optical fibre is fed through two filter-wheels. The first one contains neutral density filters to attenuate the radiation by up to a factor of 10^3, while the second filter-wheel contains several bandpass filters to select the optimal wavelength range depending on the selected measurement type. The radiation entering the monochromator is focussed onto the entrance slit of 60 mm width and 1 mm height. The parabolic mirror, the grating and the spherical mirror are carefully aligned to achieve the theoretical spectral resolution given by the ZEMAX simulation of the ERMIS monochromator. A further degree of freedom during the alignment process is the ability to rotate the detector around its vertical axis, which results in a nearly constant bandpass across its wavelength range.

ERMIS was characterised with the ATLAS laser system. The wavelength range in the default grating position is 294–390 nm with FWHM = 0.23 nm ± 0.01 nm (2σ) which remains constant over the 295–660 nm wavelength range (Figure 3). The oversampling is 6–12 pixels within the FWHM of the slit function.

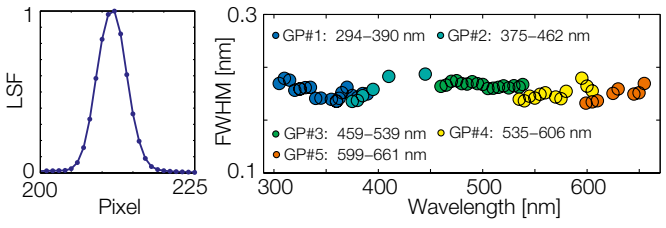

Figure 3. Left panel: Example of the slit function in the 295–390 nm range in pixel space demonstrating the achieved sampling. Right panel: FWHM of the ERMIS LSFs for five selected grating positions covering the 295–660 nm spectral range.

The ERMIS line-spread functions (LSF) for the 295–390 nm wavelength range are shown in Figure 4. The presence of dispersed light reflection of about 10^{-3} is evident which will be accounted for by applying the measured stray-light correction. An example of the high resolution direct irradiance spectrum for five spectral ranges (Figure 5) along with the normalised cross-sections of the dominant absorbing trace gas of the region, shows the potential of ERMIS.

ERMIS will be in operation in 2017 and will participate in the RBCC-E XII (Huelva, Spain) campaign where the ability to retrieve ozone will be validated.

A prototype version of the system participated in the ATMOZ campaign at Izana, Spain in September 2016 where the ozone agreement was within ±5 DU against the RBCC-E triad of reference instruments.

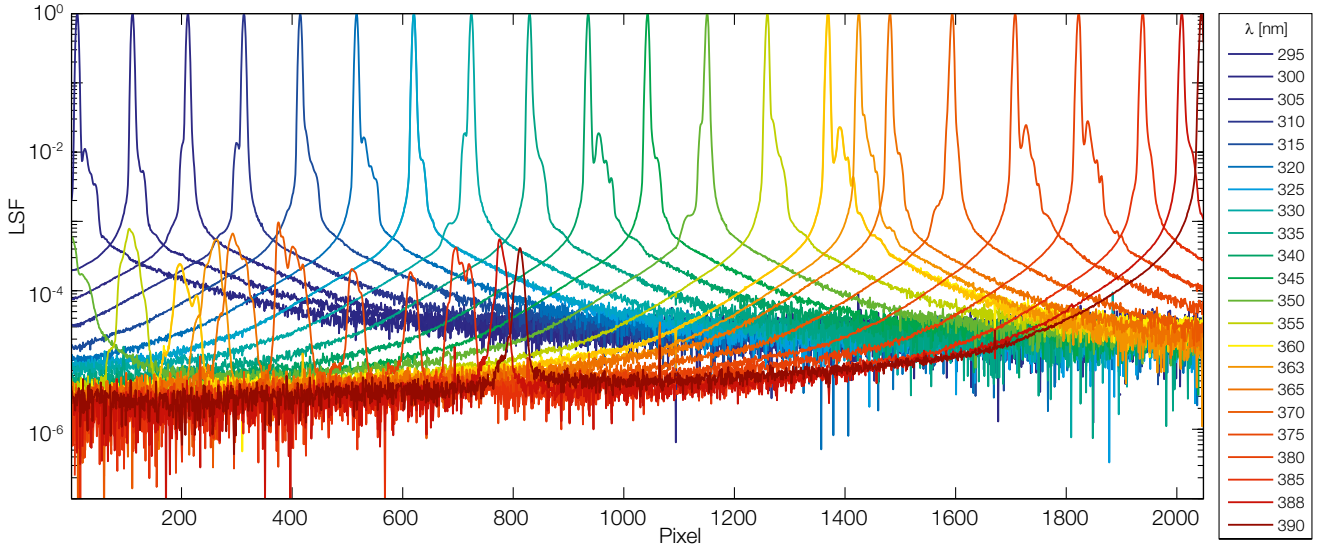

Figure 4. Line-spread functions of the ERMIS spectrometer for the 295–390 nm primary wavelength range.

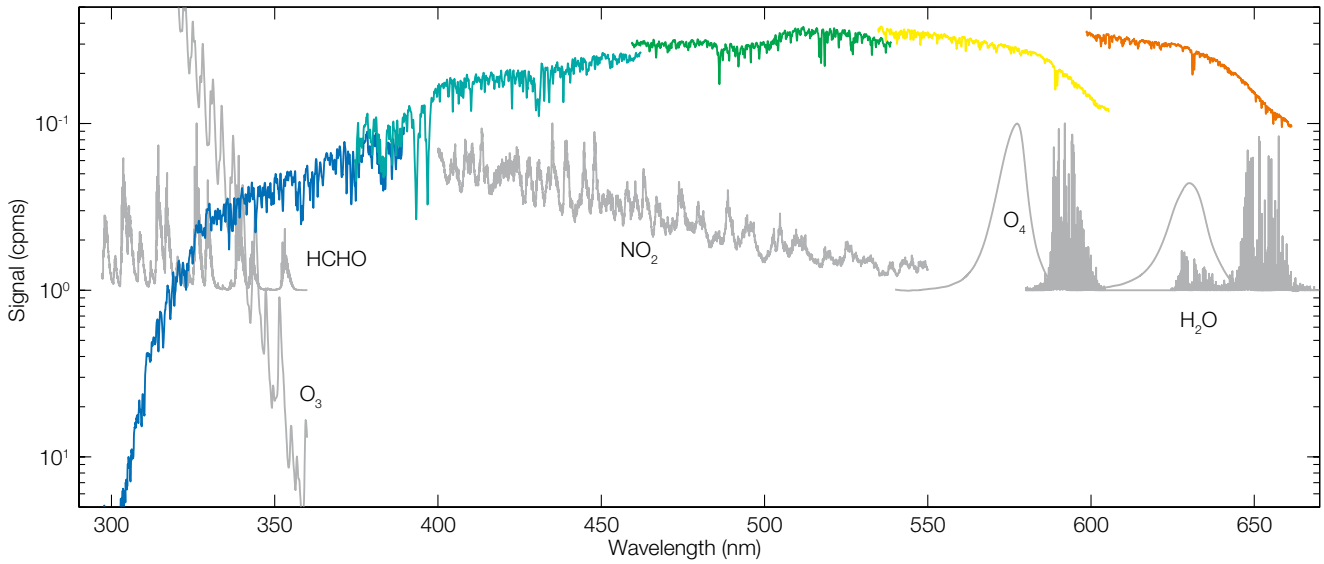

Figure 5. Direct irradiance spectra (counts per ms) measured with the ERMIS spectroradiometer for the five selected grating positions along with the signature of the dominant absorbers of each spectral region.

Space Experiments

Manfred Gyo, Lloyd Beeler, Wolfgang Finsterle, Matthias Gander, Nuno Guerreiro, Patrik Langer, Pierre Luc Lévesque, Margit Haberreiter, Johnathan Kennedy, Silvio Koller, Philipp Kuhn, Nathan Mingard, Andri Morandi, Dany Pfiffner, Pascal Schlatter, Yanick Schoch, Marcel Spescha, Benjamin Walter, and Werner Schmutz

EUI

The Extreme UV Imager (EUI) experiment, a payload onboard the ESA/NASA Solar Orbiter Mission.

PMOD/WRC is responsible for the optical bench structure (OBS) of the EUI instrument. In 2016, the main focus was on the qualification test campaign and qualification review. During the test campaign, the validation of the alignment was not working as expected, and a problem with the mirror-mount assembly was found to be the root cause. After resolving this problem, the environmental test gave good results. The qualification review was thus finished by the end of 2016 when the EUI instrument was deemed to be "qualified".

The optical bench for the Flight Model (FM) was manufactured at APCO Technologies in spring 2016. A first bake-out was conducted at PMOD/WRC with all parts surviving temperatures of up to 100°C. The parts were sent back to APCO for finalisation and to assemble the optical bench unit. A second bake-out was then performed on the assembled unit at 80°C. It was demonstrated that the first bake-out had been efficient, and that only low outgassing values were being monitored. The additional outgassing is driven by those parts which do not survive at 100°C and have not been subjected to a first bake-out. At the end of the two-stage bake-out, the cleanliness and outgassing criteria were attained. After final 3D measurements at APCO Technologies, the delivery review was successfully held at the end of July 2016.

The optical bench was delivered in August 2016 to Centre Spatial de Liège (CSL, Liège, France) in order to start with the integration of the sub-systems, optical alignment of the three channels, and final assembly of the instrument FM. The instrument is now ready for the acceptance test campaign and final calibration (Figure 1). The delivery to Airbus for integration into the EUI instrument is scheduled for spring 2017.

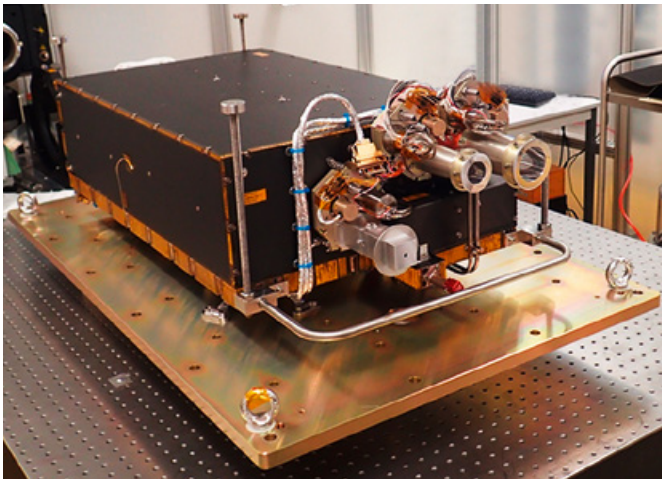

Figure 1. The fully assembled EUI Flight Model.

SPICE

The Spectral Imaging of the Coronal Environment (SPICE) experiment, a payload onboard the ESA/NASA Solar Orbiter Mission.

Low Voltage Power Supply (LVPS)

During 2016, only solder verification and component stand-off verification was pending. This entailed a vibration test with sample boards soldered at PMOD/WRC. Afterwards, a thermal cycling of the sample boards was carried out in the climate chamber for almost two months. Finally, micrographs (Figure 2) from some of the solder joints and components were taken. The solder verification was successfully passed, but the stand-off verification needs some additional work in 2017.

Figure 2. Micrograph of a component from the solder verification board.

Slit Change Mechanism (SCM)

In 2016, the FM and the flight spare model (FS) were assembled and acceptance testing was conducted. Figure 3 shows the preparation for a thermal vacuum test. With a view towards full qualification of the mechanism, the FM and FS were delivered to the Rutherford-Appleton Laboratory (England) in August for integration into the instrument. The qualification of the mechanism continued further, and the tests were finished in 2016. Final inspection, at the beginning of 2017, included a full strip-down of the mechanism.

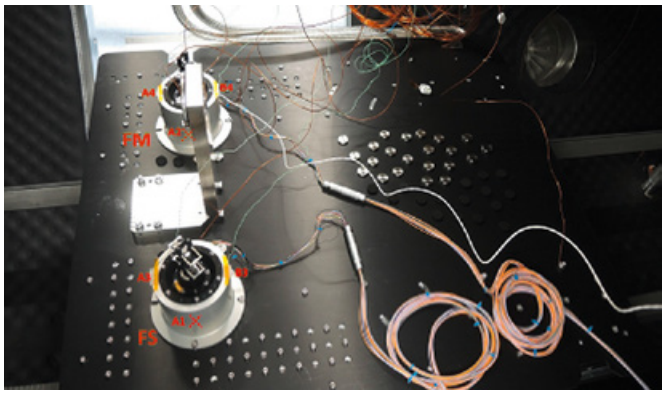

Figure 3. SCM FM and FS being prepared for thermal vacuum testing.

SPICE Door Mechanism (SDM)

The work in 2016 was dominated by the wait for the replacement of the qualification model (QM) motor. It was delivered late in 2016 so that the reassembly of the QM took place at the beginning of 2017. Similar to the SCM work-schedule, the FM of the door mechanism was assembled (Figure 4) and acceptance tested. It was delivered in August 2016 for integration into the SPICE instrument.

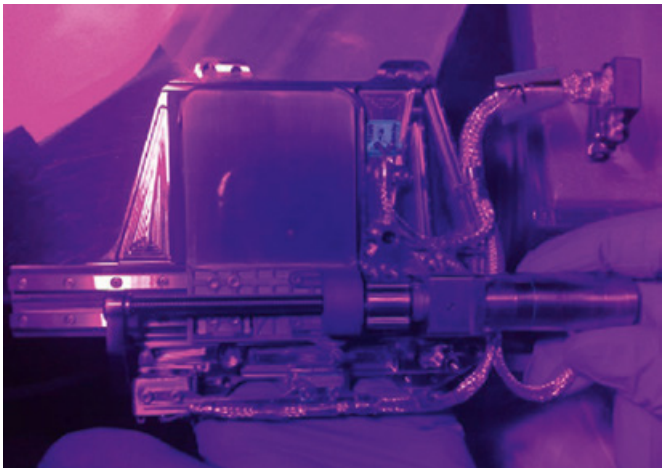

Figure 4. Inspection of the SPICE Door Mechanism (SDM) Flight Model under UV light during final assembly.

SPICE Instrument

The SPICE door mechanism was sent to the Rutherford-Appleton Laboratory in autumn 2016 for assembly into the SPICE instrument (Figure 5) and started the test campaign. A proto-FM approach is used at "instrument" level which means that the qualification and acceptance steps are conducted simultaneously.

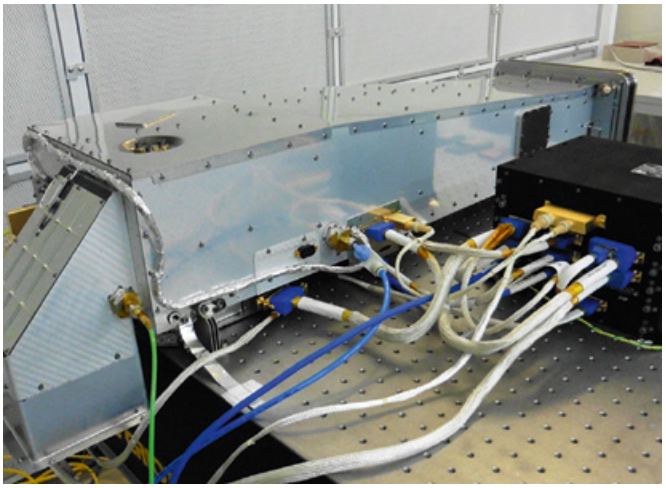

Figure 5. SPICE Flight Model.

CLARA

The Compact Lightweight Absolute Radiometer (CLARA), a payload onboard the Norwegian NORSAT-1 nano-satellite.

CLARA, shown in Figure 6, was mounted on the NORSAT-1 spacecraft and shipped to Kourou French Guyana to be launched in spring 2016. Unfortunately a late change in the rocket payload was announced when ESA engineers discovered an incompatibility between the satellite and the launcher supporting structure provided by Arianespace. NORSAT-1 was therefore not launched.

A new launch date was scheduled for mid-summer 2017, and during this waiting period the preparation of the commissioning procedure was finished and the required command sequences were defined and prepared.

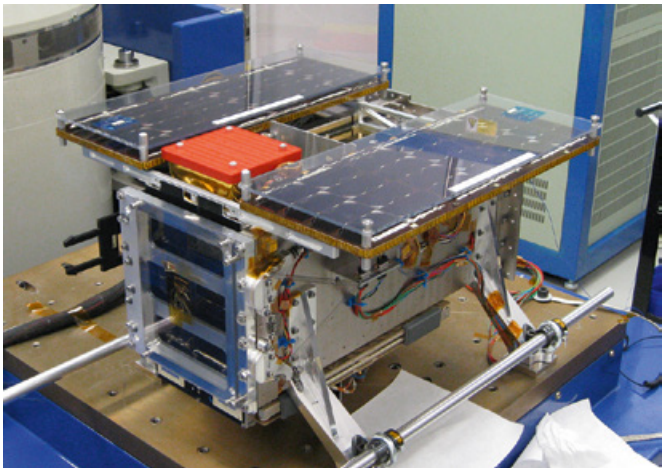

Figure 6. CLARA (with red cap) mounted on the NORSAT-1 structure.

DARA

The Digital Absolute Radiometer (DARA), a payload onboard ESA's PROBA-3 formation flying mission.

One of the project goals was to implement possible design improvements based on “lessons learned” with the CLARA radiometer during its first few months in orbit.

Unfortunately, the NORSAT-1 launch with CLARA onboard had to be postponed and is now re-scheduled for the first quarter in 2017. Nevertheless, the DARA space radiometer made good progress in all mechanical, electrical and software aspects. Mechanical aspects of the Engineering Model were finished by the end of November 2016. A vibration test was then conducted, which simulated the vibration loads during satellite launch.

Figure 7 shows the vibration test set-up with different accelerometers placed on the structure. A vibration test is performed to assess the mechanical stability of the structure and to determine instrument specific characteristics, such as Eigen-modes or damping behaviour. The results of such a test are further compared with predictions of the mechanical structural analysis, based on a finite-element model. This correlation helps to adjust some of the model parameters and thus improve its significance and accuracy.

The load specifications during the upcoming PROBA-3 launch will be rather high (24.3 grms, out-of-plane), and application of these specifications during vibration testing led to some failures within the Engineering Model structure. Therefore, some design modifications will be required.The electronics boards of the DARA Engineering Model were also ready for further development towards the end of the year. Thus, first solar measurements with the complete DARA Engineering Model are planned to commence at the beginning of 2017.

Figure 7. DARA Engineering Model on a vibration adapter during testing.

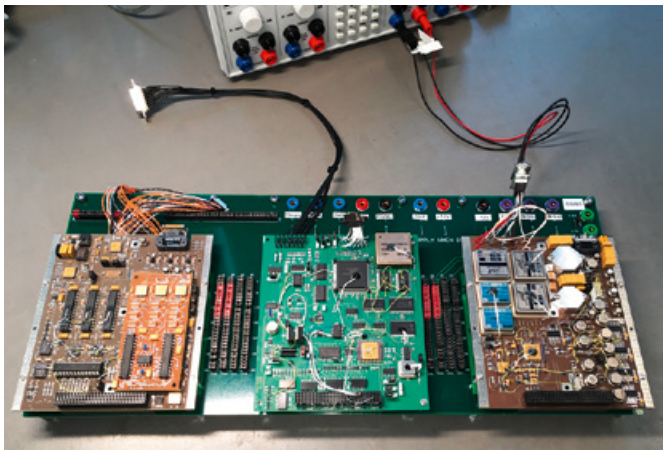

Figure 8. Electronics boards of the DARA Engineering Model.

The electronics and embedded software were developed simultaneously, and most of the radiometer functions have already been implemented. Figure 8 shows the three separate electronics boards of the DARA Engineering Model on a test adapter.

The mission schedule foresees the Critical Design Review milestone in spring 2017. When this milestone is reached, the instrument design will be frozen. Delivery of the flight units is still scheduled for mid-2018. Launch of PROBA-3 should take place in 2019.

The Critical Design Review milestone will also release the project phase C/D of the JTSIM-DARA “Sister Experiment” for the FY-3E Chinese mission. The JTSIM-DARA radiometer is very similar to the DARA radiometer on the PROBA-3 mission.

JTSIM

Joint Total Solar Irradiance Monitor (JTSIM), a payload onboard the Chinese FY-3 mission.

After a successful feasibility study, the JTSIM project was ready to begin the implementation phase. A "PROgramme de Développement d'Expériences scientifiques" (PRODEX) proposal for Phase B and C/D was submitted and approved just before the New Year. The proposal shows different challenges following the standard PRODEX guidelines for that project.

There will be a different kind of collaboration for industry contracts: namely, an adapted approach as the Chinese collaboration is new in the community and is a very direct approach determined by the tight time-line of the project. With the PROBA-3 mission and the current status of DARA in the Engineering Model test and verification phase, an approach only involving a proto-Flight Model is being adopted.

During the feasibility phase A, the team from the Royal Meteorological Institute of Belgium (IRMB) were unable to proceed further due to budget restrictions and lack of resources. As a consequence, the initial scope of the standard space group changed and will now consist of two radiometers flying on the FY-3 mission: One DARA type designed by PMOD/WRC and the SIAR radiometer (Figure 9) designed by the Changchun Institute of Optics, Fine Mechanics and Physics (CIOMP). Due to the great efforts which will be required to complete the technical

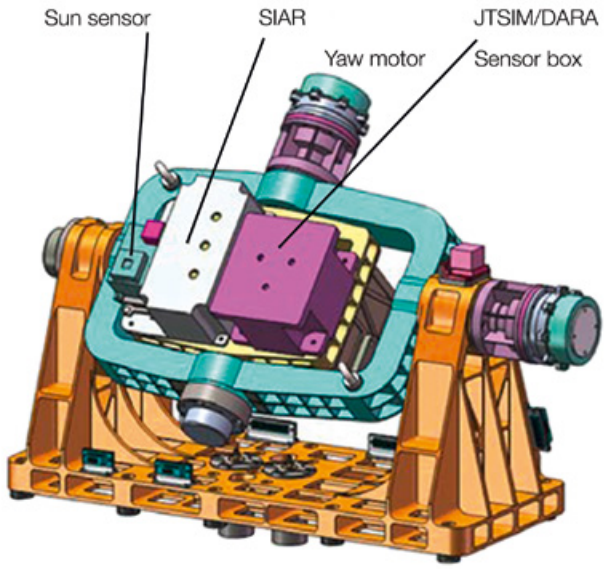

Figure 9. Sun tracker with the SIAR and DARA instruments planned for the FY-3E mission.

Figure 10. Project Meeting in 2016 at the Changchun Institute of Optics, Fine Mechanics and Physics (CIOMP), China. Participants were (from left to right): Jin Qi (Chinese Meteorological Administration, CMA), Yefei Li (Shanghai Academy of Spaceflight Technology, SAST), Frank (Interpreter), Hong Qiu (CMA), Silvio Koller (PMOD/WRC), Philipp Kuhn (PMOD/WRC), Wolfgang Finsterle (PMOD/WRC, DARA PI), Xuejun Zhang (CIOMP, vice president of CIOMP), Wei Fang (CIOMP, JTSIM PI), Hui Wang (CIOMP, co-head of international cooperation department), Hongrui Wang (CIOMP), Rong Li (CIOMP), Lingtong Zhang (CIOMP).

design and manufacturing of the flight unit, an additional electronics engineer was hired at the PMOD/WRC.

As the flight electronics will be manufactured, tested and qualified internally at PMOD/WRC, a great amount of manpower is needed. The mechanical design and manufacturing will be conducted with known partners and can be covered by existing, experienced staff.

A collaboration with LATMOS (Laboratoire Atmosphères, Milieux, Observations Spatiales) at the IPSL (Institute Pierre Simon Laplace) was established in order to conduct thermal and mechanical simulations. LATMOS will also act as a Co-Investigator regarding research questions. The project team has been put together and is operational. As the timeline is tight, it will only be possible to implement minimal hardware changes. Hence, DARA was chosen as a base instrument. Nevertheless, the concept does look optically different as both boxes will be spatially separated.

The sensor-head will be directly integrated onto the sun-pointing unit whereas the electronics box will be mounted inside the FY-3 spacecraft. This concept has some noticeable advantages leading to a design which will be more robust against mechanical stress. An electrical board has been designed and manufactured to test the communication Interface. The thermal and mechanical simulation of the concept design has been tested, and the design has been optimised to increase the performance of the radiometer.

Scientific Research Activities

Overview

Werner Schmutz

Projects at PMOD/WRC are related to solar radiation in which we address questions regarding the radiation energy budget in the terrestrial atmosphere, as well as problems in solar physics in order to understand the mechanisms concerning the variability of solar irradiance. Hardware projects at our institute are part of investigations into Sun-Earth interactions which involve measurements of solar irradiance.

The choice of projects to be conducted at the institute is governed by the synergy between the know-how obtained from the Operational Services of the WRC and other research activities. Basically, the same instruments are built for space-based experiments as are utilised for ground-based measurements. The research activities can be grouped into three themes:

- Climate modelling
- Terrestrial radiation balance
- Solar physics

Research activities are financed through third party funding. Last year, seven projects were supported by the Swiss National Science Foundation and in addition other funding sources were: i) a project through Swiss participation in the EU's COST actions, ii) two projects by MeteoSwiss in the framework of Swiss contributions to the Global Atmosphere Watch programme of the WMO, iii) a project through the Horizon 2020 programme of the European Commission, and iv) two projects through the European Metrology Research Programme. These funding sources have supported four PhD Theses and eight post-doctoral positions. Swiss participation in ESA's PRODEX (PROgramme de Développement d'Expériences scientifiques) programme funds the hardware development for space experiments. The institute's five PRODEX projects paid for the equivalent of eight technical department positions. Another space-related contribution is the ESA IDEAS+ project which is using the institute's laboratory calibration equipment.

The project, *Future and Past Solar Influence on the Terrestrial Climate* (FUPSOL) ended in March 2017. It was funded through the so-called Sinergia programme of the Swiss National Science Foundation, which supports multi-institute collaborative research. The FUPSOL partners were from the EAWAG, IAC ETHZ, University of Bern, and the Oeschger Centre for Climate Change Research. The past three-year project was the continuation of a previous three-year project and thus, we now have the results of six years of collaborative research. In total, over the six years and all partner institutes, the project has produced 66 papers, which are included in the core collection of the Web of Science. Up to now, these publications have received 966 citations. Of these, an author with a PMOD/WRC affiliation was a co-author of 55 publications, which have been cited 662 times. In our opinion, these are impressive numbers, which underline the full success of the FUPSOL project.

The Swiss National Science Foundation published a press release on 27 March 2017, coinciding with the final project meeting in Davos. The news headline and lead paragraph were as follows:

> *"Sun's impact on climate change quantified for first time. For the first time, model calculations show a plausible way that fluctuations in solar activity could have a tangible impact on the climate. Studies funded by the Swiss National Science Foundation expect human-induced global warming to tail off slightly over the next few decades. A weaker sun could reduce temperatures by half a degree."* [1]

While we scientists usually use a more moderate tone in our statements, it was nevertheless rewarding to see that there was quite a large reaction by the Swiss and also to some extent by European and even the world press. Coverage in Switzerland included a contribution on the evening news of Swiss television and a scientific discussion on the renowned "Echo der Zeit" radio programme which discusses background information on topical matters. Scientifically, it is an important result, showing that natural forcing could potentially be substantial enough to have a measurable influence on climate change. This is not so much for the magnitude of its effect, which is, including the large uncertainties, at most a fraction of the anthropogenic forcing. What we should keep in mind though, is that the damping effect through a weaker Sun could possibly mask the real extent of the anthropogenic influence on climate. If this occurs it will be important to credibly determine how much the natural effect is contributing, and will be more authentic if scientific publications already exist.

A considerable number of publications also result from the research activities of the groups responsible for the World Radiation Center. These papers do not usually get a high number of citations. Nevertheless, it is fundamentally important that research connected to the calibration activities is conducted because only through active research can we be a leading institute for radiation calibration. Figure 1 statistically illustrates the good reputation of PMOD/WRC research and the interest of the science community.

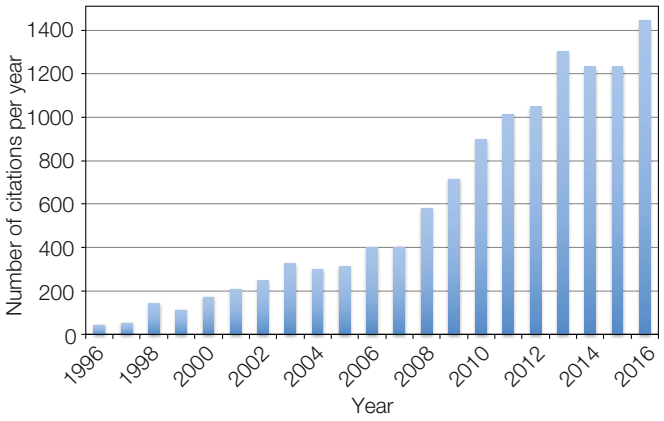

Figure 1. Number of annual citations to articles including an author with a PMOD/WRC affiliation. In April 2017, there were 12850 citations to 572 articles included in Thomson Reuter's Web of Science. The articles were selected using the search criteria address = (World Rad C*) OR (PMOD* NOT PMOD Technol*) OR (Phys* Met* Obs*).*

[1] Press release can be accessed via the SNF news archive: www.snf.ch/en/researchinFocus/newsroom/news-archive/Pages/default.aspx

Solar Conversion Constants Recommended in the IAU 2015 Resolution B2

Margit Haberreiter and Werner Schmutz in collaboration with the IAU Inter-Division A-G WG Nominal Units for Stellar and Planetary Astronomy

At the General Assembly of the International Astronomical Union, Resolution B2 was adopted that recommends the use of a number of nominal solar and planetary parameters. Amongst these parameters are the Nominal Solar Radius and the Nominal Solar Irradiance. The recommended values are based on research at PMOD/WRC.

It is common practice in stellar astrophysics to express properties of stars in terms of solar values, such as the solar mass or solar radius. A problem arises when these quantities need to be transformed to the International System of units (SI). More often than not, authors do not report the conversion constants used in their work, and the differences that stem from using different published values are in some instances no longer negligible.

To address this issue, the IAU Inter-Division A-G Working Group on *Nominal Units for Stellar and Planetary Astronomy* was established to determine nominal solar and planetary conversion constants that were compiled in the Resolutions B2 and B3 (https://www.iau.org/static/resolutions/IAU2015_English.pdf) and adopted in 2015 at the XXIXth General Assembly of the International Astronomical Union (IAU) in Honolulu, Hawaii. The constants to which research activities at PMOD/WRC have made considerable contributions are listed in Table 1. These are briefly summarised below.

Nominal Solar Radius

The revised value is based on the work by Haberreiter et al. (2008) who explain the systematic difference between the solar radius determined from inflection point measurements and the radius that relates to the layer where τ_{500}=1. Haberreiter et al. (2008) determine this discrepancy to be 0.33 Mm, and the solar radius 695.66 ± 0.140 Mm. This result was ultimately defined as the Nominal Solar Radius.

Nominal Solar Irradiance, Luminosity and Effective Temperature

The solar luminosity is derived from the observed solar irradiance integrated over all wavelengths. The observations by PREMOS/PICARD (Schmutz et al., 2013) are the first measurements of the solar irradiance in space, which are traceable to SI units by end-to-end calibration. The PREMOS/PICARD value independently confirmed the results obtained by SORCE/TIM (Kopp and Lean, 2011), which are based on component-characterisation of their instrument. The TIM and PREMOS measurements were the basis for the recommended Nominal Solar Irradiance value shown in Table 1.

The Nominal Solar Luminosity and the Nominal Effective Temperature are then further derived from the above-mentioned values. As such, the research activities at PMOD/WRC in solar physics and solar metrology have had a substantial impact on the IAU 2015 Resolution.

IAU recommends using these values in all astronomical applications when stellar parameters are reported with respect to solar parameters as well as the corresponding SI units.

Table 1. Nominal solar conversion constants, amongst others, as recommended by the IAU 2015 Resolution B2 (from Prša et al., 2016).

Nominal Parameters	Solar Conversion Constants
Solar Radius, 1 $R_\odot^N$	6.957 x 10^8 m
Solar Irradiance, 1 $S_\odot^N$	1361 Wm^{-2}
Solar Luminosity, 1 $L_\odot^N$	3.828 x 10^{26} W
Solar Effective Temp., 1 $T_\odot^N$	5772 K

References:

Haberreiter M., Schmutz W., Kosovichev A.: 2008, Solving the discrepancy between the seismic and photospheric solar radius, Astrophys. J. Letts., 675, 1, article id. L53.

Kopp G., Lean J.L.: 2011, A new, lower value of total solar irradiance: Evidence and climate significance, Geophys. Res. Letts., 38, CiteID L01706.

Prša A., Harmanec P., Torres G., Mamajek E., Asplund M., Capitaine N., Christensen-Dalsgaard J., Depagne É., Haberreiter M., Hekker S., Hilton J., Kopp G., Kostov V., Kurtz D.W., Laskar J., Mason B.D., Milone E.F., Montgomery M., Richards M., Schmutz W., Schou J., Stewart S.G.: 2016, Nominal values for selected solar and planetary quantities, IAU 2015 Resolution B3, Astron. J., 152, 2, article id. 41, 7.

Schmutz W., Fehlmann A., Finsterle W., Kopp G., Thuillier G.: 2013, Total solar irradiance measurements with PREMOS/PICARD, AIP, 1531, 1, pp. 624–627.

Future and Past Solar Influence on the Terrestrial Climate (FUPSOL-2)

Werner Schmutz (PI), Eugene Rozanov (project manager) in collaboration with teams from EAWAG, IAC ETHZ, CEP Uni Bern, and Oeschger Centre for Climate Change Research

The FUPSOL-2 project involves partners from the Institute for Atmosphere and Climate Sciences of the ETH Zürich (IAC ETH), the Swiss Federal Institute of Aquatic Science and Technology, Dübendorf (EAWAG), the Physics Institute (KUP) and Institute of Geography (GIUB) of the University of Bern, and the Oeschger Centre for Climate Change Research. It aims to study solar forcing and its influence on the Earth's atmosphere, ozone layer and climate in the past and future. The project ended in March 2017. The main aims of all sub-projects were mostly fulfilled.

Using the Code for the High Spectral ResolutiOn recoNstructiOn of Solar irradiance model (CHRONOS), we completed the reconstruction of the spectral solar irradiance covering the period from 6000 BCE to the end of the 21st century, by: i) applying an improved set of solar structure models, ii) modified treatment of the long-term irradiance evolution of the quiet sun, iii) a new calculation approach for the active region filling factors, and iv) several recently published solar modulation potential data sets. A comparison of the new SSI data sets with observations during the satellite era showed better performance when compared to our previous reconstruction.

In Figure 1, we compare the annual mean TSI calculated by CHRONOS with the PMOD composite of different satellite observations and TSI prepared within the framework of the IPCC CMIP6 project. The deviation of TSI calculated with CHRONOS from the PMOD/WRC composite is within 0.2–0.4 $W m^{-2}$. The comparison with the CMIP6 data demonstrates that the CHRONOS performance, despite a rather simplified treatment of the active regions, is close to that of other models.

In the framework of sub-project "B", we investigated the influence of auroral electron precipitation on the atmosphere using a new parameterisation of the NO_Y influx from the thermosphere. Our model results show that this approach allows good agreement of the simulated NO_Y enhancement and ozone depletion with measurements from satellite data. These results are presented by Arsenovic et al. (2017) in greater detail. The planned simulations of 20th century climate are ongoing and will be completed in March 2017.

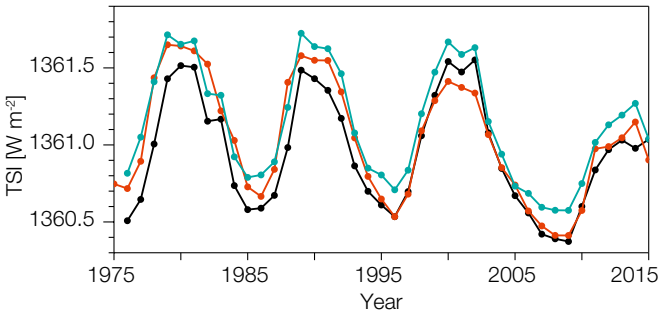

Figure 1. Evolution of the total solar irradiance (TSI) calculated with CHRONOS (red line) compared to the PMOD/WRC composite (black line) and TSI prepared in the framework of the CMIP6 project (light-blue line).

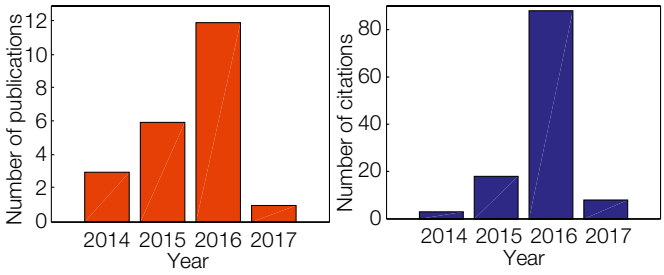

Figure 2. Total number of publications (left) and citations (right) relevant to FUPSOL-2. The data are from Thomson-Reuter's Web of Science.

Sub-project "C" was completed in 2015. The analysis of the sensitivity simulations with and without chemistry-climate interactions, which show the importance of interactive chemistry for climate change prediction, was published by Muthers at al. (2016). Sub-project "D" team continued to analyse the influence of solar activity on European weather. A time-series of daily weather types from MeteoSwiss was reconstructed back to 1763 (Schwander et al., 2017a). This novel weather type classification (CAP7) focusses on the Alpine region and Central Europe and is composed of 7 weather types.

The influence of the 11-year solar cycle on European climate was analysed by Schwander et al. (2017b), which showed that the combination of changes in the occurrence of weather types and within-type differences lead to colder temperatures over Central Europe under low phases of the 11-year solar activity. However, these results have not been found in our climate model results.

The general success of the FUPSOL-2 project is reflected by the number of publications and citations since 2014, illustrated in Figure 2.

References:

Arsenovic P., Damiani A., Rozanov E., Funke B., Peter T.: 2017, Evaluation of modeled NO_X and ozone responses to energetic particle precipitation in the South Hemispheric winter, GRL, submitted.

Muthers S., Raible C., Rozanov E., Stocker T.: 2016, Response of the AMOC to reduced solar radiation – the modulating role of atmospheric chemistry, Earth Syst. Dynam., 7, 877–892, doi: 10.5194/esd-7-877-2016.

Schwander M., Brönnimann S., Delaygue G., Rohrer M., Auchmann R., Brugnara Y.: 2017a, Reconstruction of central European daily weather types back to 1763, Int. J. Clim, doi: 10.1002/joc.4974.

Schwander M., Rohrer M., Brönnimann S., Malik A., 2017b, Influence of solar variability on the occurrence of Central European weather types from 1763 to 2009, Clim. Past Discuss., doi: 10.5194/cp-2017-8.

Revised Historical Solar Forcing Using Updated Model and Proxy Data

Tatiana Egorova, Eugene Rozanov, and Werner Schmutz in collaboration with MPS (Göttingen, Germany), University of Oulu (Finland), EAWAG (Switzerland), and IAC ETHZ (Switzerland)

In the framework of the FUPSOL-2 project, we reconstructed the spectral solar irradiance from 6000 BCE to the present day using the CHRONOS (Code for the High spectral ResolutiOn recoNstructiOn of Solar irradiance) code (Egorova et al., 2017), which uses the sunspot number to calculate the contribution from active regions and the solar modulation potential to obtain secular changes of the quiet Sun irradiance. CHRONOS improves the Shapiro et al. (2011) approach to obtain a more reliable reconstruction of the variability in spectral solar irradiance on decadal to millennial time-scales.

The long-term evolution of the irradiance of the quiet Sun, $I_{qs}(\lambda,t)$, is driven by slowly changing small-scale magnetic fields. We have to make sure that equal activity levels in the past and present agree and yield the same quiet Sun irradiance. Accordingly, changes of the quiet Sun irradiance can be described by the following equation:

$$I_{qs}(\lambda,t) = I_C(\lambda)+(I_B(\lambda)-I_C(\lambda)) \times (\phi_{1996} - \phi(t)) / (\phi_{1996} - \phi_{min})$$

where $\phi(t)$ is the time-evolving 22-year mean solar modulation potential, ϕ_{1996} is the solar modulation potential for the year 1996, and ϕ_{min} represents the smallest solar modulation potential measured during the considered time period (6000 BCE–2015). The parameter $I_B(\lambda)$ is the SSI which represents the case when solar activity is a minimum, and $I_C(\lambda)$ is the SSI for the current quiet Sun.

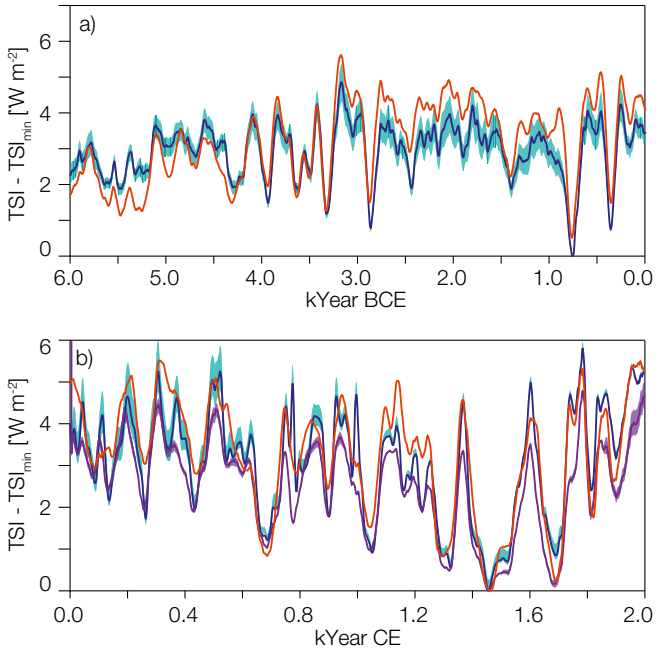

Figure 1. Deviation of TSI from its minimum, calculated with CHRONOS using PHI-MC17 (red), PHI-US16 (blue) and PHI-MU16 (violet) reconstructions of the solar modulation potential. Time-series were smoothed with a 100 and 11-year window for the upper and lower panels, respectively.

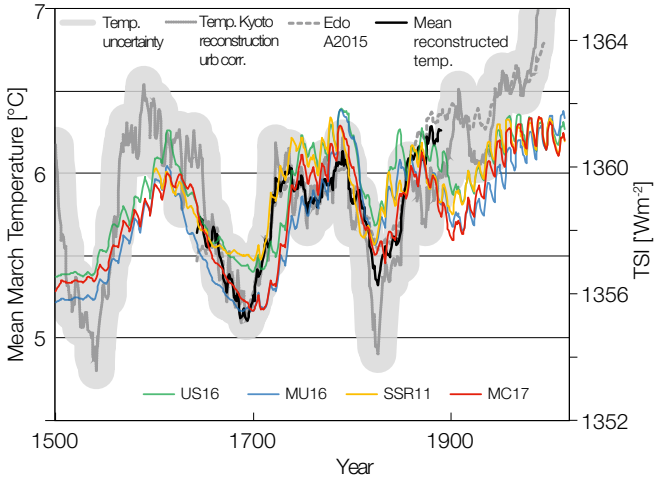

Figure 2. Mean of March temperatures at Kyoto and Edo (Tokyo), Japan (black line), reconstructed by Aono and Kazui (2008, dotted line) and Aono (2015, dashed line) compared to Total Solar Irradiance computed with CHRONOS using PHI-MC17 (red), PHI-US16 (green) and PHI-MU16 (blue) reconstructions of the solar modulation potential.

Figure 1 illustrates the TSI variability on millennial time-scales calculated with CHRONOS using three recently published solar modulation potential time-series. The BCE period is covered by PHI-MC17 (McCracken and Beer, personal communications) and PHI-US16 (Usoskin et al., 2016) datasets. The CE period is also covered by the PHI-MU16 data (Muscheler et al., 2016).

According to all three reconstructions, TSI reaches its minimum value around 1450 CE, while the maximum value (around 5.5 W m^{-2}) appears around 300 CE. Thereafter, all datasets exhibit a gradual decrease of the mean TSI level up to 1600 CE.

Figure 2 illustrates the TSI variability over the last 500 years in comparison with the mean of March temperatures in Kyoto and Edo (Tokyo). This comparison reveals a remarkably similar overall pattern and is highly indicative that historic terrestrial temperatures are influenced by variability in solar irradiance.

References:

Aono Y.: 2015, Int. J. Biometeorol. 59, 427, doi: 10.1007/s00484-014-0854-0.

Aono Y., Kazui K.: 2008, Int. J. Climatol. 28, 905, doi: 10.1002/joc.1594.

Egorova T. et al.: 2017, submitted to Astron. Astrophys.

Muscheler R. et al.: 2016, Sol. Phys., 291, 3025, doi: 10.1007/s11207-016-0969-z.

Shapiro A.I. et al.: 2011, Astron. Astrophys. 529, A67, doi: 10.1051/0004-6361/201016173.

Usoskin I. et al.: 2016, Astron. Astrophys., 587, A150, doi: 10.1051/0004-6361/2015272.

Evaluation of Modelled NO_Y and Ozone Responses to Energetic Particle Precipitation in the Southern Hemispheric Winter

Eugene Rozanov in collaboration with IAC ETHZ (Switzerland), CEReS (Chiba, Japan), and IAA (CSIC, Spain)

In the framework of the FUPSOL-2 project, we study the effect of auroral electrons on atmospheric chemistry. We show that during the geomagnetically active period most of the winter time reactive nitrogen oxides in the polar cap are coming from auroral electrons resulting in decrease in ozone. The ozone depletion is most prominent in mesosphere but can reach 15% in the stratosphere. Our results agree well with satellite observations.

Auroral electrons (energies <30 keV) precipitate continuously from Earth's magnetosphere. They penetrate Earth's atmosphere and deposit their energy in the thermosphere producing NO_X, which subsides in the down-welling branch of the overturning circulations affecting ozone at lower latitudes. Recent major advances in the parameterisation of auroral electrons for climate models has motivated us to investigate the extent of their contribution to odd-nitrogen production and ozone depletion.

We used the SOCOL3-MPIOM model which includes galactic cosmic rays, solar proton events and radiation belt electrons (30–300 keV). For the parameterisation of auroral electrons, we applied the semi-empirical model for NO_Y influx (Funke et al., 2016). Six simulations that cover the 2002–2010 period, were performed with all energetic particles (PAR) included and another six with the same model boundary conditions but without energetic particles (NOPAR).

The energetic particles increase mesospheric NO_X in austral winter during the geomagnetically active years (2002–2005) by 500 ppbv. Around 90% of the NO_X increase comes from auroral and 10% from radiation belt electrons at this altitude (Arsenovic et al., 2016). Ozone is severely depleted in the whole polar region above 100 hPa with a maximum in the mesosphere (500 ppbv) of which auroral electrons contribute about 60% towards ozone reduction.

The higher efficiency of radiation belt electrons in depleting ozone lies in the fact that they produce HO_X, which also destroys ozone at these altitudes. Ozone depletion in the stratosphere is around 450 ppbv (25%) of which auroral electrons contribute about 75% towards this reduction.

To validate the simulated ozone responses, we used ozone data for 2005–2010 from the Microwave Limb Sounder (MLS) observations. Figure 1 shows good agreement between the observed and modelled ozone anomaly pattern in both the mesosphere and stratosphere.

The model overestimates mesospheric ozone anomalies, but a good match is accomplished in the stratosphere. Ozone depletion of 15% is present in July and August, and reaches into the middle stratosphere. Since chemical signals coming from energetic particle precipitation can cause dynamical changes in the stratosphere that could affect regional climate, we recommend that energetic particle precipitation is included in climate models.

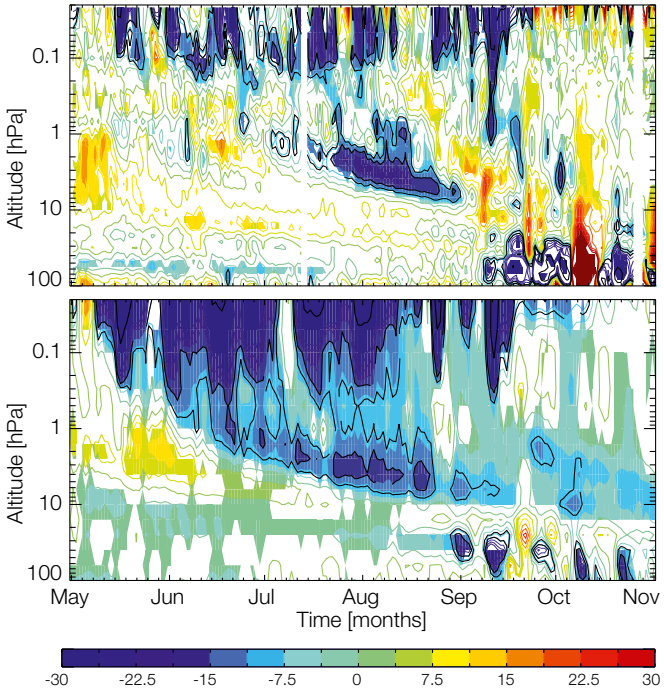

Figure 1. Mean ozone anomaly poleward of 70°S calculated as the difference of the year 2005 and the 2006–2010 average with respect to the 2005–2010 period. Upper panel), MLS observations. Lower panel), ensemble mean of PAR simulations. The colour scale highlights the changes in the middle stratosphere and mesosphere. Black lines highlight contours at -10%, -15% and -50%. Note that mesospheric ozone depletion reaches 80–90% during several strong solar proton events. Coloured regions are significant at the 95% confidence level (calculated using the Students t-test).

References:

Arsenovic P., Rozanov E., Stenke A., Funke B., Wissing J. M., Mursula K., Tummon F., Peter, T.: 2016, The influence of Middle Range Energy Electrons on atmospheric chemistry and regional climate, J. Atmos. Solar-Terrestrial Phys., 149, 180–190, doi: 10.1016/j.jastp.2016.04.008.

Funke B., López-puertas M., Stiller G.P., Versick S., Clarmann T. von: 2016, A semi-empirical model for mesospheric and stratospheric NO_Y produced by energetic particle precipitation, ACP, 16, 8667–8693, doi: 10.5194/acp-16-8667-2016.

Modelling of the Middle Atmosphere Response to 27-day Solar Irradiance Variability

Timofei Sukhodolov, Eugene Rozanov, William Ball, and Werner Schmutz in collaboration with IAC ETHZ (Switzerland)

We used a 1D Radiative Convective Photochemistry model (RCPM), a 3D Chemistry-Climate model (CCM) SOCOL v3.0, and the latest temperature re-analysis data and observations to study the influence of solar rotational variability on the Earth's middle atmosphere. For the first time, we showed a clear 3D modelled stratospheric temperature response which was obtained due to the adequate representation of radiative transfer modules in the model and due to a sufficient number of model realisations. We also examined the importance of other sources of daily variability in the middle atmosphere.

There have been many attempts to characterise the presence of the solar rotational signal in the Earth's atmosphere (Bossay et al., 2015). This could greatly contribute to an understanding of the solar UV influence on climate at longer timescales, namely the top-down mechanism starting in the middle atmosphere. However, this signal has remained highly uncertain in both models and observations. We also addressed this question, but first focussed our activity on upgrading our 3D chemistry-climate model (CCM) in terms of radiative transfer representation (Sukhodolov et al., 2014; 2016). An upgraded model and new computing facilities at IAC ETHZ have allowed us to perform more experiments with a higher horizontal resolution and accuracy.

We performed two 30-member 3-year long (2003–2005) ensemble modelling experiments with and without a rotational component in daily solar irradiance forcing. To illustrate the middle atmosphere response to 27-day SSI variability in the absence of any internally generated variability, we used a 1D model driven by the same irradiance forcing.

As shown in Figure 1, cross-correlation functions obtained from 3-D and 1D models agree well in terms of time lag. The correlations from CCM are lower than in the 1D model, but represent the highest and clearest values reported so far in the literature. The evident correlation also highlights the statistical significance of the calculated atmospheric sensitivities to the solar rotational forcing. In contrast, the temperature cross-correlation functions obtained from the re-analysis data and observations show a very weak signal.

Detailed analysis of individual ensemble members and longer time-series of re-analysis data allowed us to conclude that variability of the middle atmosphere is largely dominated by oscillations of the stratospheric polar vortices caused by natural changes in stratospheric wave-mean flow interactions. The effects of such oscillations on the tropical stratosphere are much larger in amplitude than the solar-induced changes, which highly complicates the derivation of the solar rotational signal from re-analysis data and observations, as they can be considered as the only one-model realisation which includes all internal variability of the atmospheric system.

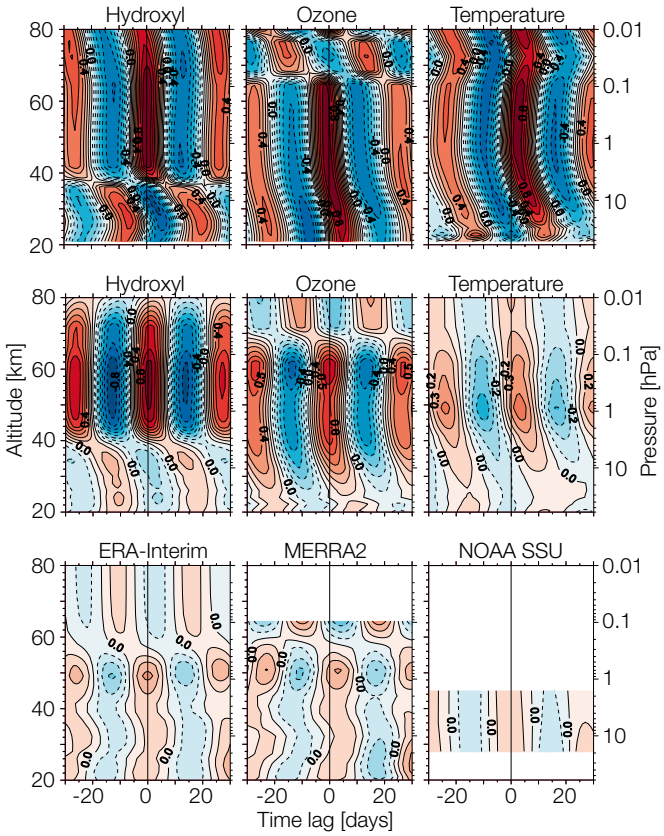

Figure 1. Cross-correlation functions of tropical hydroxyl, ozone, and temperature versus solar irradiance at 205 nm, from 1D RCPM and 3D CCM SOCOLv3 (ensemble mean) for the 2003–2005 period. Contour lines are plotted at 0.1 intervals where red (blue) represents positive (negative) correlations. The lower panel shows the same cross-correlations but from temperature re-analysis and observational data.

In the case of the model, a large number of model realisations allows the role of internal variations to be lessened, which are random in the model, thus increasing the signal-to-noise ratio of the 27-day variability component. These results have been recently published in the literature (dx.doi.org/10.1016/j.jastp.2016. 12.004).

References:

Bossay S. et al.: 2015, Atmos. Sol.-Terr. Phys., 130–131, 96–111, doi: 10.1016/j.jastp.2015.05.014.

Sukhodolov T. et al.: 2014, Evaluation of the ECHAM family radiation codes performance in the representation of the solar signal, Geosci. Model Dev., 7, 1–8, doi: 10.5194/gmd-7-1-2014.

Sukhodolov T. et al.: 2016, Evaluation of the simulated photolysis rates and their response to solar irradiance variability, J. Geophys. Res., 2015JD024277.

Volcanic Eruptions and Their Impact on Future Climate (VEC) Project: First Steps

Timofei Sukhodolov, Eugene Rozanov, William Ball, and Werner Schmutz in collaboration with IAC ETHZ (Switzerland)

Understanding of the future change in climate is a problem of utmost importance for the scientific community, society and policymakers. The large influence of powerful volcanic eruptions on climate was recognised long ago. Recently, it was suggested that small volcanic eruptions are also important for climate. However, projections of future climate change in the recent and up-coming IPCC reports do not take into account any effects from either infrequent, explosive or more-numerous small volcanic eruptions, rendering our knowledge of future climate incomplete. Our new VEC project aims to address this missing component in future climate change projections.

To achieve the project goals, we will make use of a new coupled atmosphere-ocean-aerosol-chemistry-climate model (AOACCM), which will provide a powerful tool to investigate interaction between sulphate aerosols, atmospheric chemistry, ocean dynamics and climate. We aim to prepare such a model by coupling our current chemistry-climate model (SOCOLv3, Stenke et al., 2013), SOCOLv3 with the sulphate aerosol module (SOCOL-AER, Sheng et al., 2015), and the Max Planck Institute Earth System Model (MPI-ESM, Giorgetta et al., 2013). Here we present the first steps of the project implementation, namely, the results of the installation and tests of MPI-ESM and the installation of emissions from smaller (non-major) volcanoes to SOCOL-AER.

The MPI-ESM model consists of: i) coupled general circulation models for the atmosphere, ECHAM6 (successor of ECHAM5 used in SOCOLv3), and ocean, MPIOM, and ii) the subsystem models for land and vegetation, JSBACH, and for marine biogeochemistry, HAMOCC5. The main benefit of the ECHAM6 dynamical core compared to ECHAM5 is the better scaleability, which will allow us to use the new model with a higher horizontal and vertical resolution. The fully coupled Earth system will also allow us to take many climate feedbacks into account. As an illustration of the new model advantages, Figure 1 shows an annual mean spatial distribution of dimethyl sulphide (DMS), an important source of sulphur in the atmosphere, which is now interactively calculated by the HAMOCC5 module of MPI-ESM and was previously prescribed in SOCOL-AER.

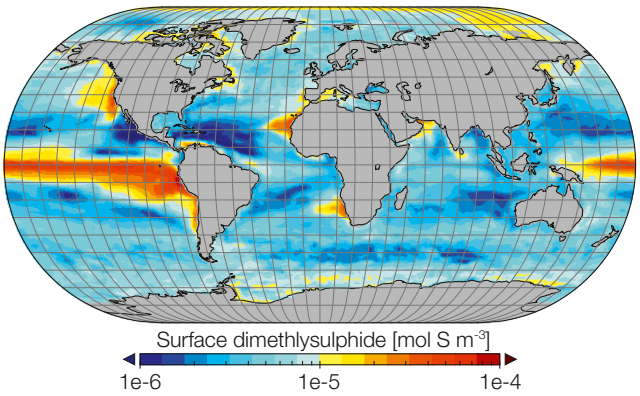

Figure 1. Annual mean surface DMS calculated by MPI-ESM for pre-industrial conditions.

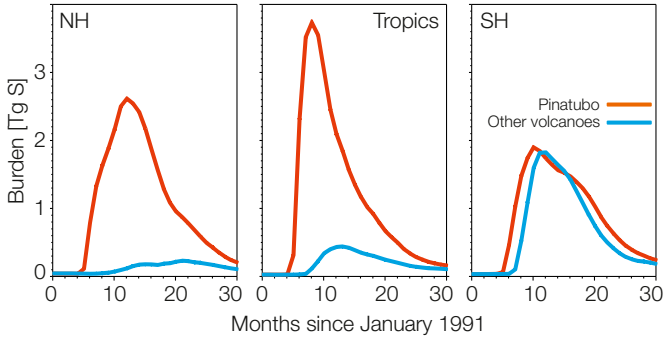

Figure 2. Evolution of the stratospheric burden of liquid sulphuric acid [S] aerosol in the Northern Hemisphere (NH), tropics, and the Southern Hemisphere (SH) calculated by SOCOL - AER for Pinatubo only (red) and all other eruptions without Pinatubo (blue).

The sulphate aerosol part of the model, developed in our group, is capable of explicitly calculating the sulphate aerosol properties and therefore treating different types of volcanic eruptions as well as other sources of sulphur containing species. This module did not previously take the temporal evolution of emissions from smaller volcanic eruptions into account. We now address this issue by preparing and installing new emissions based on a NASA SO_2 volcanic database. This provides information about location, amount of SO_2 released, volcanic cloud column height, and volcano elevation for 1979–2010 eruptions of all intensity including de-gassing eruptions.

Figure 2 shows the evolution of the stratospheric sulphur burden contained in liquid sulphate aerosols, calculated for the strong Pinatubo eruption and for all other weaker eruptions from newly installed emissions. As can be seen, SO_2 from additional volcanoes can significantly contribute to the stratospheric sulphur burden. In particular, the largest contribution is caused by the eruption of a high-latitude Hudson volcano, which is usually omitted when modelling the effects of Pinatubo by models with interactive sulphate aerosol modules. Further, we will combine the 1979–2010 SO_2 statistics with the 1950–2014 volcanic eruption intensity statistics from NGDC/NOAA to produce future scenarios of volcanic activity.

References:

Giorgetta M.A. et al.: 2013, JAMES, doi: 10.1002/jame.20038.

Sheng J.-X. et al.: 2015, J. Geophys. Res., 120, 256–276, doi: 10.1002/2014JD021985.

Stenke A. et al.: 2013, Geosci. Model Dev., 6(5), 1407–1427, doi: 10.5194/gmd-6-1407-2013.

Modelling of Sulphate Deposition for the CMIP6 VolMIP Activity

Eugene Rozanov and William Ball in collaboration with IAC ETHZ (Switzerland) and ICAS (Univ. Leeds, England)

We applied our chemistry-climate model with sulphate aerosol microphysics (CCMA) SOCOL-AER (Sheng et al., 2015) to calculate the sulphate deposition for background conditions as well as after the Mt. Tambora eruption in 1815. This activity is in the framework of the "Model Intercomparison Project on the climatic response to Volcanic forcing" (VolMIP). The comparison of the simulated deposition rates with observations shows that the model tends to overestimate observational data for background and post-Tambora experiments. The work to elucidate the problem is ongoing.

The evaluation of the impact of volcanic eruptions on climate requires information about aerosol surface area density (SAD) and spectral optical properties. For the satellite era this information can be obtained from different satellite observations. For the past, however, the main source of information about volcanic aerosol is measurements of sulphate in ice-cores, which can be converted to global aerosol distribution using appropriate model tools. Therefore, it is of great importance to evaluate model performances in the simulation of the sulphate deposition rates.

The eruption of Mt. Tambora in April 1815 was one of the most powerful volcanic eruptions in recent history. Its clear signature in the ice-core provides a good reference to study the simulation of aerosol deposition in climate models. The simulation of the background and post-Tambora sulphate deposition rates were performed in the VolMIP framework using five state-of-the-art aerosol-climate models including CCMA SOCOL-AER (Sheng et al., 2015).

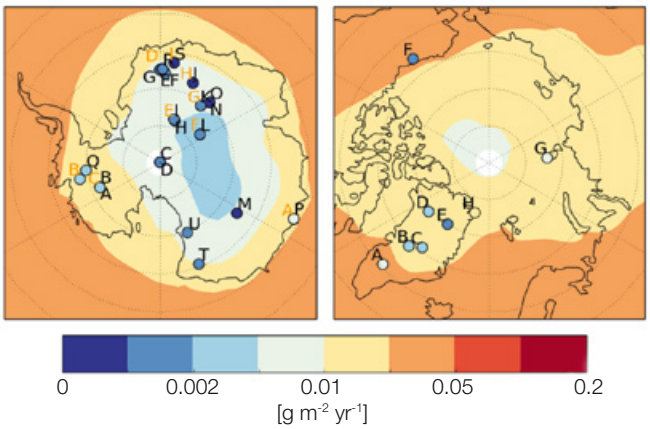

Figure 1. Simulated annual mean total (wet+dry) SO_4 deposition [g S m^{-2} y^{-1}] for Antarctica (left) and the Arctic (right) compared to pre-industrial ice core SO_4 fluxes (filled circles). Figure is adapted from Marshall et al. (2017).

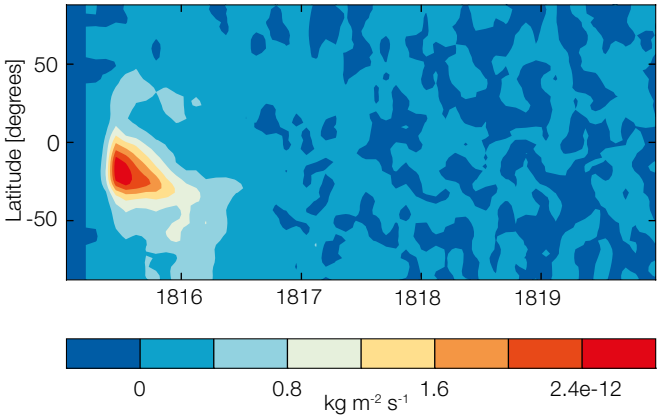

Figure 2. Simulated zonal mean volcanic SO_4 deposition [kg SO_4 km^{-2}] after the onset of the eruption (1 April 1815). Volcanic SO_4 deposition is calculated as the difference in total SO_4 deposition (wet + dry) between the perturbed and control simulations.

The comparison of the simulated background sulphate deposition rate with ice-core data is shown in Figure 1 for sites in Antarctica and Greenland. The model substantially (by up to 100%) overestimates sulphate deposition rates for both cases except for the one site in North Greenland, where the model and observations agree well.

The simulated aerosol deposition is shown in Figure 2. The major fraction of volcanic sulphur is eliminated one year after the eruption. Deposition occurs mostly in the tropical area and is more intense in Antarctica than in the Arctic. The latter feature is visible but not so pronounced in the latest analysis of ice-core data, which shows only about 20% more deposition in Antarctica. The simulated deposition intensity is overestimated and the pattern does not agree well with other model results. However, it should be noted that the difference between models is large (Marshal et al., 2017). The causes of large uncertainty in the simulation results can include microphysics and transport of the aerosol as well as the parameterisation of subgrid-scale deposition processes, which is the most complicated for ice-covered surfaces. The results illustrate the necessity to improve the representation of aerosols in the models with special attention to wet and dry deposition processes.

References:

Marshal L. et al.: 2017, Multi-model comparison of the volcanic sulfate deposition from the 1815 Mt. Tambora eruption, in preparation for Atmos. Chem. Phys.

Sheng J.-X., Weisenstein D.K., Luo B.-P., Rozanov E., Stenke A., Anet J., Bingemer H., Peter T.: 2015, Global atmospheric sulfur budget under volcanically quiescent conditions: Aerosol-chemistry-climate model predictions and validation, J. Geophys. Res. Atmos., 120, 256–276, doi:10.1002/2014JD021985.

Study to Determine Spectral Solar Irradiance and its Impact on the Middle Atmosphere (SIMA)

William Ball, Eugene Rozanov, and Werner Schmutz in collaboration with IAC ETHZ (Switzerland), Imperial College (England), BIRA (Belgium) and CNRS (France)

Project SIMA aims to use atmospheric measurements and 2D and 3D atmospheric and climate models to constrain spectral solar irradiance (SSI) variability. The consequence of constraining SSI will lead to a better understanding of the response of atmospheric chemistry and dynamics to the solar forcing.

Success of the project requires an accurate estimate of the solar cycle (SC) response in ozone observations, from which estimates of ozone changes from models allows (within a Bayesian framework) an extraction of the solar cycle changes that induce the ozone change seen in the observations (Work package 1, WP1). Our original aim was to use a set of recent ozone composites from which to extract the SC ozone changes.

However, we found that the use of multiple linear regression to estimate the SC ozone response led to very different SC changes estimated from four ozone composites that we considered (colours, Figure 1), and indeed, in decadal ozone trends. Thus, in order to determine a reliable SC response, we developed a procedure to correct the ozone composites and remove artefacts that were the cause of the different multiple linear regresion SC estimates. The approach uses particle filtering, a sequential Bayesian Monte Carlo estimator, and a procedure that can account for jumps and drifts. A major result is improved decadal trend estimates, as well as other additional results that are currently being prepared for publication. The major step forward for SIMA is a new ozone composite, free from artefacts that interfere with multiple linear regresion estimates of the SC (black line, Figure 1; see Ball et al., 2017).

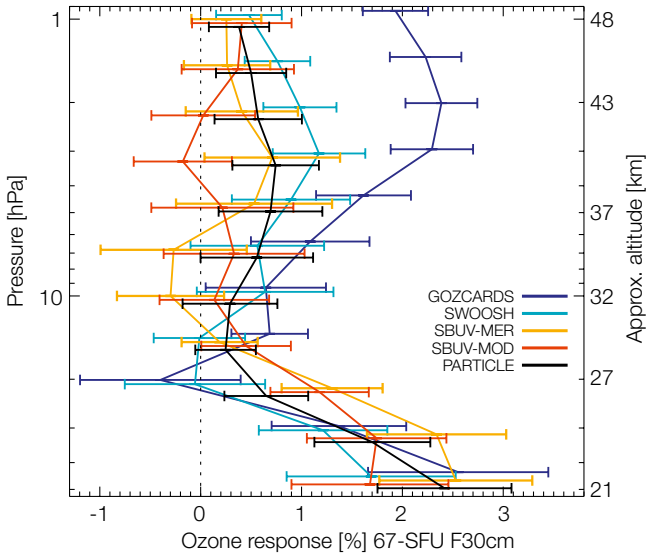

Figure 1. Equatorial (25°S–25°N) solar cycle change in ozone from four composites and the particle filter ozone composite (Ball et al., 2017) using multiple linear regression to extract the signal. Error bars are uncertainties at the 95% level.

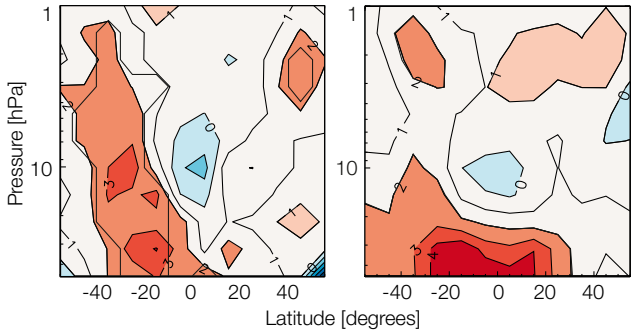

Figure 2. The solar cycle ozone response extracted from the particle filter ozone composite (Ball et al., 2017) using dynamical linear modelling (left) and multiple linear regression (right). Contours are in 1%-levels; red represents positive changes, and blue negative; crosses are not statistically significant at the 95% level.

Our work has also determined that multiple linear regresion does not robustly estimate SC changes, due to the large unaccounted for variance, and the short observation period available. We find that the use of dynamical linear modelling (DLM) improves the robustness of estimates (Figure 2), but the lack of a SC signal in the tropical upper stratosphere is not fully understood. Further additional considerations are therefore required. Despite the additional work to correct the ozone composites and understand the lack of a solar signal in the tropics, the next step to integrate the temperature solar cycle signal with ozone is nearly complete: the temperature response has been extracted, the Bayesian method expanded to include temperature with ozone, and all required 2D modelling runs completed. Upon finalising the ozone signal, this milestone will be completed (Ball et al., in prep.).

Following a meeting in Brussels between collaborators at PMOD/WRC, BIRA and CNRS to progress simultaneous work needed to complete the remainder of the project, by constraining coherent SC changes at different wavelengths, a clear methodology has been determined of how to estimate wavelength dependent priors that will constrain SSI changes. The implementation is currently ongoing. In addition, work on integrating these spectral variation constraints with H_2O and OH in a 2D model has commenced. A 3D model will later be used that also includes realistic dynamics, whereupon all information can then be combined to reconstruct solar irradiance variations from atmospheric observations, which is the ultimate goal of the project.

References: Ball W.T. et al.: 2017, Reconciling differences in stratospheric ozone composites, ACPD, doi: 10.5194/acp-2017-142, in review.

Ball W.T. et al.: in prep., Estimate of ultraviolet solar cycle changes from stratospheric ozone and temperature observations.

Mt. Pinatubo Eruption Effects Simulated with CCMI and CMIP6 Stratospheric Aerosol Datasets

Eugene Rozanov and Timofei Sukhodolov in collaboration with Bodeker Sci. (New Zealand) and IAC ETHZ (Switzerland)

In the framework of the Chemistry-Climate Model Initiative (CCMI) project, we study the effects of the Mt. Pinatubo eruption on the stratospheric temperature and ozone layer and their dependence on the applied aerosol data set. We conducted two experiments with our chemistry-climate model (CCM) SOCOL v3 (Stenke et al., 2013) driven by two aerosol data sets recommended for the international model inter-comparison campaigns. We show that the temperature response obtained with the "Coupled Model Intercomparison Project phase 6" (CMIP6) datasets agrees better with the satellite observations, while the ozone response is not sensitive to the choice of the aerosol data set.

In order to simulate the impacts of volcanic eruptions on the atmosphere, chemistry-climate models need monthly, spatially resolved values of aerosol surface area density (SAD) and spectral optical properties. SAD is necessary to calculate heterogeneous reaction rates, and optical properties are used to calculate photolysis and heating rates in the atmosphere. For phase 1 of the Chemistry-Climate Model Initiative (CCMI-1) project, a stratospheric aerosol dataset was compiled from SAGE-II satellite data by applying the so-called SAGE-4λ algorithm.

Satellite datasets usually ignore measurements below 15 km to reduce potential interference from clouds, which is problematic since a significant amount of aerosol is contained between the tropopause and 15 km. To correct this, a new stratospheric aerosol dataset has been compiled for phase 6 of the Coupled Model Intercomparison Project (CMIP6). This dataset was compiled from multiple satellite sources using the SAGE-3λ algorithm, and corrected data from optical particle counters was applied below 20 km. Overall, aerosol radiative properties and stratospheric aerosol surface area densities are improved in the CMIP6 stratospheric aerosol dataset, and smaller particles are included in the lower stratosphere.

We performed simulations of the recent past using our chemistry-climate model (CCM) SOCOL v3 (Stenke et al., 2013) driven by the CCMI and CMIP6 stratospheric aerosol datasets to evaluate the effects of the Mt. Pinatubo eruption. Figure 1 illustrates time-series of temperature and ozone anomalies at 30 hPa averaged over the 15°N–15°S zonal belt. While stratospheric warming and ozone loss is overestimated by approximately 3 K and 0.2 ppmv, respectively, in our simulations with CCMI stratospheric aerosol, less heating occurs following the eruption in our simulations with CMIP6 stratospheric aerosol because of radiative scattering and cooling effects induced by small particles in the lower stratosphere. As a result, simulated temperatures in our CMIP6 simulations agree favourably with observational data.

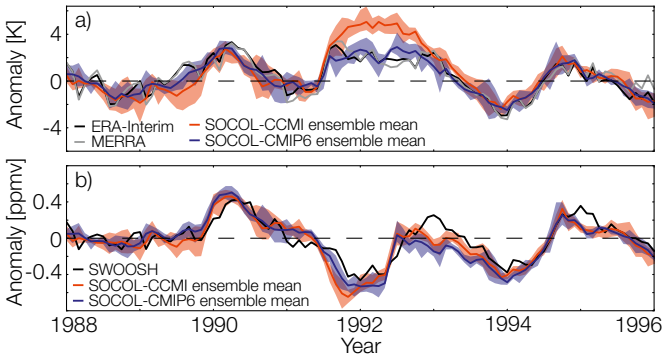

Figure 1. Time-series of: a) temperature, and b) ozone anomalies at 30 hPa, 15°N–15°S. The thick red and blue lines denote the ensemble mean of the SOCOL simulations using the CCMI and CMIP6 stratospheric aerosol datasets, respectively. The shaded areas either side denote the range of simulated anomalies within each ensemble.

Less heating following the eruption in the CMIP6 simulations leads to a weaker intensity of the catalytical ozone oxidation cycles and reduces ozone depletion by the heterogeneous chemistry on/in sulphate aerosols. Moreover, less warming also means that the rate of tropical upwelling does not strengthen as much as it does in the simulations with CCMI aerosol, and dynamical uplift of ozone does not occur to the same extent leading again to a reduced ozone loss. However, the shift in the aerosol size distribution to smaller particles increases surface area density, and intensifies the heterogeneous reactions and chlorine activation leading to enhanced ozone depletion. The combined effect of these processes results in good agreement of the simulated and observed ozone depletion obtained with the CCMI dataset.

Our results help to resolve a long-standing problem with the overestimation of the temperature response to volcanic aerosol after the Pinatubo eruption and support the use of the CMIP6 stratospheric aerosol dataset in future global model intercomparison projects. The results of this study will be presented and discussed in greater detail in a forthcoming publication by Revell et al. (2017).

References: Revell L. et al.: 2017, Chemistry-climate model simulations of the Mt. Pinatubo eruption using CCMI and CMIP6 stratospheric aerosol datasets, in preparation for Atmos. Chem. Phys.

Stenke A., Schraner M., Rozanov E., Egorova T., Luo B., Peter T.: 2013, The SOCOL version 3.0 chemistry-climate model: Description, evaluation, and implications from an advanced transport algorithm, Geosci. Model Dev., 6, 1407–1427, doi: 10.5194/gmd-6-1407-2013.

Solar Spectral Irradiance Reconstruction Data for the Paleoclimate Model Intercomparison Project (PMIP)

Tatiana Egorova, Eugene Rozanov, and Werner Schmutz in collaboration with MPS (Göttingen, Germany)

The relative contributions of the various forcing and feedback terms to global and regional climate change are poorly understood. Some studies have emphasised the contribution of solar irradiance variability to the cooling during the Little Ice Age, others have suggested that volcanic aerosols and greenhouse gases had a dominant role. Also, the importance of orbital variations, and ocean and sea ice feedbacks has been highlighted in the literature. To quantify climate forcing and feedbacks over the last Millennium, the Paleoclimate Model Intercomparison Project (PMIP) was organised to perform transit climate model simulations driven by boundary conditions of the last millennium. The task for PMOD/WRC was to provide a solar variation reconstruction for the 850–1850 period.

The reconstruction of the spectral solar irradiance (SSI) for the PMIP activity (Jungclaus et al., 2016) is based on the Shapiro et al. (2011) approach. The spectral solar irradiance was calculated with the Code for Solar Irradiance (COSI) solar radiation code using solar atmosphere structure models representative of different regions or components on the Sun. These components are the quiet Sun, faculae, active network, and sunspots. Filling factors are calculated using the sunspot number (SSN) instead of high resolution solar magnetograms, as detailed information about the solar magnetic field is not available for the investigation period.

We applied several improvements to the original approach of Shapiro et al. (2011). For instance, smoothed SSN time-series from Usoskin et al. (2016) were used instead of the solar modulation potential, and a relative scaling to avoid problems with the absolute calibration of the time series was applied.

Finally, we followed conclusions by Judge et al. (2012) based on their re-analysis of sub-mm data from the James Clerk Maxwell telescope, and also replaced the model "A" from Fontenla et al. (1999) used by Shapiro et al. (2011) for the quiet Sun irradiance during the minimum solar activity state by a model "B". We constructed model "B" using the requirement formulated by Judge et al. (2012) that the minimum model of the quiet sun should produce the irradiance at an intermediate level between the models "A" and "C".

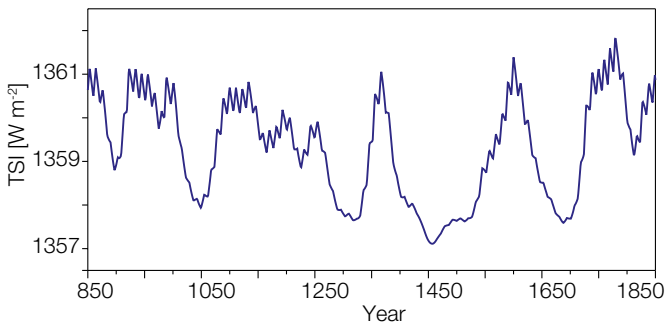

Figure 1. Reconstructed evolution of TSI from 850 to 1850.

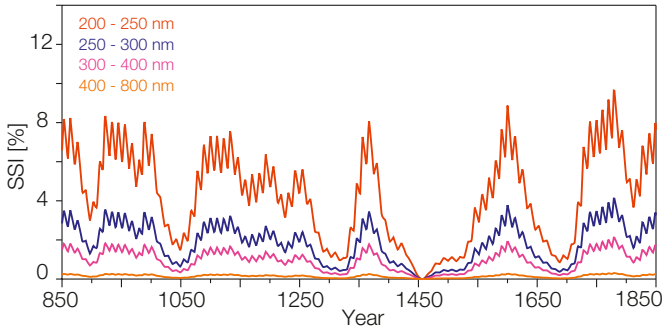

Figure 2. Reconstructed evolution of the spectral solar irradiance from 850 until 1850 integrated over several spectral intervals relative to the minimum (%).

The evolution of TSI during the investigation period is shown in Figure 1. TSI changes over a range of up to 4 Wm^{-2}, which is slightly lower than in Shapiro et al. (2011) because the present reconstruction is based on model "B" instead of "A" for the quietest solar states. The same is true of the SSI variability shown in Figure 2 for several spectral intervals.

References:

Fontenla J. et al.: 1999, Calculation of solar irradiances. I. Synthesis of the solar spectrum, Astrophys. J., 518, 1, 480–499, doi: 10.1086/307258.

Judge P. et al.: 2012, Confronting a solar irradiance reconstruction with solar and stellar data. Astron. Astrophys. 544, A88, 6, 2012, doi: 10.1051/0004-6361/201218903.

Jungclaus et al.: 2016, The PMIP4 contribution to CMIP6 - Part 3: the Last Millennium, Scientific objective and experimental design for the PMIP4 past 1000 simulations, Geosci. Model Dev. Discuss., doi: 10.5194/gmd-2016-278.

Shapiro A.I. et al.: 2011, A new approach to long-term reconstruction of the solar irradiance leads to large historical solar forcing, Astron. Astrophys. 529, A67, doi: 10.1051/0004-6361/201016173.

Usoskin I. et al.: 2016, Solar activity during the Holocene: the Hallstatt cycle and its consequence for grand minima and maxim. Astron. Astrophys., 587, A150, doi: 10.1051/0004-6361/201527295.

High Resolution Extraterrestrial Solar Spectrum Determined from Ground-Based Measurements of Direct Solar Irradiance

Julian Gröbner, Luca Egli, and Gregor Hülsen in collaboration with PTB Braunschweig (Germany)

A high resolution extra-terrestrial (ET) solar spectrum was determined from ground-based measurements of direct solar irradiance for the 300 – 500 nm wavelength range. The retrieved solar ET spectrum has an expanded uncertainty of 2% between 305 nm to 500 nm, providing a benchmark dataset for validating space-based measurements of solar irradiance in this wavelength range.

In this study, we present ground-based direct spectral solar irradiance measurements obtained with the transportable reference double monochromator spectroradiometer QASUME (Hülsen et al., 2016) and a high resolution Fourier Transform Spectrometer (FTS) over the 300 – 500 nm wavelength range. A high resolution absolute ET solar spectrum is then derived by applying the Langley-plot technique to the measurements of each instrument before combining them to a single solar spectrum.

The measurements were performed at the Izaña Atmospheric Observatory (IZO) located on Tenerife, (Canary Islands, Spain) from 12–25 September 2016. IZO is a high mountain station at an elevation of 2373 m.a.s.l. above a strong subtropical temperature inversion layer, which acts as a natural barrier for local pollution and low-level clouds.

Direct solar irradiance measurements were performed from 14–24 September 2016. The ET solar spectrum was retrieved from the measurements by applying the Langley-Plot method to individual half-days in which there were cloud-free conditions.

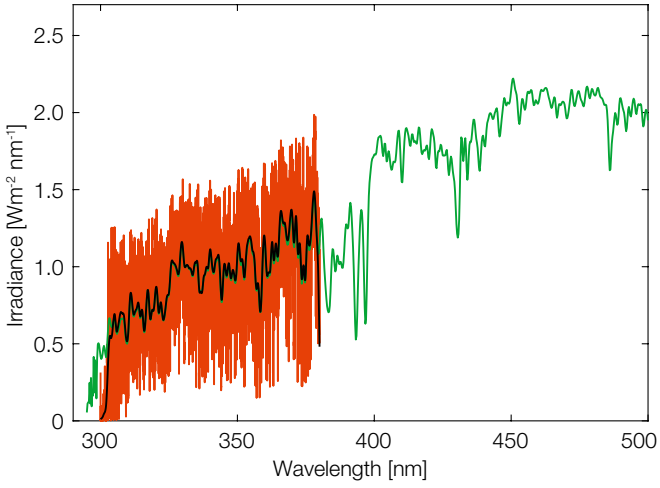

Figure 1. Solar ET spectra derived from QASUME (green) and FTS measurements (red). The black curve represents the FTS ET spectrum convolved with the QASUME slit function.

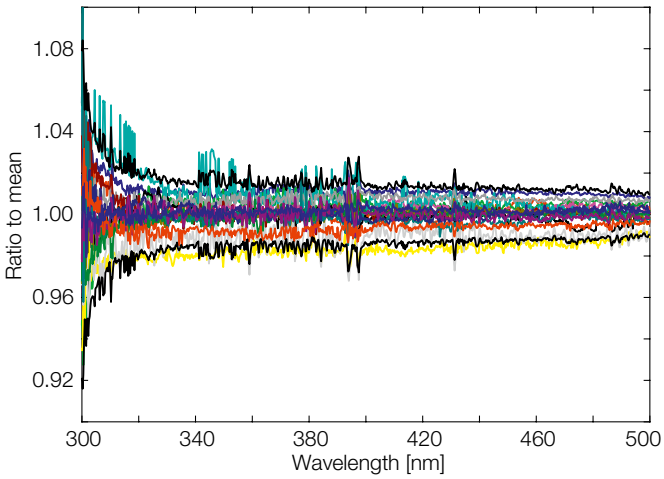

Figure 2. Ratio of the 17 solar ET spectra retrieved from QASUME measurements. The black curves represent the standard deviation of the measurements multiplied by two.

In total, 17 half-days are available from QASUME to derive a solar ET spectrum. Figure 1 shows the ratio of all 17 solar ET spectra to their average. The variability of the retrieved solar ET spectra is shown in Figure 1 as the thick black line and represents twice the standard deviation σ of the measurements. The variability originates both from the uncertainty of the measurement and instability of atmospheric conditions which is considered to be uncorrelated in-between successive days.

The resulting relative expanded uncertainty U of the average QASUME solar ET spectrum ($U = \sigma/\sqrt{N}$, $N = 17$, $k = 2$, assuming a 95% coverage probability) is less than 2% between 305 nm and 500 nm, and increases to 3% at 300 nm. The same procedure was applied to the FTS measurements to derive a solar ET spectrum. In the case of the FTS, measurements from 20– 22 September with a spectral resolution of 0.025 nm were used. Figure 2 shows the solar ET spectrum derived from QASUME, the high resolution FTS solar spectrum, and the FTS solar spectrum convolved with the QASUME slit function.

This work was supported by the European Metrology Research Programme (EMRP) within the joint research project EMRP ENV59 “Traceability for atmospheric total column ozone.” EMRP is jointly funded by the EMRP participating countries within EURAMET and the European Union. The solar spectrum is freely available at ftp.pmodwrc.ch/pub/people/julian.groebner/QASUMEFTS.dat.

References: Hülsen G., Gröbner J., Nevas S., Sperfeld P., Egli L., Porrovecchio G., Smid M.: 2016, Traceability of solar UV measurements using the QASUME reference spectroradiometer, Appl. Opt. 55, 7265–7275, 2016.

Sky Brightness Temperature and Fractional Cloud Cover Using an All-Sky Infrared Cloud Camera

Julian Gröbner and Christine Aebi

The Infrared Cloud Camera (IRCCAM) measures the thermal infrared radiation emitted from the atmosphere in the 8–14 µm wavelength range. The fractional cloud cover is retrieved from the sky images by comparison to a clear-sky model of the atmosphere. The comparison to a visible clear-sky camera has shown that the two systems agree to within 1 octa cloud cover in more than 70% of cases.

The IRCCAM consists of a commercial infrared camera with a microbolometer detector array of 640 x 480 pixels. The camera looks down onto a convex gold-plated mirror which images the upper hemisphere on the detector. The camera was calibrated using the blackbody of the Infrared Section of the World Calibration Center at PMOD/WRC with a resulting calibration uncertainty of ±1 K. The resulting images are corrected for the distortion resulting from the imaging mirror and are then calibrated. An example of a brightness temperature map of the upper hemisphere is shown on the right of Figure 1 for an image taken at PMOD/WRC on 3 July 2016.

The consistency of the temperature calibration can be assessed by comparing the brightness temperature at the horizon with the air temperature measured at PMOD/WRC. Both temperatures are expected to be nearly equal (small differences arise due to the difference between a point temperature measurement and the averaged atmospheric emission temperature). As can be seen in Figure 2, the brightness temperatures measured by the IRCCAM, averaged over the 89–90° zenith angle range, agree well with the daily variability of the air temperature measured at PMOD/WRC at a 2 m screen-level height. When analysing the period from April to October 2016, the average difference between the IRCCAM and the ambient air temperature is -0.6 K with a standard deviation of 2 K.

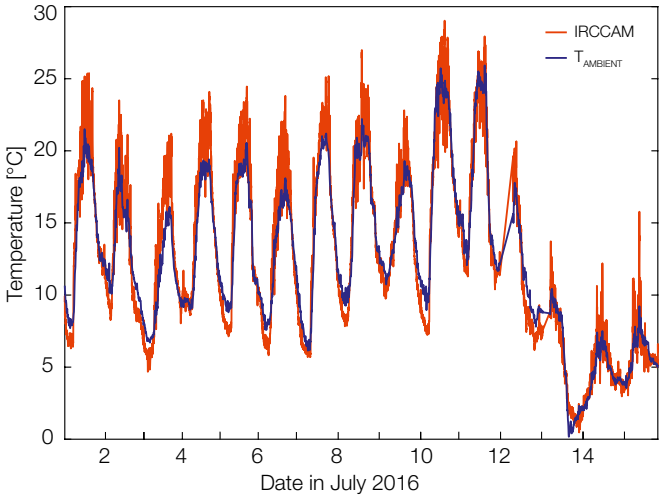

Figure 2. Air temperature (blue curve) measured at a 2 m screen-level height and the horizon brightness temperature measured by the IRCCAM for the period 1–15 July 2016.

The sky brightness temperature images can also be analysed with respect to a clear-sky background obtained from a look-up table based on radiative transfer calculations to retrieve the fractional cloud cover. A clear-sky background image map is generated for every single sky brightness image using the surface air temperature and relative humidity measured at PMOD/WRC.

The middle panel in Figure 1 shows the fractional cloud cover observed by the algorithm and on the left the corresponding image from a visible sky camera. The cloud fraction derived from the visible camera was compared to the cloud fraction derived from the IRCCAM for the period from January to October 2016. Of the 123,307 coincident images obtained, about 65% and 85% agreed to within a cloud cover of 1 and 2 octas, respectively. Only 10% showed differences larger than 3 octas.

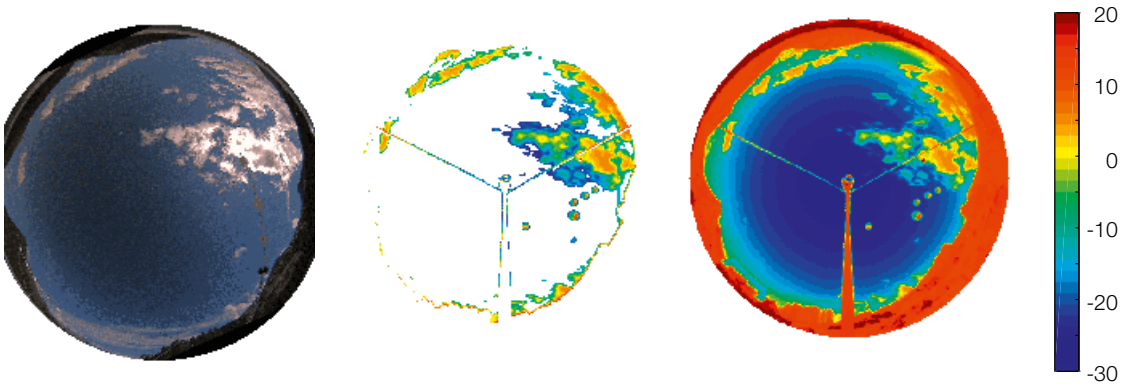

Figure 1. Sky image from 3 July 2016 showing: left) an image taken with a visible sky camera, middle) clouds detected by the infrared camera, and right) the sky brightness temperature map. The colours in the two right-hand pictures represent the sky temperatures [°C] as shown in the colour-bar.

Climatology of Cloud Radiative Effect, Cloud Fraction and Cloud Type at two Stations in Switzerland

Christine Aebi and Julian Gröbner in collaboration with University of Bern (Switzerland) and MeteoSwiss (Switzerland)

In the framework of the project "A comprehensive radiation flux assessment (CRUX)", the role of clouds on the surface radiation budget is analysed. A climatology of cloud fraction, cloud type and cloud radiative effect has been calculated using hemispherical sky cameras.

The climatology of cloud fraction, cloud type and cloud radiative effect (CRE) has been calculated for a time period of 3–4 years at Davos and Payerne. The CRE is separately calculated for the short-wave (SW; 0.3–3 µm) and long-wave (LW; 3–100 µm) radiation range. In our study, the CRE is calculated as the difference of a measurement value minus a clear-sky model value for the same atmospheric conditions. The cloud fraction and the cloud type are retrieved from images taken by visible all-sky cameras installed at the two aforementioned stations. The characterised cloud classes are stratocumulus (sc), cumulus (cu), stratus-altostratus (st-as), cumulonimbus-nimbostratus (cn-ns), cirrocumulus-altocumulus (cc-ac) and cirrus-cirrostratus (ci-cs). Radiation data are measured with pyranometers for the SW and pyrgeometers for the LW. The clear-sky model for SW is a look-up table based on LibRadtran with measured input parameters (solar zenith angle, total ozone content, integrated water vapour (IWV) and aerosols). The clear-sky model for LW is an empirical model using measurements of water vapour and surface temperature with a climatology of the atmospheric temperature profile.

March and December are the months with the greatest frequency of cloud-free cases at Davos, whereas this occurs more often in the summer half-year at Payerne. During cloudy periods, the st-as cloud class occurs most often at Davos (in 35% of the studied cases) while sc occurs most often at Payerne (in 29% of cases).

Figure 1 shows a non-linear increase in the long-wave cloud radiative effect (LCE) with increasing fractional cloud coverage for the cumulus clouds in Davos. This non-linear increase is also observed for other cumulus-type cloud classes, but cannot be explained at present. The LCE values for low-level clouds (sc, cu, st-as, cn-ns) and 8 octas cloud coverage are between 58

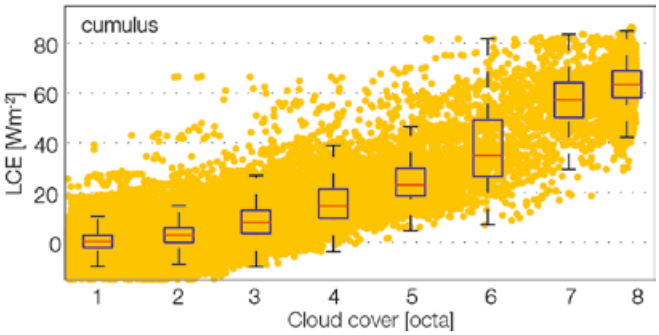

Figure 1. Dependence of LCE on cloud coverage at Davos for the time period from 7 Aug 2013 to 31 Oct 2016, and cumulus. Data points (yellow dots) are shown as well as box plots per octa with the median (red line), the interquartile range (blue box) and spread without outliers.

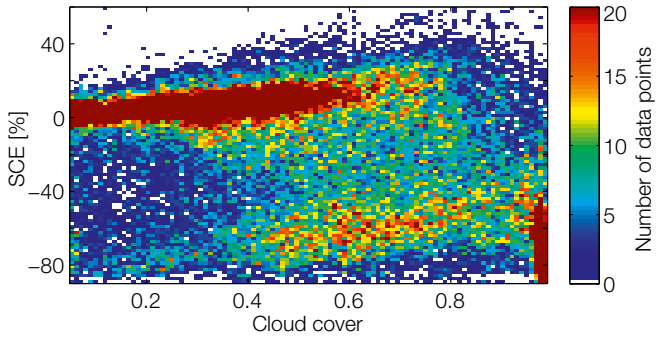

Figure 2. The density distribution of the dependence of SCE on cloud coverage at Davos for mid-level clouds (cc-ac). The density colour distribution represents the number of data points.

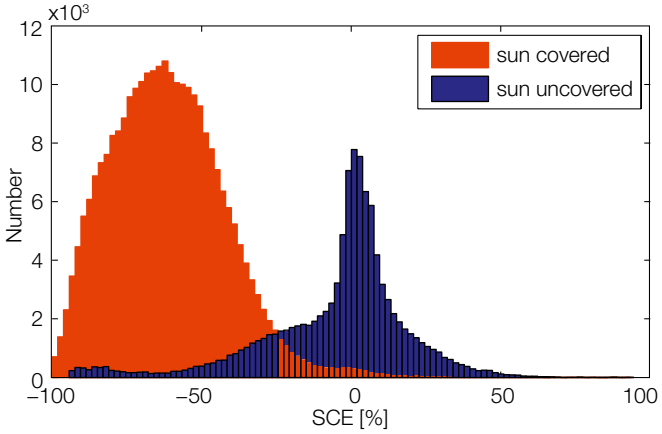

Figure 3. The density distribution of the dependence of SCE on cloud coverage at Davos for mid-level clouds (cc-ac). The density colour distribution represents the number of data points.

and 72 Wm^{-2} with the highest values for cn-ns. The LCE values for the mid-level cc-ac cloud class are clearly lower. There is a difference in the LCE between the two stations ranging from 7 to 25 Wm^{-2}. The influence of cloud base height and IWV on LCE has been analysed.

Figure 2 shows the density distribution of the dependence of the short-wave cloud radiative effect (SCE) on cloud coverage at Davos for mid-level cc-ac clouds. There are two groups of the relative SCE values - one around 0% and the other around -60 to -70 Wm^{-2}. These two groups can be explained by the fact that the sun is either covered or uncovered by a cloud (Figure 3).

Figure 3 shows a histogram of the SCE for low-level clouds in Davos. The red histogram shows the distribution of SCE values when the sun is directly covered by a cloud, and the blue one when the sun is uncovered. In 14% and 8% of the cloud cases in Davos and Payerne, respectively, a so-called cloud radiative enhancement has been detected. A cloud radiative enhancement is defined as a minimum SCE value of +5%.

References: Aebi C. et al.: Time-series of cloud radiative effect, cloud fraction and cloud type at two stations in Switzerland using hemispherical sky cameras, to be submitted.

The Arosa-Davos Total Column Ozone Intercomparison

Luca Egli and Julian Gröbner in collaboration with MeteoSwiss

To evaluate the spatial dependency of total ozone column observations and in view of a potential transfer of the long-term ozone monitoring time-series of MeteoSwiss from LKO Arosa to PMOD/WRC at Davos, simultaneous Brewer ozone measurements have been performed since 2011. The comparison reveals that on most days of the year the ozone measurements in Davos are in good agreement with observations in Arosa. On some specific days, a small time-lag of the diurnal evolution of ozone is observed.

To ensure the long-term ozone monitoring activities in Switzerland and to develop adequate support to continue the historical Dobson and Brewer series initiated at the Lichtklimatisches Observatorium (LKO) in Arosa, MeteoSwiss has initiated a strategy of rapprochement between the LKO and the PMOD/WRC. The objective is to compare total column ozone measurements performed at LKO Arosa and PMOD/WRC, which are only 13 km apart, with a view to the eventual transfer of ozone monitoring activities to PMOD/WRC. In order to achieve this objective, a multi-year project was initiated in 2011. One Brewer spectrophotometer (#072) [WMO, 2013] from the Arosa triad was moved to PMOD/WRC in 2011, with some interruptions due to re-calibration at LKO. Preliminary results have been presented at international conferences and have shown good agreement of the Brewer instruments to within about ±1% in total column ozone between both stations.

In January 2016, an automatic Dobson instrument (D101) [WMO, 2013] was transferred to the measurement site in Davos (Figure 1) in order to evaluate the agreement with ozone retrieval, based on a different instrument than the Brewer.

An example of daily total column ozone measurements from the two Brewer spectrophotometers located at PMOD/WRC (Br#072 and Br#163), and the Brewers still stationed at LKO (Br#040 and Br#156) are displayed in Figure 2, indicating good agreement between the four instruments and both locations. This is observed on most days. However, on a few days of the year, TOC observed in Arosa shows a small time-lag in its diurnal development. Figure 3 shows an example day, where the ozone peak occurs about 1 hour earlier in Arosa than in Davos. This time-lag highlights the large-scale stratospheric transportation processes of the trace gas ozone.

Figure 1. Picture of the measurement site at PMOD/WRC with the Dobson container on the left and the Brewer #072 on the right.

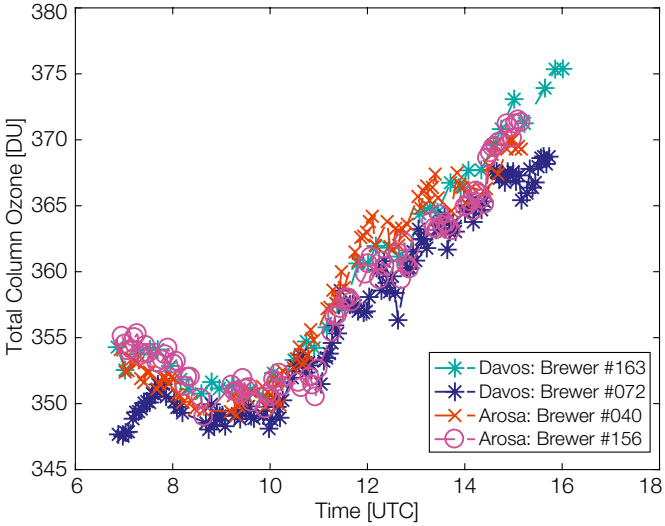

Figure 2. Comparison between four Brewers located in Davos and Arosa on 22 March 2016.

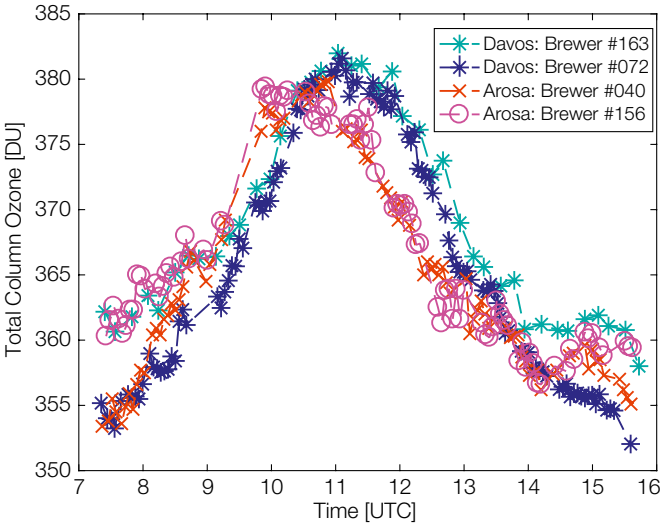

Figure 3. Observation of a time-lag between daily peak ozone observed in Arosa and Davos.

The impact of such specific events on ozone climatology in terms of monthly or yearly averages, and the corresponding ozone trend analysis should be further investigated. A decision on the eventual transfer of the monitoring activities of LKO Arosa to PMOD/WRC is scheduled for 2017, and will be based on a rigorous scientific evaluation of the measurement results in concert with the international scientific ozone community.

References: World Meteorological Organization (WMO): 2013, Comparison of total ozone measurements of Dobson and Brewer spectrophotometers and recommended transfer function, Global Ozone Res. Monit. Proj. Rep. 149, Geneva, Switzerland.

Uncertainty Calculations of Total Column Ozone Retrievals from Spectral Direct Irradiance Measurements

Luca Egli and Julian Gröbner in collaboration with Aalto University (Finland)

In the framework of the European ATMOZ EMRP project, different methods and software tools for calculating the overall uncertainty budget for total ozone column retrieval are investigated. This research activity studies the total uncertainty budget with Monte-Carlo based ensemble runs applied to multi-spectral UV measurements from two different PMOD/WRC instruments. The instruments for direct UV radiation measurements were operated during the first ATMOZ field campaign at the Izaña atmospheric observatory, Tenerife, Spain.

The European EMRP project ATMOZ "Traceability for atmospheric total column ozone" aims to evaluate the overall uncertainty of total column ozone (TOC) from different instruments which measure direct solar irradiance such as Brewers, Dobsons or from multispectral measurements with double monochromators or array spectroradiometers, as operated at the WCC-UV section of the WRC at PMOD/WRC. Direct solar spectra used for this TOC uncertainty study were measured at the first ATMOZ field campaign on 17 September 2016 at the Izaña atmospheric observatory on Tenerife, Spain. In order to assess the overall uncertainty budget for multispectral TOC retrieval, two instruments were selected:

1. The QASUME double monochromator based scanning spectroradiometer, which is the portable world reference for global UV radiation operated by PMOD/WRC and which was also equipped with a specially designed collimator.

2. The AVODOR system consisting of a commercially available array spectroradiometer, assembled by PMOD/WRC with direct optics connected through a fibre and temperature stabilised weather-proofed housing.

TOC from multispectral measurements were retrieved according to the method of Huber et al. (1995). The algorithm basically derives TOC by a linear least square fit model to the measured direct solar spectra, based on the Beer-Lambert law. The overall uncertainty of TOC was calculated by Monte-Carlo ensemble runs, randomly varying the spectra and the different input parameters of the retrieval model within the uncertainty of these parameters. Random variation means that a Gaussian distribution with the standard deviation (standard uncertainty) of the known uncertainty was generated and then randomly applied to each input spectrum. The standard deviation of the Gaussian distribution was selected as follows: i) QASUME: 1% for the full spectrum and 0.01 nm for the wavelength shift, according to Hülsen et al. (2016), and ii) AVODOR: 5% for the full spectrum and also 0.01 nm for the wavelength shift, according to laboratory measurements in Izaña.

The input parameters for the atmospheric model were also randomly varied within their expected uncertainties. For the effective ozone temperature, the values were randomly selected from a uniform distribution between 223 and 232 K. The extra-terrestrial spectrum was varied with a 3% standard deviation having a Gaussian distribution, while both ozone cross-sections were varied with Gaussian white noise having a standard deviation of 2.5%. The variation of all parameters was applied at the same time for all 600 runs for each spectrum, retrieval model parameter, and for the cross-sections. The overall uncertainty was finally given as the standard deviation of all ensemble runs and both cross-sections.

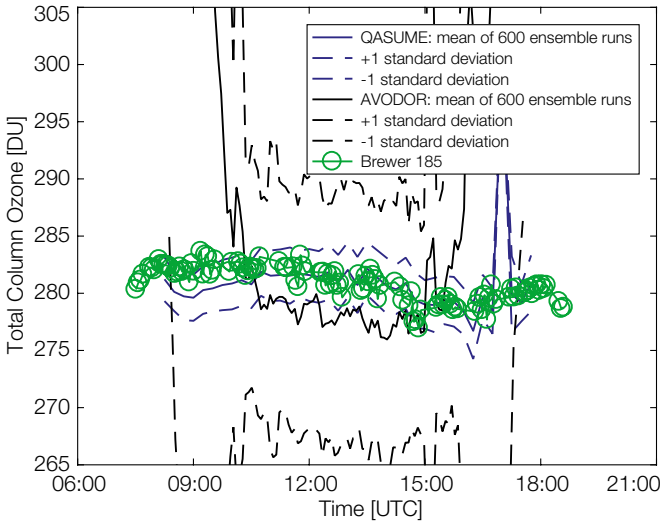

Figure 1. TOC retrieval for QASUME and AVODOR in terms of averages and standard deviations of the ensemble runs on 17 September 2016. Brewer 185 results are included for comparison.

The results in Figure 1 show that the standard uncertainties for QASUME range from 0.7%, in the morning and evening at low solar zenith angles, to 0.9% at local noon. The uncertainties for TOC retrievals with AVODOR are considerably larger (around 4%) than for TOC estimates with QASUME. Moreover, TOC from AVODOR showed a bias of -3 DU compared to QASUME and the Brewers, indicating that the retrieval also depends on the quality of the instrument used.

In summary, the well-calibrated and characterised QASUME reference spectroradiometer allows TOC to be estimated with lower uncertainty (~2 DU) than the commercially available array spectroradiometer (~10 DU) which is roughly optimised for TOC retrieval.

The EMRP is jointly funded by the EMRP participating countries within EURAMET and the European Union.

References: Huber M., Blumthaler M., Ambach W., Staehelin J.: 1995, Total atmospheric ozone determined from spectral measurements of direct solar UV irradiance, Geophys. Res. Lett. 22, 53–56.

Hülsen G., Gröbner J., Nevas S., Sperfeld P., Egli L., Porrovecchio G., Smid M.: 2016, Traceability of solar UV measurements using the QASUME reference spectroradiometer, Appl. Opt. 55, 7265–7275.

Revising Short and Long-Wave Radiation Archives in View of Possible Revisions of the WSG and WISG Reference Scales: Methods and Implications

Stephan Nyeki, Julian Gröbner, and Wolfgang Finsterle in collaboration with ASIAQ (Nuuk, Greenland)

Previous studies suggest that the PMOD/WRC Standard Groups for short and long-wave irradiance (WSG and WISG) may need to be corrected. These implications are considered with respect to long-wave irradiance time-series at several international baseline stations belonging to the Baseline Surface Radiation Network.

The Baseline Surface Radiation Network (BSRN) archive of surface observations is used worldwide to validate satellite products and global climate models (GCM). Most BSRN records are traceable to the World Standard Group (WSG) for short-wave irradiance and World Infrarred Standard Group (WISG) for long-wave irradiance, hosted by the PMOD/WRC. However, the WSG and WISG have recently been found to over and underestimate irradiance values, respectively (Fehlmann et al., 2012; Gröbner et al., 2014). In view of a possible correction to both standard groups, and hence to the BSRN radiation archive, this study investigated the methods involved and their implications on BSRN time-series archives.

Fehlmann et al. (2012) recommended that a WSG scale correction of 0.3% would be necessary which can be readily applied to the short-wave time-series of network radiometers (pyrheliometers and pyranometers). However, a similar straightforward scale correction is not possible for long-wave irradiance time-series. Studies (Gröbner et al., 2014; Nyeki et al., 2017) made during the calibration of pyrgeometers at PMOD/WRC suggest that Eppley PIR and pre-2003 K&Z CG4 pyrgeometers will require a scale correction of the pyrgeometer sensitivity *C* as well as a correction accounting for the integrated water vapour (IWV) content of the atmosphere when IWV < 10 mm. On the other hand, post-2003 K&Z CG4 pyrgeometers only require a scale correction. Based on a comparison with two independent long-wave radiometers, the WISG scale would have to be provisionally increased by about +5.1 Wm^{-2} (Gröbner et al., 2014). Regarding the IWV correction, this only applies to periods when IWV < 10 mm at the BSRN station itself.

BSRN downward short and long-wave time-series were revised for a small selection of stations, including Georg von Neumayer (GVN, Antarctica), Ny Ålesund (NYA, Arctic), Payerne (PAY, Switzerland) and Davos (DAV, Switzerland). The first three stations belong to the BSRN network amongst others, and were mainly chosen due to: i) direct traceability of all pyrgeometers to the WISG with regular calibration every 2 – 4 years, ii) the ready availability of pyrgeometer raw data, and iii) the length (10+ years) and continuity of the downward long-wave irradiance (DLR) time-series.

The effect of revising the WISG reference scale increased the average all-sky DLR for the 2006 – 2015 period by 1.4 – 4.2 Wm^{-2} at the four stations. The increase was less (0.7 – 3.5 Wm^{-2}) when the dependence of the sensitivity *C* on IWV was also corrected. Average clear-sky DLR values were higher at 7.0 and 5.4 Wm^{-2}. It can therefore be reasonably argued that similar increases in DLR can be expected at other polar and mid-latitude BSRN stations.

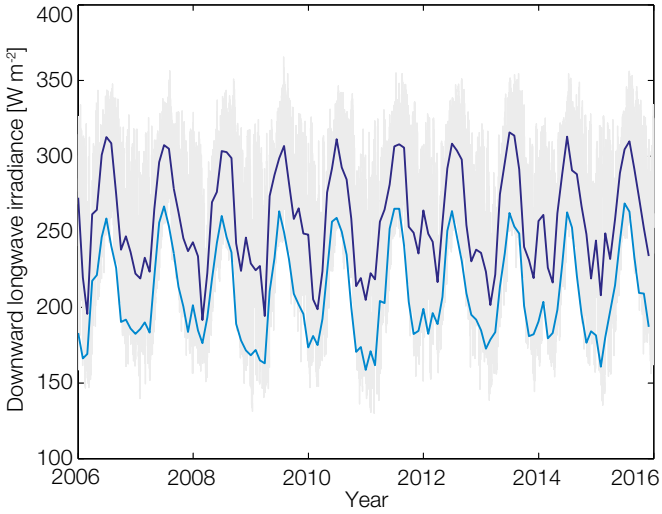

Figure 1. Monthly mean values of downward long-wave radiation for all-sky (blue) and clear-sky (light blue) conditions for the 2006 – 2015 period at NYA. Corresponding all-sky (light grey lines) and clear-sky (dark grey lines) for 1-min values are shown in the background for comparison.

A long-standing issue in climate models is a general underestimation of DLR when compared to BSRN-type surface observations (Wild et al., 2015). Although these low biases have generally decreased over time, increases in observed time-series as suggested above may imply that the underestimation of DLR continues to be a serious issue even in the latest generation of climate models used in the 5th International Panel on Climate Change (IPCC) assessment report (Wild et al., 2015). In the context of the quantification of the global energy balance, estimates making use of the information contained in the surface observations over many years have suggested a higher global mean DLR than typically advocated in various published global energy balance estimates, such as those given in the IPCC assessments up to the 4th assessment report. An increase in observed DLR time-series may further support such higher DLR estimates within the global energy balance.

References:

Fehlmann A. et al.: 2012, Fourth World Radiometric Reference to SI radiometric scale comparison and implications for on-orbit measurements of the total solar irradiance, Metrologia, 49, S34–S38, doi: 10.1088/0026- 1394/49/2/S34.

Gröbner J. et al.: 2014, A new absolute reference for atmospheric longwave irradiance measurements with traceability to SI units, J. Geophys. Res. Atmos., 119, doi: 10.1002/2014JD021630.

Nyeki S. et al.: 2017, Revising short and longwave radiation archives in view of possible revisions of the WSG and WISG reference scales: Methods and implications, Atmos. Meas. Tech, submitted.

Wild M. et al.: 2015, The energy balance over land and oceans: An assessment based on direct observations and CMIP5 climate models. Clim. Dyn., 44, 3393–3429, doi: 10.1007/s00382-014-2430-z.

A Pulsed Tunable Laser System for the Characterisation of Spectrometers (ATLAS)

Julian Gröbner, Natalia Kouremeti, and Stelios Kazadzis

The project aims to improve the accuracy of array spectroradiometers that are widely used for satellite validation of various atmospheric products. More specifically, it is intended to measure the stray-light and linearity of spectroradiometers, and to develop algorithms and post-correction functions to deal with these aspects.

Surface-based optical radiation measurements are a key requirement for the validation of remote-sensing products from satellites. State-of-the-art systems consist of array spectroradiometers to measure solar radiation in the UV-VIS-NIR range in order to determine a large range of parameters, from surface radiation to atmospheric composition products such as the total concentration of trace gases as well as their profiles. In order to fulfil their role as reference systems for the validation of satellite products, traceable surface-based measurements to the international system of units are required, including a comprehensive uncertainty budget based on an extensive characterisation of the measuring system. One key aspect in this chain is the radiometric characterisation of the optical system, including its stray-light characteristics and non-linearities in order to produce correction functions for these parameters.

Figure 1 shows the ATLAS set-up in the PMOD/WRC optical laboratory. The in-range stray-light correction of array spectroradiometers are based on line-spread function (LSF) measurements across the whole wavelength range of the spectrometer (Nevas et al., 2014). Figure 2 shows the LSF measurements for Precision Spectroradiometer (PSR) #006 which are used to determine the stray-light matrix according to the Zong et al. (2006) procedure.

The non-linearity of the array spectroradiometer was measured using the same ATLAS facility by analysing the LSF while varying either the integration time or the radiation level. This is shown in Figure 3 for PSR #006. Similar results are found when varying the intensity as well, showing that PSR #006 has negligible non-linearities over its measurement range.

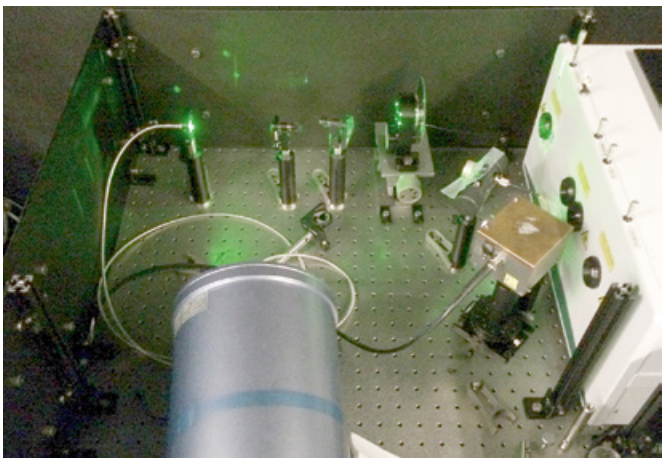

Figure 1. The ATLAS tunable laser facility with the optical conditioning beam unit consisting of a trap diode, a micro-lens-array system and a neutral density filter-wheel. An optical fibre transmits radiation into the PSR.

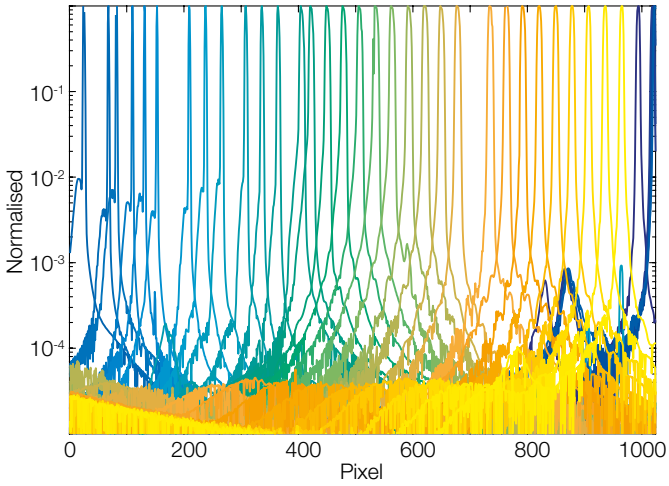

Figure 2. Line-spread functions of PSR #006 measured with ATLAS. The measurements cover the 300 – 1000 nm wavelength range.

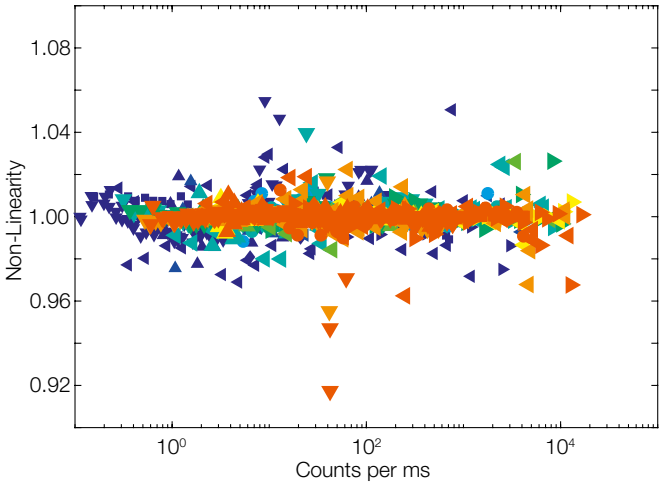

Figure 3. Relative non-linearity correction of PSR #006 versus intensity changes (counts per ms).

In phase 2 of the ATLAS project, a Pandora system (#120) operating at PMOD/WRC will be similarly characterised for non-linearity and stray-light to demonstrate the improvements in trace gas retrievals for a well-characterised system.

The project is funded by ESA/SERCO under IDEAS+/SER/SUB/11.

References:

Nevas S., Gröbner J., Egli L., Blumthaler M.: 2014, Stray light correction of array spectroradiometers for solar UV measurements, Appl. Opt., 53, 19, 4313–4319.

Zong Y., Brown S.W., Johnson B.C., Lykke K.R., Ohno Y.: 2006, Simple spectral stray light correction method for array spectroradiometers, Appl. Opt., 45, 1111–1119.

Aerosol Absorption Retrieval at Ultraviolet Wavelengths

Stelios Kazadzis, Panagiotis Raptis, and Natalia Kouremeti in collaboration with FMI (Finland), NASA Langley Research Center (USA) and NOA (Athens, Greece)

We investigated the spectral dependence of aerosol columnar absorption properties, including the single scattering albedo. Using five years of simultaneous sun-photometric and multi-filter diffuse and global irradiance measurements, we found that an extrapolation of such aerosol properties from the visible and near IR to the UV wavelength region leads, in most cases, to an underestimation of the aerosol absorption.

A comprehensive review of the assessment of the aerosol direct effect (see IPCC, 2013) emphasises that significant aerosol absorption uncertainties in global single scattering albedo (SSA) constitute one of the largest single sources of uncertainty in current modelling estimates of aerosol climate forcing. SSA is the ratio of scattering to total extinction (scattering plus absorption), and depends strongly on chemical composition, particle size, mixture, relative humidity and wavelength. Comprehensive measurements are crucial to understand their effects and to reduce SSA uncertainties that propagate into aerosol radiative forcing estimates. Several other issues can be clarified with accurate knowledge of aerosol absorption properties, and include the following:

• Aerosol effects on UV trends may enhance, reduce or reverse effects of stratospheric ozone change.

• Solar irradiance satellite retrieval algorithms are directly affected by the presence of absorbing aerosols.

• They have an impact on the uncertainty of commonly used atmospheric radiative transfer applications and codes.

In the visible (VIS) part of the spectrum, advanced retrieval algorithms for microphysical aerosol properties have been developed in the framework of the Aerosol Robotic Network Network (AERONET) (Dubovik and King, 2000). As AERONET does not provide any information about SSA in the UV, compared to the visible spectral region, only a few publications have dealt with aerosol absorption at UV wavelengths.

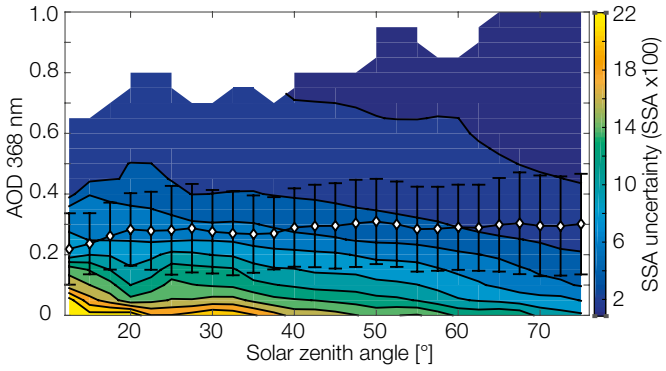

Figure 1. Uncertainty estimate (colour) for the SSA retrieval from UV-MFR as a function of AOD and solar zenith angle for λ = 368 nm. Superimposed, mean AODs for 2.5° bins of the solar zenith angle are shown.

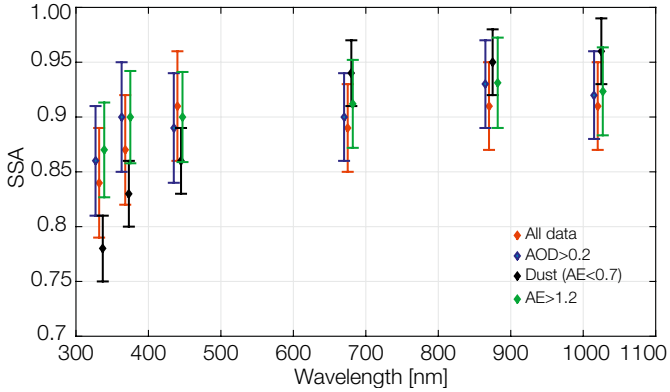

Figure 2. Wavelength dependence of SSA from concurrent CIMEL and UV-MFR data. Black symbols represent only dust aerosol cases.

In this work, we present estimates of SSA at two independently retrieved UV wavelengths (332 and 368 nm) for an urban site in Athens, Greece. The analysed measurement period is from July 2009 to May 2014. Radiative transfer model (RTM) calculations were used to retrieve SSA by using global and/or diffuse spectral irradiance, solar zenith angle (SZA), total column ozone, and aerosol optical depth (AOD), amongst others. Our approach uses measurements of the direct to global irradiance ratios and AOD from a UV–MFR instrument. They are used as basic RTM input parameters for the calculation of SSA at 332 and 368 nm. The advantage of this method is that the same detector and filter measures global and direct irradiance, thus there is no need for absolute irradiance calibration, and hence raw voltage measurements can be used. The enhanced aerosol absorption (lower SSA) found when comparing UV and visible spectra results, shows that we expect:

• A systematic overestimation of modelled solar UV irradiance using SSA from extrapolation from the visible range as input to RTMs.

• A possible decrease in specific days/cases of regional ozone due to the enhanced aerosol absorption.

• An overestimation of the UV irradiance (UV index) calculations for cloudless cases under dust and/or brown carbon presence when using SSA values from the visible range. This is a combination of the overestimated SSA and the high AOD during such events.

References: Dubovik O., King M.D.: 2000, A flexible inversion algorithm for retrieval of aerosol optical properties from Sun and sky radiance measurements, J. Geophys Res., 105, 20673–20696.

IPCC: 2013, Climate Change 2013: The Physical Science Basis, edited by: Stocker, Univ. Press, Cambridge.

One Decade of Irradiance Scale Realisation at the WCC-UV

Gregor Hülsen and Julian Gröbner

The annual irradiance scale realisation of the WCC-UV has now been conducted for one decade. The stability of the seven transfer standard lamps used for this procedure is defined as a deviation from the group mean. The best lamp is stable to within ±0.1%.

The absolute spectral responsivity of a spectroradiometer is determined by measuring the radiation from calibrated transfer standards. These lamps themselves are calibrated against primary standards, such as high temperature blackbody cavities. Filter radiometers are used to determine the blackbody temperature. Their spectral responsivity is calibrated against a silicon trap detector, which is directly calibrated against an absolute cryogenic radiometer. The lamp irradiance calibration is linked to SI units in $W m^{-2} nm^{-1}$ through this source-based traceability chain.

The QASUME spectral irradiance responsivity is calibrated annually in the optical laboratory of the World Calibration Center for UV (WCC-UV) against a group of seven spectral irradiance standard lamps directly calibrated by the PTB. At PMOD/WRC, this procedure is conducted using the reference spectroradiometer QASUME as a transfer device. The method includes repeated measurements of monitor lamps to take QASUME responsivity changes into account during the 1–2 day calibration period. In the measurement set-up for the 1000 W transfer standards, the 8.1 A lamp current is controlled using a feedback loop consisting of a power supply, voltmeter and 100 mΩ precision shunt. Two lamps can be measured after each other, which facilitates a fast repetition of measurements together with a safe cooling phase of the lamps. Stray-light is reduced by the dark environment of the laboratory but mainly by a baffle in front of the input optic of the spectroradiometer.

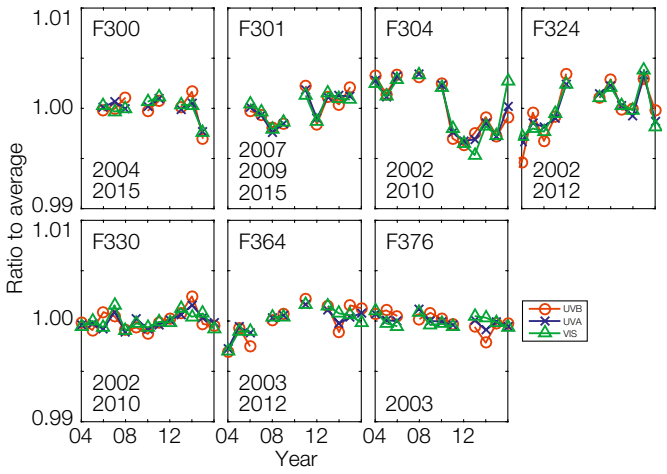

Figure 1. QASUME irradiance scale uncertainty for all seven lamps belonging to the WCC-UV standard group. Calibrations conducted at the PTB are indicated by the year in each plot.

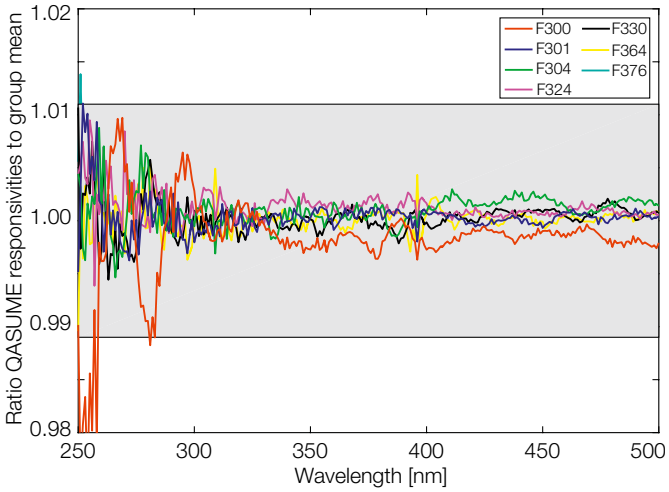

Figure 2. Irradiance measurements with QASUME of the seven WCC-UV transfer standard lamps as a ratio of the total mean. The grey-shaded area represents the expanded uncertainty of the measurements ($k=2$).

The radiometric traceability chain, as described above, mostly determines the uncertainty of the radiometric calibration of a spectroradiometer. This uncertainty between 300 nm and 400 nm is ~0.8% ($k=2$) at the WCC-UV (Hülsen et al., 2016). By using a set of seven transfer standards each calibrated directly against the PTB blackbody, the expanded uncertainty of QASUME is finally determined to be 1.1% ($k=2$).

The stability of the individual lamps is shown in Figure 1 as a deviation from the group mean. The best lamp, F376 has shown no drift during the past decade and is stable to within ±0.1%. Lamp F324 increased in intensity by almost 1% in the first years of operation and remained stable to within ±0.2% afterwards. The second lamp with larger deviations of ±0.5% is F304. This lamp was taken to PTB in 2010 for a re-calibration. As the PTB certification of the lamp did not change, the mechanical disturbance caused by the travel back to Davos was most likely the reason for the change in intensity.

The irradiance of lamps F324 and F364, as calibrated by the PTB, showed larger deviations from the other lamps before the re-calibration in 2012. Therefore, all measurements before 2012 were recalculated using the new certificates. Hence, Figure 1 shows only the stability of the lamps and not the change caused by the re-calibration. Figure 2 shows the agreement of the seven lamps during the last irradiance scale realisation in December 2015. The irradiance measured with QASUME is plotted against the group mean. Both figures show that all seven lamps have been well within the radiometric calibration uncertainty stated above during more than 10 years of measurements.

References: Hülsen G., Gröbner J., Nevas S., Sperfeld P., Egli L., Porrovecchio G., Smid M., Traceability of solar UV measurements using the QASUME reference spectroradiometer, Appl. Opt. 55, 7265–7275, 2016.

A Travel Standard for Aerosol Optical Depth in the UV

Thomas Carlund, Stelios Kazadzis, Natalia Kouremeti, and Julian Gröbner in collaboration with AEMET (Madrid, Spain)

One of the main objectives of the European Brewer Network (EUBREWNET; COST Action ES1207) is the retrieval of aerosol optical depth (AOD) in the ultraviolet (UV) spectral range. A UV precision filter radiometer (UV-PFR) developed at PMOD/WRC was established as a travelling standard for AOD measurements in order to facilitate the necessary calibrations of the EUBREWNET field instruments.

Based on the results of this study, the UV-PFR appears to be a stable high quality radiometer for AOD determination in the UV. However, due to the ~1 nm wide spectral response functions of the UV-PFR, the calibration constants from Langley plot calibrations underestimate the true extra-terrestrial signals, especially at the shortest wavelengths. The UV-PFR filter bandwidths also result in an apparent decrease in ozone optical depth with increasing airmass. An adjusted formula for AOD, with correction terms for the filter bandwidth influence, has therefore been introduced (Carlund et al., 2017).

For a reference instrument, calibration accuracy and stability are issues of major importance. The UV-PFR has therefore been absolutely calibrated by Langley plots at the high altitude station Izaña Observatory, Tenerife, Spain, where stable aerosol atmospheric conditions and columnar ozone concentrations often occur. Calibrations performed during two periods about 14 months apart showed that the UV-PFR sensitivity changed by ≤1 % per year at all four wavelengths. The UV-PFR has also been found to give stable and consistent AOD values compared to a reference standard PFR for over a 12-month measurement period at PMOD/WRC.

Figure 1. The UV-PFR during the site visit in July 2016 to AEMET, Madrid.

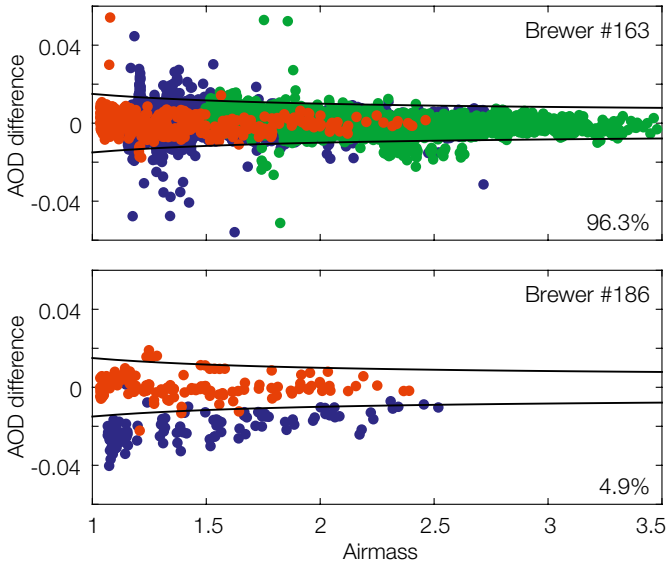

Figure 2. Difference in AOD at the 310.1 nm wavelength between: Upper panel: Brewer #163 and UV-PFR#01 during autumn 2015 (green) and spring 2016 in Davos, and lower panel: Brewer #186 and UV-PFR#01 during a week in late July 2016 in Madrid. AOD differences during the calibration at the RBCC-E campaign in 2015 are shown in red. Black lines are the WMO traceability limits and the percentages of the data points within these limits are given.

In 2015, the UV-PFR participated in the 10th Regional Brewer Calibration Centre for Europe (RBCC-E) campaign at the El Arenosillo station in southern Spain. During this campaign 21 Brewer spectrophotometers were calibrated for AOD against the UV-PFR. Within a 14-month period after this campaign, visits were performed with the UV-PFR to two of the participating Brewer home sites. AOD differences at the RBCC-E campaign and at a following site visit are shown for one of the Brewer wavelengths in Figure 2.

The stability of Brewer #163 was confirmed during two months in autumn 2015 and two months in spring 2016 at PMOD/WRC. During a one week visit to Brewer #186 at AEMET in Madrid, it became clear that the sensitivity of Brewer #186 had increased by 2–4 % since the 10th RBCC-E campaign about 14 months earlier. These findings both highlight the suitability for Brewers to measure AOD at a high precision, as well as the necessity of regular calibration.

References: Carlund T., Kouremeti N., Kazadzis S., Gröbner J.: 2017, Aerosol optical depth determination in the UV using a four-channel precision filter radiometer, Atmos. Meas. Tech., 10, 905–923, doi: 10.5194/amt-10-905-2017.

Aerosol Effect on Solar Radiation/Energy (GEO-CRADLE)

Stelios Kazadzis and Panagiotis Raptis in collaboration with NOA (Athens, Greece)

GEO-CRADLE (geocradle.eu/en/) has received funding from the EU Horizon 2020 Research and Innovation Programme (February 2016–July 2018) with the aim of promoting the uptake and exploitation of Earth Observation (EO) activities in North Africa, the Middle East and the Balkans. To this end, the project has brought together 25 partners from 3 continents to work in a highly-complementary team that combines a strong background in EO coordination activities with proven scientific excellence in four key thematic areas: i) adaptation to climate change, ii) improved food security and water extremes management, iii) access to raw materials, and iv) access to energy).

Within GEO-CRADLE, there are four pilot thematic studies that have been chosen in order to build the scientific basis that will lead to a specific application for the area under study. PMOD/WRC leads the Solar Energy Now-casting SystEm (SENSE) pilot. The aim of the pilot is to coordinate, improve and support the regional EO infrastructures and capabilities related to "access to energy". The niche for this pilot is the operational, satellite-driven and real-time system for solar energy now-casting. SENSE will be a starting point for energy related short future investments towards and beyond the implementation of GEO, GEOSS and Copernicus Energy related activities, envisioning innovative high-end applications and technologies.

The SENSE final product is spectral solar irradiance which can be used for solar energy related applications. It is based on the synergy of Radiative Transfer Model (RTM) and Neural Network (NN) simulations, using real-time satellite retrievals. A NN is trained with a large-scale (2.5 million record) look-up table of clear and cloudy sky RTM simulations to convert satellite cloud and aerosol products directly into solar radiation spectra (Figure 1).

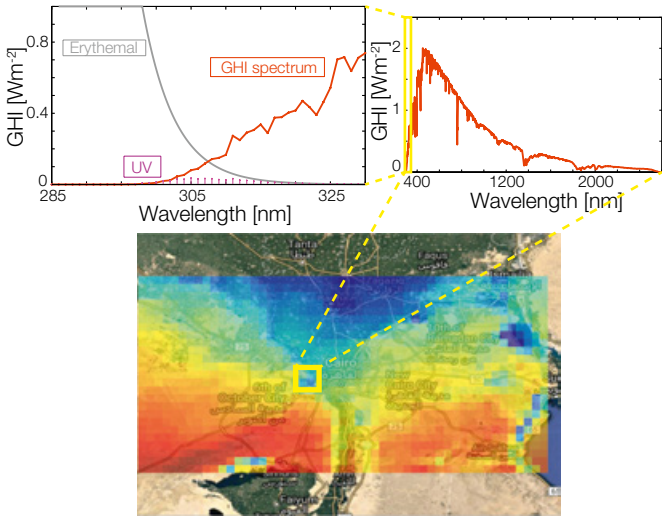

Figure 1. SENSE pilot graphical representation. From right to left: the Global Horizontal Irradiance (GHI) for Cairo (Egypt), the insolation spectrum in a single pixel, and finally, the spectrally-weighted UV radiation spectrum.

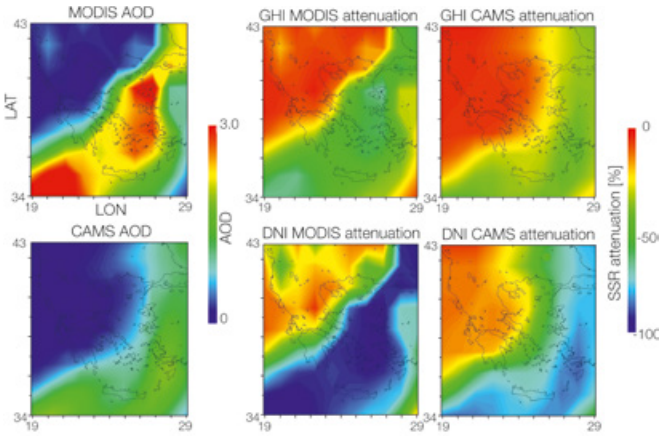

Figure 2. Left: AOD from MODIS satellite and CAMS for the SE Mediterranean area. Right: Impact of aerosols on calculated GHI and DNI. Results are for an extreme dust case on 1 Feb. 2015 over Greece.

As a result, SENSE is capable of producing maps of spectrally-integrated irradiances of about 10,000 to 100,000 pixels within 1 minute and hence provides the capability needed to serve high precision solar power applications for energy planning. Surface spectra for Direct Normal Irradiance (DNI), which applies to Concentrated Solar Plants, as well as Global Horizontal irradiance (GHI), which applies to photovoltaic installations, are produced at high resolution (wavelength step: 1 nm; spatial grid: 5 km; time step: 15 minutes). These use input data from the Copernicus Atmosphere Monitoring Service (CAMS; a combination of satellite surface-based and modelling aerosol database) for aerosols optical properties and from the Spinning Enhanced Visible and Infrared Imager (SEVIRI) onboard the Meteosat Second Generation (MSG) for cloud optical properties.

One basic aspect investigated during the SENSE activity is the quantification of the impact of aerosols on the solar radiation and solar energy potential. This effect becomes very important especially for areas with a low probability of cloud presence and areas in the proximity of the Saharan desert, where the aerosol impact on solar radiation becomes important (e.g. Northern Africa).

The effect of aerosols was investigated using various sources as inputs to the SENSE related radiative transfer modelling tool. Surface-based AOD measurements, satellite-based aerosol observations and the CAMS aerosol product have been used to serve this purpose. An example of the aerosol impact on solar energy for a selected aerosol dust event over Greece is shown in Figure 2. MODIS satellite-based AOD measurements and CAMS aerosol forecast products have been used to calculate the impact on solar radiation and energy calculations.

Integrated Water Vapour Retrieval Using a Precision Solar Spectroradiometer

Panagiotis Raptis, Stelios Kazadzis, Natalia Kouremeti, and Julian Gröbner

We have developed an algorithm to retrieve Integrated Water Vapour (IWV) from Precision Solar Spectroradiometer (PSR) measurements. The sensitivity of the retrieved IWV values at different wavelengths has been investigated. The algorithm was applied to the PSR data set that was recorded during the 4th Filter Radiometer Comparison (FRC-IV) campaign at PMOD/WRC in October 2015 and retrievals were compared with CIMEL/AERONET and GPS IWV retrievals.

Integrated Water Vapour (IWV) is the depth of water in a column of the atmosphere if all the water in that column were precipitated as rain. IWV is critical to earth's climate as water vapour is a primary greenhouse gas, and responsible for heat transport and latent heat of vapourisation. In addition, it has high importance in radiative transfer calculations where uncertainties can lead to the erroneous determination of the solar radiation attenuation vertical profiles.

The PSR has been developed at PMOD/WRC during the last decade, and is designed to measure the solar spectrum in the 300–1020 nm wavelength range with a spectral resolution varying from 1.5 to 5 nm (full-width-at-half-maximum). In this study, we use data from PSR#006 which was given an absolute calibration in the PMOD/WRC optical laboratory just before the FRC-IV campaign.

Spectral AOD was calculated using the absolute direct irradiance, corrected for stray-light and a theoretical extra-terrestrial (ET) spectrum, and was then compared to other sun-photometers during the campaign. Results of PSR-retrieved AOD were found to be well within the WMO recommended limits (±0.005 + 0.01/*m*, where *m* is the airmass), compared with the PFR WORCC reference triad.

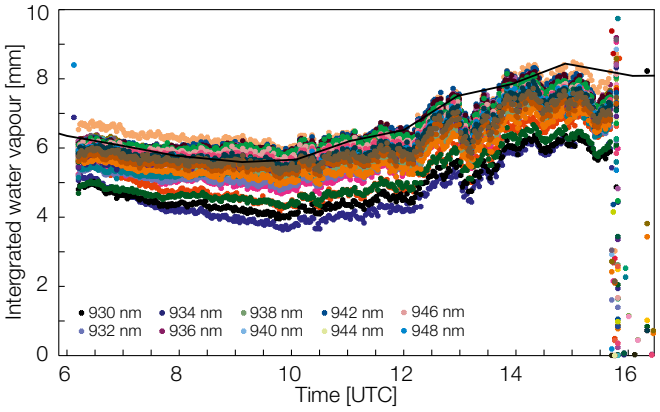

Figure 1. PSR IWV retrieved at all available wavelengths in the 928 – 950 nm range (not all wavelengths shown) on 30 September 2015. GPS retrieval corresponds to the black line.

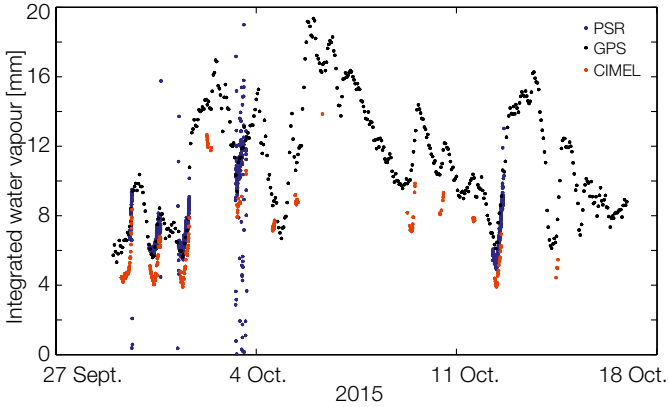

Figure 2. IWV data during FRC-IV. PSR retrieved at λ = 946 nm direct irradiance. GPS is hourly averaged data. CIMEL appears to permanently underestimate in the area of Davos.

For the IWV retrieval, we used the method described by Ingold et al. (2000). An empirical IWV transmittance function was constructed for each wavelength using MODTRAN Radiative Transfer Model outputs (convolved to PSR wavelengths by using the PSR relative slit functions), which relates transmittance of IWV and absolute IWV. In addition, transmittances for aerosol (through AOD values at 846 nm and extrapolated at the corresponding wavelength) and Rayleigh scattering were calculated, as well as absolute transmittance using the ET values and measured direct irradiance. We retrieved IWV with this procedure using all spectral measurements in the 928–950 nm range, where maximum absorption due to water is expected (Figure 1).

We used the GPS retrievals (hourly averaged values) to validate results, and co-located CIMEL retrievals (which appear to underestimate by a constant value of ~20%). It was observed that the best agreement is with the retrieval at 946 nm (R^2 = 0.77 compared to GPS retrievals, using 44 hourly averages), which is in accordance with WMO recommendations for IWV. All data using retrieved values from this wavelength are shown in Figure 2 along with IWV from GPS and CIMEL. Values from the CIMEL retrieval are always ~10% lower, and R^2 = 0.71 for the 241 simultaneous values.

References: Ingold T., Schmid B., Matzler C., Demoulin P., Kämpfer N.: 2000, Modeled and empirical approaches for retrieving columnar water vapor from solar transmittance measurements in the 0.72, 0.82, and 0.94 mu m absorption bands, J. Geophys. Res., 105(D19), 24327–24343.

Improved Observational SSI Composite

Margit Haberreiter and Werner Schmutz in collaboration with CNRS (France) and AUTh (Greece)

The impact of solar variability on the Earth's climate has a long history as a research field, and has also become a hotly debated topic. Although there is strong evidence for this natural forcing to be weak in comparison to that of man-made greenhouse gases, large uncertainties remain regarding the magnitude of the variation of the solar spectral irradiance dataset and thus also on the magnitude of its impacts.

We have refined the previously described SSI observational composite and present an updated version. The individual SSI datasets that go into the composite were evaluated by Schöll et al. (2016), and the overall approach is described in detail by Haberreiter et al. (2017). One challenge for this composite has been the fact that for wavelengths longer than 410 nm, only the SIM/SORCE instrument provides observations. In addition, the SIM instrument seems to have changed its performance considerably during the course of the SORCE mission (see Figure 1). From 2003 to 2009 (see colour-coded crosses), the relative SIM variation at 500 nm shows a negative correlation with the relative TSI change, while it is positively correlated after 2010 (grey-overlayed crosses).

The positive correlation after 2010 is similar to observations by Wehrli et al. (2013) who found a significant positive correlation of VIRGO data at 500 nm with TSI from the SOHO mission. From this, we conclude that the SIM data are reliable after 2010 and we incorporate these in the composite. The relative annual mean variation of the new SSI composite for the 2003 - 2008 period years 2003 to 2008 is shown in Figure 2. The contribution of the change in SSI from 120 nm to 200 nm explains 98.9% of the TSI variation.

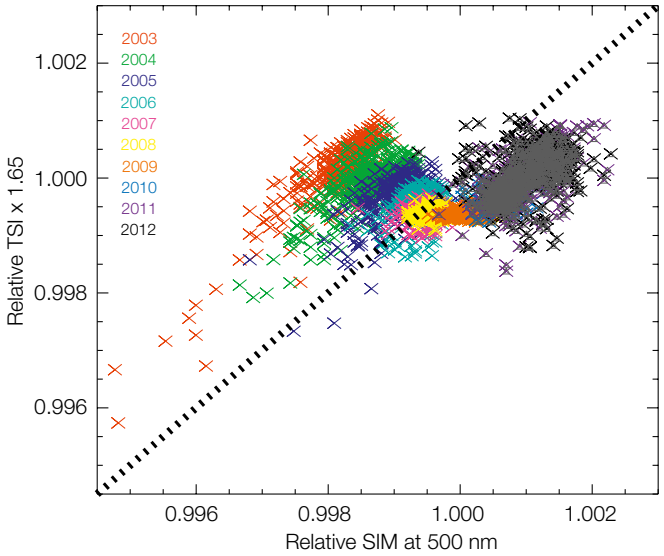

Figure 1. Solar Irradiance Data Exploitation (SOLID) composite (black line) along with the individual irradiance datasets used to produce it, as an example at 121.5 nm.

Acknowledgement: This work has received funding from the EC 7th Framework Prog. under grant agreement no 313188 (SOLID).

References: Haberreiter M. et al.: 2017, J. Geophys. Res., in press, doi: 10.1002/2016JA023492.

Schöll M. et al.: 2016, SWSC, 6, A14.

Wehrli C. et al.: 2013, Astron. Astrophys., 556, id.L3.

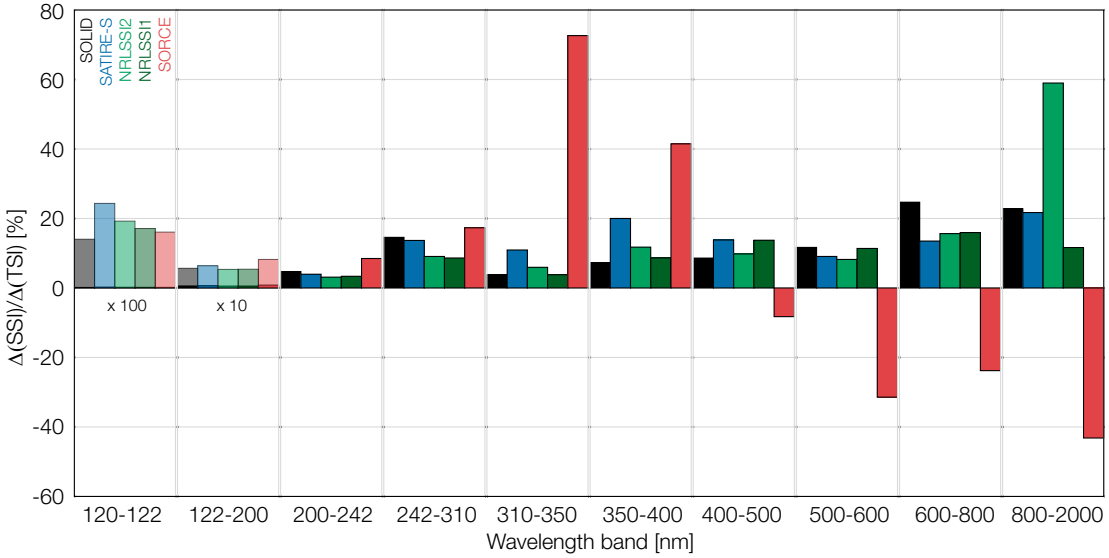

Figure 2. Change of the annual SSI mean in different spectral bins from 2003 to 2008 with respect to TSI variations for the same time interval. Shown are the relative changes for the latest version of the SOLID composite (black), SATIRE-S (blue), NRLSSI1 and NRLSSI2 (dark and light green), and the SORCE composite (red). For better illustration, the first and second spectral bins are multiplied by 100x and 10x, respectively, and are shown with partly transparent colours.

Understanding the Implication of Small-Scale Heating Events in the Solar Upper Atmosphere

Nuno Guerreiro, Margit Haberreiter, and Werner Schmutz in collaboration with the University of Oslo (Norway)

Small-scale heating events (SSHEs) result from the impulsive release of magnetic energy in the solar atmosphere. These SSHEs release energy in the 10^{17} to 10^{27} erg range and are considered to have important implications in the understanding of coronal heating, acceleration of spicules and the pervading redshifts in the lower transition region. We use a method developed at PMOD/WRC applied to 3D magneto-hydrodynamic (MHD) simulations to study the properties and potential of the SSHEs to better understand the structure of the solar atmosphere.

The developed method is based on the idea that every SSHE always has a maximum region in its interior where the energy dissipation is at a maximum which is above a defined background. The method identifies this region for the individual SSHEs, then calculates the SSHE's volume at each instant and follows them over time. We used two 3D MHD models with different resolutions and different magnetic field distributions. The model with low resolution is identified as LRM and the model with high resolution is identified as HRM. The models represent volumes of the solar atmosphere that span from the top of the convection zone to the corona.

The application of the method to the models yields several important results. We find that the SSHEs that have the potential to heat the corona have a lifetime shorter than 4 minutes and typically they have a total energy (E_T) that ranges from 10^{20} erg to 10^{24} erg. Figure 1 displays the probability distribution of E_T in a logarithmic scale versus the lifetime of the SSHEs. The left panels correspond to the LRM and the right panels to the HRM. The top panels represent the SSHEs selected with a background of 1×10^{18} erg s^{-1} and the lower panels with a background of 1×10^{17} erg s^{-1}. We can see that the choice of the background affects the lower E_T cut-off of the SSHEs studied. The panels representing the SSHEs computed using the 1×10^{18} erg s^{-1} background indicate that the bulk energy of the SSHEs ranges from 10^{21} erg to 10^{24} erg, while with a background of 1×10^{17} erg s^{-1} the bulk energy of the SSHEs ranges from 10^{20} erg to 10^{24} erg. The figure also shows that the lifetime range of the SSHEs is less than four minutes and that many of the detected SSHEs are above the limit of detectability that is currently about 10^{24} erg. This opens the possibility to compare the properties of the SSHEs with those observed in the Sun. This possibility will provide a better understanding of the physics and the response of the atmospheric plasma to the energy dissipated by the SSHEs that occur in the different layers of the solar atmosphere.

The application of our method has also helped to estimate the angles for which the rate of energy dissipation is maximum. We find that in the models we used, the energy dissipated is at a maximum when the magnetic field presents an angle in the vicinity of the energy dissipation that ranges from 5° to 15°. The energy that is dissipated when the angles reach these amplitudes results from two SSHE types: i) SSHEs where there is a violent reconnection process, and ii) SSHEs where reconnection occurs as a slower process. A detailed description of the above findings can be found in Guerreiro et al. (2017).

References: Guerreiro N., Haberreiter M., Hansteen V., Schmutz W.: 2017, Small-scale heating events in the solar atmosphere. II. Life-time, total energy and magnetic properties, Astron. Astrophys., doi: https://doi.org/10.1051/0004-6361/201629795.

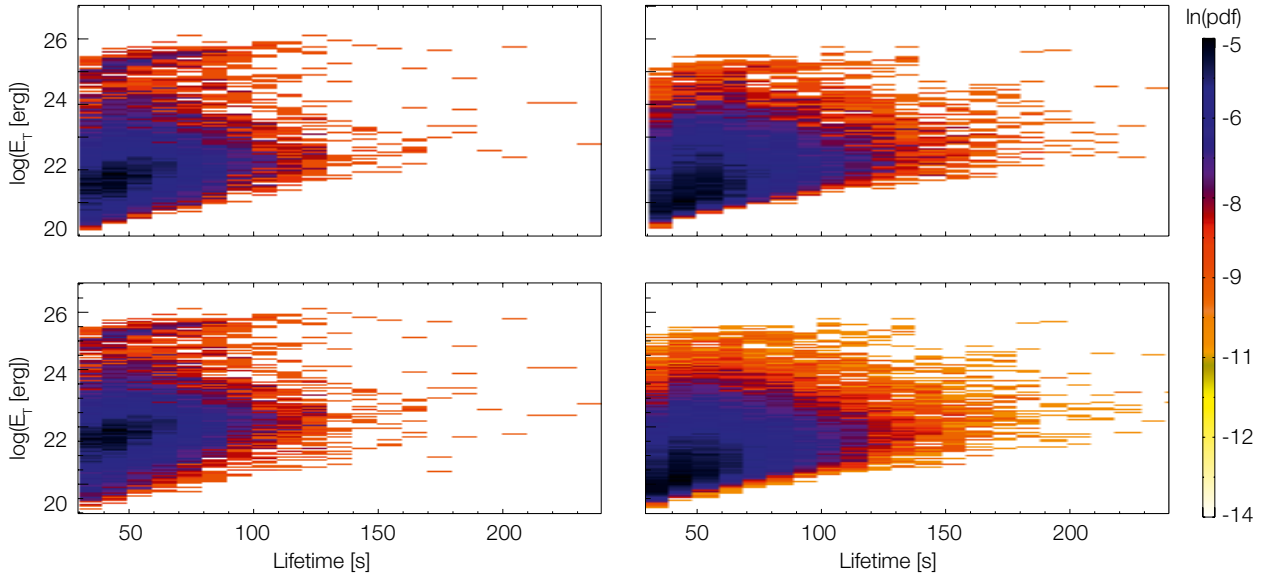

Figure 1. Probability distribution function (PDF) of the total energy (E_T) of the individual SSHEs versus their lifetime considering SSHEs selected using different backgrounds for the LRM (left) and HRM (right). The backgrounds are 10^{18} erg s^{-1} and 10^{17} erg s^{-1} for the upper and lower panels, respectively. Darker regions correspond to a high SSHE concentration, light yellow regions to a low concentration and white regions represent locations with no SSHEs.

Nine Years of Total Solar Irradiance Measurements on FY-3 Satellites with Primary Corrections

Hongrui Wang and Wolfgang Finsterle in collaboration with CIOMP (Changchun, China)

Total Solar irradiance (TSI) has been measured on three Feng Yun 3 (FY-3) satellites ever since the FY-3A satellite was sent into space in 2008. TSI measurements from FY-3 satellites have shown that the Sun's radiative output at the maximum of solar cycle 24 increased by about 1.29 $W m^{-2}$ compared with the low TSI value recorded on FY-3A around the solar minimum of solar cycle 24. This is much smaller than that of solar cycle 23. Future work will be required to correct the degradation of the TSI instruments on the FY-3 satellites.

FY-3 satellites are meteorological satellites which have been placed on sun-synchronous polar orbits. They have been mainly developed for Earth observation, in order to provide accurate observations of the atmosphere, ocean, and land surface. However, solar activity has also been recorded on FY-3 nadir-pointing spacecraft to record the Earth's energy input from the Sun (Wang et al., 2015; Wang et al., 2017), including the FY-3A satellite (launched on 27 May 2008), the FY-3B satellite (launched on 5 November 2011), and the FY-3C satellite (launched on 23 September 2013). The TSI time-series from the three FY-3 satellites are shown in Figure 1 along with time-series from the SOHO and SORCE missions. Primary data corrections have been applied to the FY-3 time-series, including: the Sun-Earth distance, the thermal background, and solar pointing (Wang et al., 2017).

Electrical substitution radiometers, which have a similar design of the cavity detectors and optical arrangements, have been used to measure TSI during the past three FY-3 missions. Measurements began in 2008 around the solar minimum in solar cycle 24. Solar instruments on the FY-3A and FY-3B satellites operate in a scanning manner. Since the vehicle axis of the FY-3A or FY-3B satellite is always aligned with a nadir reference by using a three-axis-stabilised system, the solar radiometers can only measure the Sun when the satellite passes close to Earth's North Pole, and when the Sun is in the field-of-view of the radiometers (Wang et al., 2015). The TSI value observed on the FY-3A satellite in September 2008, around the solar minimum in solar cycle 24, was 1364.19 $W m^{-2}$.

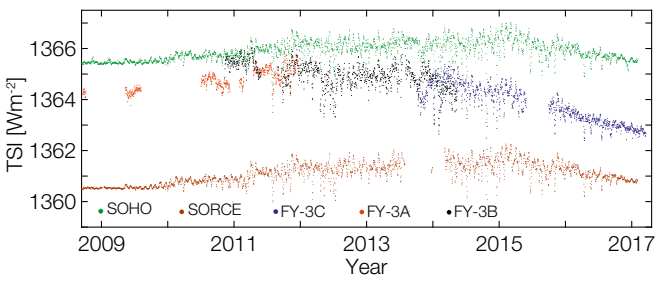

Figure 1. TSI measurements on the FY-3A, FY-3B and FY-3C satellites along with those from the SOHO and SORCE missions.

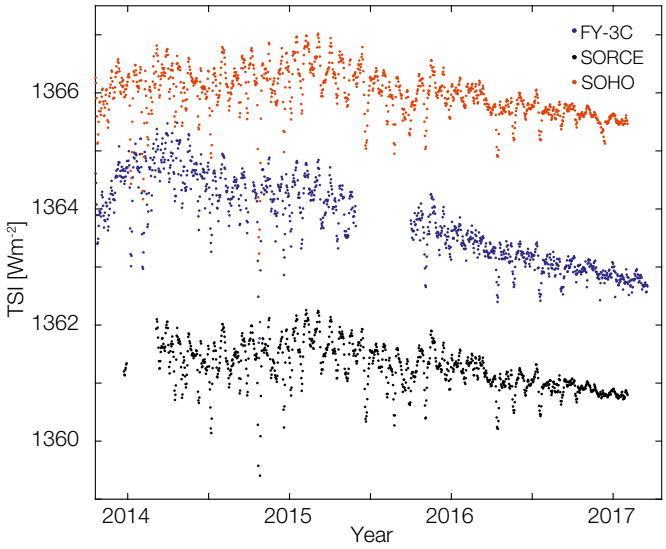

Figure 2. TSI observations from the FY-3C satellite. The data dropout in the FY-3C time-series in the middle of 2015 was due to limitations to the power supply.

In order to avoid complex corrections as a result of solar pointing, as experienced with the FY-3A and FY-3B missions, a new TSI instrument with a solar pointing system was developed which allows accurate solar pointing and stable thermal control of the nadir FY-3C satellite. TSI is measured about 26 times each day by the new solar instrument onboard the FY-3C satellite as shown in Figure 2. Since receiving "first light" on 1 October 2013, this TSI instrument has operated normally, and has recorded solar activity around the solar maximum in the current solar cycle.

TSI results from the FY-3C satellite with primary corrections are shown in Figure 2. The TSI value around the solar maximum in solar cycle 24 is 1365.48 $W m^{-2}$. As shown in Figure 2, TSI data recorded on FY-3C decreased much faster than VIRGO/SOHO or TIM/SORCE after 2016. This is mainly attributed to degradation corrections which will need to be performed on the cavity detector in the TSI routine channel on the FY-3C satellite. Further work will be conducted in the future to account for such corrections.

References:

Wang H., Li H., Qi J., Fang W.: 2015, Total Solar Irradiance monitor for the FY-3B satellite – Space experiments and primary data corrections, Solar Physics, 290, 645–655.

Wang H., Qi J., Li H., Fang W.: 2017, Initial in-flight results: The Total Solar Irradiance monitor on the FY-3C satellite, an Instrument with a pointing system, Solar Physics, 292, 9.

Understanding and Improving the Cavity Absorptance of Space TSI Radiometers

Alberto Remesal Oliva, Wolfgang Finsterle, and Benjamin Walter

PMO6-type radiometers for ground and space-based operation have used Aeroglaze Z302 to date as the black absorptive coating to absorb all incoming radiation to the cavity. This study investigates whether carbon nanotube coatings could improve the cavity characteristics, especially degradation.

Since the PMO6-type radiometer was first developed in the 1980s (Brusa and Fröhlich, 1986), Aeroglaze Z302 has been the black absorptive coating used by PMOD/WRC in all cavities. Aeroglaze Z302 is a polyurethane black coating with a glossy surface. The geometry of the PMO6-type cavities make use of the glossy finish in such a way that each incident beam of light is reflected five times within the cavity before it leaves through the entrance aperture again (Suter, 2015). In space, all PMO6-type radiometers have shown a long-term sensitivity loss of ~0.3% (Figure 1). The degradation rate depends on the exposure time *t* of the coating to solar radiation. The first goal of the project is to understand the physical and/or chemical processes which cause the degradation.

In recent years, advancements have been made in the field of absorptive coatings, mainly based on the use of carbon nanotubes. The second goal of the proposed research project is to find out if such a coating is feasible for use in TSI space radiometers, as well as examining the manufacturing process and thermal properties of the coating. The PMO6 and DARA-type cavities have cone shapes which are optimised for the specular surface of the Aeroglaze Z302 coating. A different coating may require different cavity shapes to optimise the absorptance and/or for manufacturing reasons. The third goal of the proposed research project is to develop a cavity receiver which is optimised for the new coating.

Degradation has always been a problem for the black coatings on radiometers in space. The degradation of two detectors (one active cavity, one reference cavity which had always been shaded), used in a PMO6-type radiometer that had been measuring in space for more than one year, was analysed by means of the reflectance map measurements as shown in Figure 2. The results show that the active (exposed) cavity has a higher reflectance (1384 ppm) because of the degradation of the black coating. On the other hand, the maximum reflectance is lower in the reference cavity (908 ppm) because the paint has most probably become more diffuse (ie less glossy) due to degradation.

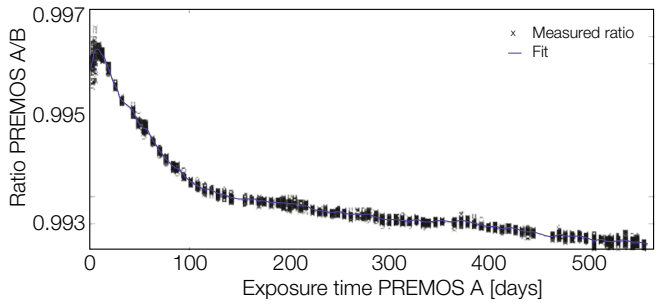

Figure 1. The RSI ratio of the active and backup channels of the PMO6/PREMOS radiometers onboard the PICARD satellite.

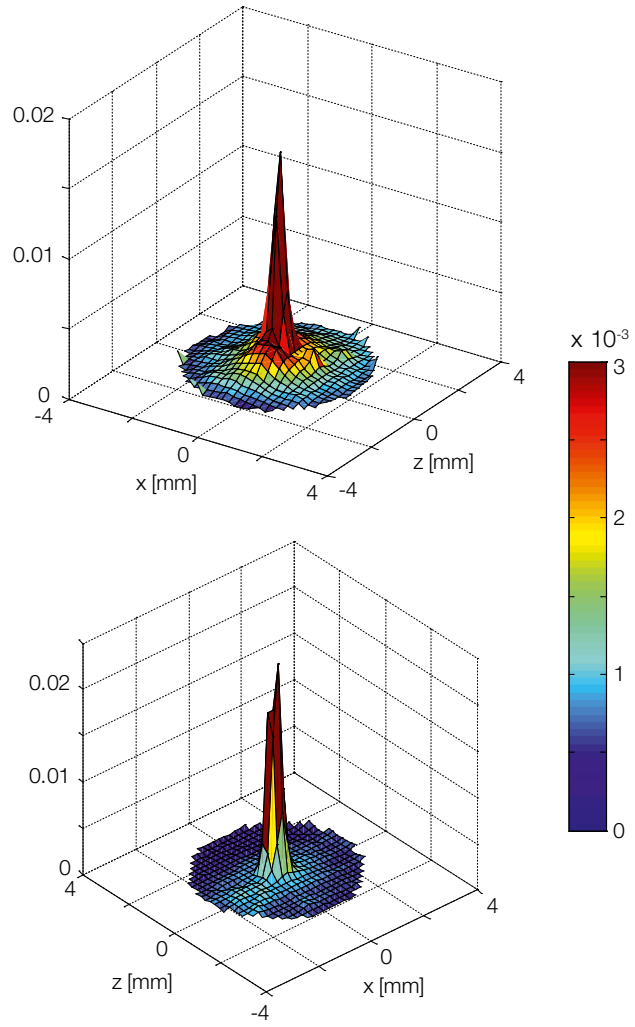

Figure 2. Reflectance maps of PMO6-type radiometer from the Solar Variability (SOVA) experiment previously onboard the de-commissioned Eureca satellite. Upper panel: Active cavity. Lower panel: The reference cavity.

References: Brusa R.W., Fröhlich C.: 1986, Absolute radiometers (PMO6) and their experimental characterization, Appl. Opt. 25, 4173.

Suter M., 2015, Advances in Solar Radiometry, PhD Thesis Univ. Zürich, Zürich, Switzerland.

Publications and Media

Refereed Publications

Arsenovic P., Rozanov E., Stenke A., Funke B., Wissing J.M., Mursula K., Tummon F., Peter T.: 2016, The influence of Middle Range Energy Electrons on atmospheric chemistry and regional climate. JASTP, 149, 180–190, doi: 10.1016/j.jastp.2016.04.008.

Ball W.T., Kuchař A., Rozanov E.V., Staehelin J., Tummon F., Smith A.K., Sukhodolov T., Stenke A., Revell L., Coulon A., Schmutz W., Peter T.: 2016, An upper-branch Brewer-Dobson circulation index for attribution of stratospheric variability and improved ozone and temperature trend analysis, Atmos. Chem. Phys., 16, 15485–15500, doi: 10.5194/acp-16-15485-2016.

Ball W.T., Haigh J.D., Rozanov E.V., Kuchar A., Sukhodolov T., Tummon F., Shapiro A.V., Schmutz W.: 2016, High solar cycle spectral variations inconsistent with stratospheric ozone observations Nature Geoscience 9, 206–209, doi: 10.1038/ngeo2640.

Ball W.T., Schmutz W., Fehlmann A., Finsterle W., Walter B.: 2016, Assessing the beginning to end-of-mission sensitivity change of the PREcision MOnitor Sensor total solar irradiance radiometer (PREMOS/PICARD), J. Space Weather Space Clim., 6, A32, 8 pp, 2016, doi: 10.1051/swsc/2016026.

Barreto Á., Cuevas E., Granados-Muñoz M.-J., Alados-Arboledas L., Romero P. M., Gröbner J., Kouremeti N., Almansa A. F., Stone T., Toledano C., Román R., Sorokin M., Holben B., Canini M., Yela M.: 2016, The new sun-sky-lunar Cimel CE318-T multiband photometer - a comprehensive performance evaluation, Atmos. Meas. Tech., 9, 631-654, doi: 10.5194/amt-9-631-2016.

Brönnimann S., Malik A., Stickler A., Wegmann M., Raible C., Muthers S., Anet J., Rozanov E., Schmutz W.: 2016, Multidecadal variations of the effects of the Quasi-Biennial Oscillation on the climate system, Atmos. Chem. Phys.. 16, 15529-15543, doi: 10.5194/acp-16-15529-2016.

Cessateur G., Schmutz W., Wehrli C., Gröbner J., Haberreiter M., Kretzschmar M., Rozanov E., Schöll M., Shapiro A., Thuillier G., Egorova T., Finsterle W., Fox N., Hochedez J.-F., Koller S., Meftah M., Meindl P., Nyeki S., Pfiffner D., Roth H., Rouzé M., Spescha M., Tagirov R., Werner L., Wyss J.-U.: 2016, Solar irradiance observations with PREMOS filter radiometers on the PICARD mission: In-flight performance and data release, Astron. Astrophys. 588, A126, 16 pp, doi: 10.1051/0004-6361/201527577.

Diémoz H., Eleftheratos K., Kazadzis S., Amiridis V. and Zerefos C.S.: 2016, Retrieval of aerosol optical depth in the visible range with a Brewer spectrophotometer in Athens, Atmos. Meas. Tech., 9, 1871–1888.

Edkins N., Schmutz W., Egli L., Davies R., Aoki T., McFarquhar G.: 2016, The International Radiation Symposium 2016, Adv. Atmos. Sci., 33, 1325–1328, doi: 10.1007/s00376-016-6180-1.

Egli L., Gröbner J., Hülsen G., Bachmann L., Blumthaler M., Dubard J., Khazova M., Kift R., Hoogendijk K., Serrano A., Smedley A., Vilaplana J.-M.: 2016, Quality assessment of solar UV irradiance measured with array spectroradiometers, Atmos. Meas. Tech., 9, 1553-1567, doi: 10.5194/amt-9-1553-2016.

Founda D., Kazadzis S., Mihalopoulos N., Gerasopoulos E., Lianou M., Raptis P.I.: Long-term visibility variation in Athens (1931–2013): 2016, A proxy for local and regional atmospheric aerosol loads, Atmos. Chem. Phys., 16, 11219-11236, doi: 10.5194/acp-16-11219-2016.

Giamarelou M., Eleftheriadis K., Nyeki S., P. Tunved S., Torseth K., Biskos G.: 2016, Indirect evidence of the composition of nucleation mode atmospheric particles in the high Arctic, J. Geophys. Res. Atmos., 121, 965–975, doi: 10.1002/2015JD023646.

Gkikas A., Basart S., Hatzianastassiou N., Marinou E., Amiridis V., Kazadzis S., Pey J., Querol X., Jorba O., Gassó S., Baldasano J.M.: 2016, Mediterranean intense desert dust outbreaks and their vertical structure based on remote sensing data, Atmos. Chem. Phys., 16, 8609-8642, doi: 10.5194/acp-16-8609-2016.

Gratsea M., Vrekoussis M., Richter A., Wittrock F., Schönhardt A., Burrows J., Kazadzis S., Mihalopoulos N., Gerasopoulos E.: 2016, Slant column MAX-DOAS measurements of nitrogen dioxide, formaldehyde, glyoxal and oxygen dimer in the urban environment of Athens, Atmos. Environ., 135, 118-131, ISSN 1352-2310, dx.doi.org/10.1016/j.atmosenv. 2016.03.048.

Hülsen G., Gröbner J., Nevas S., Sperfeld P., Egli L., Porrovecchio G., Smid M.: 2016, Traceability of solar UV measurements using the QASUME reference spectroradiometer, Applied Optics, 55, 26, 7265-7275.

Kazadzis S., Raptis P., Kouremeti N., Amiridis V., Arola A., Gerasopoulos E., Schuster G.L.: 2016, Aerosol absorption retrieval at ultraviolet wavelengths in a complex environment, Atmos. Meas. Tech., 9, 5997-6011, doi: 10.5194/amt-9-5997-2016.

Klimenko M., Klimenko V., Bessarab F., Korenkov Yu., Rozanov E., Reddmann T., Zakharenkova L., Tolstikov M.:2016, Application of the models of the middle and upper atmosphere to simulation of total electron content perturbations caused by the 2009 stratospheric warming, Russ. J. Phys. Chem. B, 10, 1, 109–116, doi: 10.1134/S1990793116010097.

Misios S., Mitchell D., Gray L., Tourpali K., Matthes K., Hood L., Schmidt H., Chiodo G., Thieblemont R., Rozanov E., Krivolutsky A.: 2016, Solar signals in CMIP-5 simulations: Effects of atmosphere-ocean coupling, QJMS, 142, 928-941, doi: 10.1002/ qj.2695.

Muthers S., Raible C., Rozanov E., Stocker T.: 2016, Response of the AMOC to reduced solar radiation – the modulating role of atmospheric chemistry, Earth Syst. Dynam., 7, 877–892, doi: 10.5194/esd-7-877-2016.

Poulain V., Bekki S., Marchand M., Chipperfield M., Khodri M., Dhomse S., Bodeker G., Toumi R., De Maziere M., Pommereau J.-P., Pazmino A., Goutail F., Plummer D., Rozanov E., Mancini E., Akiyoshi H., Lamarque J.-F., Austin J.: 2016, Evaluation of the inter-annual variability of stratospheric chemical composition in chemistry-climate models using ground-based multi species time series, JASTP, 145, 61-84, doi: 10.1016/j.jastp.2016.03.010.

Proestakis M., Kazadzis S., Lagouvardos K., Kotroni V., Kazantzidis A.: 2016, Lightning activity and aerosols in the Mediterranean region, Atmos. Res., 170, 66–75, dx.doi.org/10.1016/j.atmosres.2015.11.010.

Proestakis E., Kazadzis S., Lagouvardos K., Kotroni V., Amiridis V., Marinou E., Price C., Kazantzidis A.: 2016, Aerosols and lightning activity: The effect of vertical profile and aerosol type, Atmos. Res., doi: 10.1016/j.atmosres.2016.07.031.

Prša A., Harmanec P., Torres G., Mamajek E., Asplund M., Capitaine N., Christensen-Dalsgaard J., Depagne E., Haberreiter M., Hekker S., Hilton J., Kopp G., Kostov V., Kurtz D.W., Laskar J., Mason B. D., Milone E.F., Montgomery M., Richards M., Schmutz W., Schou J., Stewart S.G.: 2016, Nominal values for selected solar and planetary quantities: IAU 2015 Resolution B3, Astron. J., 152, 41, 7 pp, doi: 10.3847/0004-6256/152/2/41.

Revell L., Stenke A., Rozanov E., Ball W., Lossow S., Peter T.: 2016, The role of methane in projections of 21st century stratospheric water vapour, Atmos. Chem. Phys., 16, 13067–13080, doi: 10.5194/acp-16-13067-2016.

Rozanov E., Georgieva K., Mironova I., Tinsley B., Aylward A.: 2016, Foreword: Special issue on “Effects of the solar wind and interplanetary disturbances on the Earth's atmosphere and climate”, JASTP, 149, 146-150, doi: 10.1016/j.jastp.2016.08.012.

Schöll M., Dudok de Wit T., Kretzschmar M., Haberreiter M.: 2016, Making of a solar spectral irradiance dataset I: observations, uncertainties, and methods, J. Space Weather Space Clim., 6 (27), A14, doi: 10.1051/swsc/2016007.

Shapiro A.I., Solanki S.K., Krivova N.A., Yeo K.L., Schmutz W.K.: 2016, Are solar brightness variations faculae- or spot-dominated?, Astron. Astrophys. 589, A46, 14 pp, doi: 10.1051/0004-6361/201527527.

Sukhodolov T., Rozanov E., Ball W.T., Bais A., Tourpali K., Shapiro A.I., Telford P., Smyshlyaev S., Fomin B., Sander R., Bossay S., Bekki S., Marchand M., Chipperfield M.P., Dhomse S., Haigh J.D., Peter T., Schmutz W.: 2016, Evaluation of the simulated photolysis rates and their response to solar irradiance variability, J. Geophys. Res. Atmos., 121, 6066–6084, doi: 10.1002/2015JD024277.

Taylor M., Kosmopoulos P.G., Kazadzis S., Keramitsoglou I., Kiranoudis C.T.: 2016, Neural network radiative transfer solvers for the generation of high resolution solar irradiance spectra parameterized by cloud and aerosol parameters, J. Quant. Spectr. Rad. Trans., 68, 176–192.

Vignola F., Derocher Z., Peterson J., Vuilleuimer L., Felix C., Gröbner J., and Kouremeti N.: 2016, Effects of changing spectral radiation distribution on the performance of photodiode pyranometers, Solar Energy, 129, 224-235.

Walter B., Voegeli C., Horender S.: 2016, Estimating sediment mass fluxes on surfaces sheltered by live vegetation, Bound. Layer Meteorol, doi: 10.1007/s10546-016-0224-z.

Zampila M.M., Taylor M., Bais A., Kazadzis S.: 2016, Modeling the relationship between photosynthetically active radiation and global horizontal irradiance using singular spectrum analysis, J. Quant. Spectr. Rad. Trans., 182, 240–263.

Zanchettin D., Khodri M., Timmreck C., Toohey M., Schmidt A., Gerber E., Heger G., Robock A., Pausata F., Ball W., Bauer S., Bekki S., Dhomse S., LeGrande A., Mann G., Marshal L., Mills M., Marchand M., Niemeier U., Poulain V., Rozanov E., Rubino A., Stenke A., Tsigaridis K., and Tummon F.: 2016, The Model Intercomparison Project on the climatic response to Volcanic forcing (VolMIP): experimental design and forcing input data for CMIP6, Geosci. Model Dev., 9, 2701–2719, doi: 10.5194/gmd-9-2701-2016.

Zerefos C. S., Eleftheratos K., Kapsomenakis J., Solomos S., Inness A., Balis D., Redondas A., Eskes H., Allaart M., Amiridis V., Dahlback A., De Bock V., Diémoz H., Engelmann R., Eriksen P., Fioletov V., Gröbner J., Heikkilä A., Petropavlovskikh I., Jarosławski J., Josefsson W., Karppinen T., Köhler U., Meleti C., Repapis C., Rimmer J., Savinykh V., Shirotov V., Siani A. M., Smedley A. R. D., Stanek M., Stübi R.: 2017, Detecting volcanic sulfur dioxide plumes in the Northern Hemisphere using the Brewer spectrophotometers, other networks, and satellite observations, Atmos. Chem. Phys., 17, 551-574, doi: 10.5194/acp-17-551-2017.

Other Publications

Ball W.T. et al.: 2016, A mid-latitude stratosphere dynamical index for attribution of stratospheric variability and improved ozone and temperature trend analysis, Atmos. Chem. Phys. Discuss., doi: 10.5194/acp-2016-449.

Bolduc C. et al.: 2016, NLTE calculation of the SOlar spectrum with CRoss-influence of solar ATmospheric structures, EGU General Assembly 2016, Abstract No. EGU2016-7895.

Brönnimann S. et al.: 2016, Multi-decadal variations of the effects of the quasi-biennial oscillation on the climate system, Atmos. Chem. Phys. Discuss., doi: 10.5194/acp-2016-502.

Egli L. et al.: 2016, A simulation-tool to model ozone retrieval uncertainties of Brewer and Dobson instruments, UVNews, The official newsletter of the Thematic Network for Ultraviolet Measurements, Issue 11, Aalto University.

Fludra, A., Haberreiter M. et al.: 2016, The SPICE Spectral Imager on Solar Orbiter: Linking the Sun to the Heliosphere, 41st COSPAR Scientific Assembly, Abstract D2.2-5-16.

Funke B., Ball W. et al.: 2016, HEPPA-II model-measurement intercomparison project: EPP indirect effects during the dynamically perturbed NH winter 2008–2009, Atmos. Chem. Phys. Discuss., doi: 10.5194/acp-2016-971, 2016.

Giunta A., Haberreiter M. et al.: 2016, Solar abundances with the SPICE spectral imager on Solar Orbiter, 41st COSPAR Scientific Assembly, Abstract D2.6-5-16.

Guerreiro N., Haberreiter M., Hansteen V., Schmutz W., 2016, Characterization of small-scale heating events in the solar atmosphere from 3D-MHD simulations and their potential role in coronal heating, EGU 2016, Abstract No. EGU2016-14407.

Haberreiter M. et al.: 2016, How to strengthen the legacy of European Space Projects, EGU General Assembly 2016, Abstract No. EGU2016-17984.

Halain J.-P. et al.: 2016, The qualification campaign of the EUI instrument of Solar Orbiter. In: Society of Photo-Optical Instrumentation Engineers (SPIE) Conf. Series 9605, eid. 96052X, 7 pp, doi: 10.1117/12.2232372.

Jungclaus J. et al: 2016, The PMIP4 contribution to CMIP6 - Part 3: the Last Millennium, Scientific Objective and Experimental Design for the PMIP4 past1000 simulations, Geosci. Model Dev. Discuss., doi: 10.5194/gmd-2016-278, 2016.

Meftah M. et al: 2016, Main Results of the PICARD mission. In: Society of Photo-Optical Instrumentation Engineers (SPIE) Conf. Series 9904, eid. 99040Z, 14 pp, doi: 10.1117/12.223202.

Morgenstern O. et al.: 2016, Review of the global models used within the Chemistry-Climate Model Initiative (CCMI), Geosci. Model Dev. Discuss., doi: 10.5194/gmd-2016-199.

Revell L. et al.: 2016, The role of methane in projections of 21st century stratospheric water vapour, Atmos. Chem. Phys. Discuss., 16, doi: 10.5194/acp-2016-545.

Rozanov E. et al.: 2016, Long-term variations of solar activity and their impacts: From the Maunder Minimum to the 21st century, Sparc newsletter, No. 46, 15–20, 2016.

Schöll M., Dudok de Wit T., Haberreiter M. et al.: 2016, A new observational solar irradiance composite, EGU General Assembly 2016, Abstract No. EGU2016-17963.

Snow M. et al.: 2016, Lyman alpha solar spectral irradiance line profile observations and models, EGU General Assembly 2016, Abstract No. EGU2016-3071.

Thuillier G. et al.: 2016, Solar spectral irradiance model validation using Solar Spectral Irradiance and Solar Radius measurements, EGU General Assembly Conf. Abstracts 18, 7407.

Walter B., Winkler R., Finsterle W., Fehlmann A., Schmutz W.: 2016, Direct solar irradiance measurements with a cryogenic solar absolute radiometer, Int. Rad. Symp., 1–2 April 2016, Auckland, New Zealand.

Walter B. et al.: 2016, A new generation of Compact Lightweight Absolute Radiometers (CLARA) for spaceborne TSI observations, 1st Swiss SCOSTEP workshop, 4–5 Oct. 2016, ISSI Bern, Switzerland.

Edited Book Chapters

Space Research 2014 – 2016 in Switzerland. Report to the 41st COSPAR meeting, planned in Istanbul, Turkey, July-August 2016. The meeting was cancelled. Publication by the Swiss Committee on Space Research (working group of the Swiss Academy of Sciences). Edited by Werner Schmutz and Stephan Nyeki, 2016, Davos, Switzerland: PMOD/WRC.

Media

"Abkühlung in Sicht", SRF Tagesschau, 19:30, 27 March 2017, https://www.srf.ch/play/tv/tagesschau/video/

"Klimaerwärmung wird vorübergehend gebremst", 27 March 2017, Panorama Sendung: https://www.srf.ch/news/panorama/klimaerwaermung-wird-voruebergehend-gebremst

Personnel Department

Barbara Bücheler

Just before the start of the 2016 World Economic Forum we were honoured to host a meeting of the US Rotary Club at the PMOD/WRC. Continuing the international context, the mid-term review of the World Bank and Global Risk Forum also took place at the PMOD/WRC on the 1 – 2 February 2016 with a meeting entitled "Afghanistan Risk Analysis".

While the Swiss Society for Astrophysics and Astronomy held their annual General Assembly on 6 – 7 October 2016 at the PMOD/WRC, our Supervisory Board presented the half-yearly financial statement during their regular autumn meeting on 21 October 2016. In addition to these events, we continued to present our strengths in the fields of solar science and technology to experts and the public through various channels including: i) television, radio and press releases, ii) guided tours of the PMOD/WRC, and iii) literature papers.

Our "PMOD/WRC team", also being interested in aero and space technology, was treated to a guided tour of the Dornier Museum in Friedrichshafen on Lake Constance in Germany. Afterwards, our educational trip was complemented with the "Tabtour" in Lindau. Equipped with a tablet, GPS instrument and a map, our teams went on a scenic and cultural hunt where exciting puzzles and team tasks had to be solved to collect points. Prizes for the "Tabtour" team-building event were awarded on the Gebhardsberg in Bregenz during a wonderful "Whoddunit" dinner. In the middle of events, we watched the police inspector conduct his investigations and were soon enough taking part in the hunt ourselves.

We are also able to proudly report on developments and personnel changes at the PMOD/WRC this year. At this juncture, we would like to congratulate our previous PhD students, Timofei Sukhodolov (2016) and Rinat Tagirov (2017) on obtaining their doctoral degrees. Since then, Timofei has been supporting our scientific group, starting in October 2016. In addition, Dr. Tatjana Egorova took on the work of Wilnelia Adams at the beginning of 2016.

Dr. Cassandra Bolduc, a Postdoc Physicist left the PMOD/WRC at the end of her contract in September 2016 in order to accept a vacancy in the field of Environment and Climate-Change in Canada. Dr. Nuno Guerreiro took over her newly-funded project in our Solar Physics Section. Dr. Gael Cessateur complemented our team for a short time in September 2016. Dr. Hongrui Wang joined us for a Chinese-Swiss joint project and PhD student, Alberto Remesal Oliva started his Thesis in the Solar Radiometry Section of the WRC. We are also pleased to be part of the Horizon 2020 project and that our collaboration with Panagiotis Raptis, a PhD student from Athens, Greece, has been extended with a stay with us in Davos from October 2016 to October 2017.

Our Technology Department has gained valuable support in the production of PMO6-CC instruments through a collaboration with Markus Suter, a former employee at PMOD/WRC who is now with the company Davos Instruments AG. In addition, Lloyd Beeler joined the Electronics Section in April 2016. We would like to congratulate Andri Morandi for passing his apprentice examination and becoming an "Elektroniker EFZ". He was succeeded by Yanick Schloch in August. Nicholas Bresina joined us for a 4-month trial which went so well that he was given a position after several weeks. Jocelyn Pleish successfully finished her 3-week commercial placement at the PMOD/WRC in July 2016. Similarly, we are pleased to have Jeanine Lehner in the Administration Section since August 2016.

We were also able to achieve many envisaged goals with the conscientious support of our versatile and creative civilian conscripts, including: Patrik Caspar, Ron De Caspar, Luca Rüegg, Luca Zurmühle, Corentin Gut, Fabian Frei, Pascal Marc Vecsei, Mathias Hermann, Marcel Schläppi and Martin Steiner.

To attain our goals, go beyond limits and to carry forward the spirit of pioneers: This is what we aim for in the future and for which we will give our best. Thank you that you have had faith in our vision and for accompanying us on our journey.

Scientific Personnel

Prof. Werner Schmutz	Director, physicist
Dr. William Ball	Postdoc climate group, physicist
Dr. Luo Beiping	Scientist climate group, physicist (until 30.11.2016)
Dr. Cassandra Bolduc	Postdoc solar physics group, physicist (until 30.09.2016)
Dr. Thomas Carlund	Scientist WORCC section, meteorologist
Dr. Gael Cessateur	Postdoc, solar physics group, physicist (01.09.2016 – 30.09.2016)
Dr. Luca Egli	Scientist WCC-UV section, physicist
Dr. Tatiana Egorova	Scientist, climate group, climate scientist
Dr. Wolfgang Finsterle	Head WRC-section solar radiometry, physicist
Dr. Julian Gröbner	Head WRC-sections IR radiometry, WORCC, and WCC-UV, physicist
Dr. Nuno Guereirro	Postdoc solar physics group, physicist
Dr. Margit Haberreiter	Head solar physics group, physicist
Dr. Gregor Hülsen	Scientist WCC-UV section, physicist
Dr. Stylianos Kazantzis	Scientist WORCC section, physicist
Dr. Natalia Kouremeti	Scientist WORCC section, physicist
Dr. Stephan Nyeki	Scientist IR radiometry section, physicist
Dr. Eugene Rozanov	Scientist climate group, physicist (since 01.12.2016)
Dr. Benjamin Walter	Postdoc solar physics group, physicist
Dr. Hongrui Wang	Postdoc, WRC-section solar radiometry, physicist (since 28.09.2016)
Alberto Remesal Oliva	PhD student, 1st year (since 01.06.2016)
Wilnelia Adams	PhD student, SNF project, 3rd year (until 31.12.2016)
Christine Aebi	PhD student, SNF project, 3rd year
Ioannis Panagiotis Raptis	PhD student, 3rd year (since 01.10.2016)
Timofei Sukhodolov	PhD student, ETHZ, 4th year (until 30.04.2016), postdoc (since 09.05.2016)
Rinat Tagirov	PhD student, ETHZ, 5th year (until 30.06.2016)

Technical Personnel

Silvio Koller	Co-Head technical dept., project manager space, quality system manager, elec. engineer
Daniel Pfiffner	Co-Head technical dept., project manager space, elec. engineer
Lloyd Beeler	Electronics engineer MSc (since 04.04.2016)
Nicholas Bresina	Trainee electronic technician (17.05.2016 – 30.09.2016)
Manfred Gyo	Project manager space, electronic engineer
Jonathon Kennedy	Mechanics engineer MSc
Philipp Kuhn	System engineer
Patrik Langer	Mechanics engineer BSc
Pierre-Luc Lévesque	Instrument engineer
Andri Morandi	Electronics apprentice, 4th year (01.08.2012–31.07.2016)
	Electronics technician (01.08.2016–31.10.2016)
Pascal Schlatter	Mechanic, head workshop, security officer
Yanick Schoch	Electronics apprentice, 1st year (since 01.08.2016)
Marco Senft	System administrator
Ricco Soder	Project manager technics, deputy quality system manager, electronics engineer
Marcel Spescha	Technician

Technical Personnel within the Science Department

Nathan Mingard	Physics laboratory technician
Christian Thomann	Technician

Administration

Barbara Bücheler	Head administration/Human Resources
Kathrin Anhorn	Administration apprentice, 2nd and 3rd year
Irene Keller	Administration, import/export
Angela Lehner	Administration, book-keeping
Jeanine Lehner	Trainee administration (since 22.08.2016)
Alexandra Sretovic	Administration apprentice, 2nd and 3rd year
Christian Stiffler	Accountant

Caretaker

Maria Sofia Ferreira Pinto	General caretaker, cleaning
Eufémia Soares Ferreira	General caretaker, cleaning (back-up)

Civilian Service Conscripts

Patrik Caspar	14.09.2015 – 12.02.2016
Ron De Caspar	12.10.2015 – 18.01.2016
Luca Rüegg	18.01.2016 – 29.04.2016
Luca Zurmühle	22.02.2016 – 31.05.2016
Corentin Gut	09.05.2016 – 31.07.2016
Fabian Frei	11.07.2016 – 30.09.2016
Pascal Marc Vecsei	18.07.2016 – 30.09.2016
Mathias Hermann	19.09.2016 – 30.11.2016
Marcel Schläppi	03.10.2016 – 31.01.2017
Martin Steiner	28.11.2016 – 31.01.2017

Meeting/Event Organisation

Rotary/World Economic Forum (WEF)	WEF Event, 22.1.2016
Global Risk Forum (GRF)	Mid-term review meeting, 01 – 02.02.2016
Stiftungsratsitzung	PMOD/WRC, 09.06.2016
Aufsichtskommission	Ordentliche Herbstsitzung, 21.10.2016
SSAA/SGAA	Schweizerische Gesellschaft für Astrophysik und Astronomie, Meeting, 06 – 07.10.2016
Obs-Ausflug	Friedrichshafen/Bregenz, 28.10.2016

Public Seminars

14.01.2016	Lionel Doppler, PMOD/WRC and DWD/MOL-RAO, Lindenberg, "15 years of instrumental collaboration".
16.02.2016	Alberto Remesal, PTB Berlin, "THz detectors".
03.03.2016	Ralph Neuhäuser, Jena, Germany, "Reconstruction of solar activity for the 8th and 17th century".
25.04.2016	Cindy Giebink, University of Hawaii's Institute for Astronomy, "HOTMOL Web Tools for Solar, Stellar and Planetary Research".
31. 05.2016	Gael Cessateur, ROB-Belgium, "Photochemical model for forbidden oxygen line emission for the Jovian moons and comets".
08.09.2016	Abdellah Bouhanik, Tunisia, "Presentation about the institute in Tunisia".
10.11.2016	John Lehman, Boulder, Colorado USA, "A New Generation of Detectors for Laser Radiometry at NIST".

Lecture Courses, Participation in Commissions

Werner Schmutz	Lecture course in Astronomy, HS 2016, ETH-ZH Examination expert in Astronomy, BSc ETH-ZH President of the International Radiation Commission (IRC, IAMAS) Member of the Comite Consulatif de Photomètrie et Radiomètrie (CCPR, OICM) Swiss delegate to the Science Programme Committee, ESA Member of the Space Weather Working Team Steering Board of ESA Swiss delegate to the council of the Committee on Space Research (COSPAR) President of the National Committee on Space Research, SCNAT Member of the Commission for Astronomy, SCNAT Member of the GAW-CH Working Group (MeteoSwiss)
Wolfgang Finsterle	Member of CIMO ET Instrument Intercomparisons Member of CIMO TT Radiation References Member of EURAMET TC PR Chairman of ISO/TC180 SC1 (Solar Energy, Climate – Measurement and Data) Member of the PROBA-3 Science Working Team Course on calibration of solar radiometers, in the framework of PTB project
Julian Gröbner	Lecture course in Solar Ultraviolet Radiation WS 2016, ETH - ZH GAW-CH Working group (Meteoswiss) Member Scientific Advisory Group for UV, WMO GAW, since 2016 Chair of the NEWRAD Scientific committee Chairman of Infrared Working group of Baseline Surface Radiation Network (BSRN) Member IAMAS International Radiation Commission Member of the CIMO Task Group on Radiation – Vice Chairman Swiss delegate to the Management Group of COST ES1207 "A EUropean BREWer NETwork - EUBREWNET" and Working Group Leader of WG1 "Instrument characterisation and calibration" Member of the EURAMET Task Group on Environment Member International Ozone Commission (IO3C), since 2016
Margit Haberreiter	Elected President of the EGU Division on Solar-Terrestrial Sciences Member of the EGU Programme Group Associate Member of the SPICE Operations Team Co-Investigator of EUI and SPICE onboard Solar Orbiter Swiss Rep. of Inter-programme Team on Space Weather, Information System and Services (IPT-SWISS) Member of the IAU Organising Committee of Commission E3 "Solar Impact throughout the Heliosphere" Topical Editor Annales Geophysicae Member of the Swiss SCOSTEP Committee
Eugene Rozanov	Co-Leader of SPARC SOLARIS-HEPPA WG3 Member of SCOSTEP VarSITI ROSMIC WG1 Member of National SCOSTEP Committee Swiss representative in European COST CA15211, WG6 leader1
Stelios Kazadzis	Scientific Advisory Group for Aerosols (WMO/GAW) GAW-CH Working Group (MeteoSwiss) Editor in Atmospheric Chemistry and Physics Co-Lecturer, MSc in Space Science Technologies and Applications, Univ. of Peloponnese, Greece

Donations

A contribution from Mr. Daniel Karbacher (from Küsnacht, ZH) made it possible to cover expenses of the CLARA/NORSAT-1 space experiment that were outside the allocated budget. Our special thanks go to Mr. Karbacher for his generous donation.

Bilanz 2016 (inklusive Drittmittel) mit Vorjahresvergleich

Aktiven	31.12.2016 CHF	31.12.2015 CHF
Flüssige Mittel	1'017'573.44	1'222'976.71
Forderungen	43'628.80	199'478.13
Aktive Rechnungsabgrenzungen	203'736.55	10'930.62
Total Aktiven	1'264'938.79	1'433'385.46
Passiven		
Verbindlichkeiten	151'914.51	215'316.65
Kontokorrent Stiftung	91'540.05	58'173.95
Passive Rechnungsabgrenzung	121'532.31	195'523.13
Rückstellungen	892'789.75	945'320.19
Eigenkapital	7'162.17	19'051.54
Total Passiven	1'264'938.79	1'433'385.46

Erfolgsrechnung 2016 (inklusive Drittmittel) mit Vorjahresvergleich

Ertrag	CHF	CHF
Beitrag Bund Betrieb WRC	1'460'000.00	1'366'976.00
Beitrag Bund (BBL)	158'003.30	0.00
Beitrag Kanton Graubünden	499'282.00	452'088.00
Beitrag Gemeinde Davos	651'168.00	589'555.00
Beitrag Gemeinde Davos, Mieterlass	160'000.00	160'000.00
Overhead SNF	117'461.69	124'866.78
Overhead EU	9'587.25	0.00
Profit Projekt ATLAS	30'844.00	0.00
Instrumentenverkäufe	114'947.95	344'849.70
Reparaturen und Kalibrationen	145'458.63	184'194.16
Ertrag Dienstleistungen	27'051.90	19'826.85
Übriger Ertrag	19'949.25	12'907.85
Finanzertrag	29.65	51.05
Ausserordentlicher Ertrag	13'623.30	3'258.95
Drittmittel	2'783'362.31	2'520'065.20
Total Ertrag	6'190'769.23	5'778'639.54
Aufwand		
Personalaufwand	4'338'549.10	4'255'398.65
Investitionen Observatorium	140'181.42	118'850.34
Investitionen Drittmittel	41'493.75	270'519.05
Unterhalt Gebäude (Beitrag Bund)	158'003.30	0.00
Unterhalt	48'485.26	33'658.55
Verbrauchsmaterial Observatorium	22'822.20	71'046.65
Verbrauchsmaterial Drittmittel	252'137.61	217'627.78
Verbrauch Commercial	126'897.56	153'452.73
Reisen, Kurse	160'966.71	157'363.70
Raumaufwand/Energieaufwand	206'804.75	211'628.80
Versicherungen, Verwaltungsaufwand	147'736.14	127'311.43
Finanzaufwand	2'839.72	3'008.81
Übriger Betriebsaufwand	41'449.32	50'640.80
Ausserordentlicher Aufwand	111'914.28	39'154.48
Nicht gedeckter Aufwand EU-Projekte	454'907.92	91'961.76
Total Aufwand	6'255'189.04	5'801'623.53
Jahresergebnis vor Auflösung Rückstellungen	-64'419.81	-22'983.99
Auflösung Rückstellungen zur Defizitdeckung	52'530.44	0.00
Jahresergebnis	-11'889.37	-22'983.99
	6'190'769.23	5'778'639.54

Abbreviations

AERONET	Aerosol Robotic Network, GSFC, USA
AIT	Assembly, Integration and Test
AOCCM	Atmosphere-Ocean-Chemistry-Climate Model
AOD	Aerosol Optical Depth
BIPM	Bureau International des Poids et Mesures, Paris, France
BSRN	Baseline Surface Radiation Network of the WCRP
CCM	Chemistry-Climate Model
CCPR	Comité Consultatif de Photométrie et Radiométrie, BIPM
CIE	Commission Internationale de l'Eclairage
CIMO	Commission for Instruments and Methods of Observation of WMO, Geneva, Switzerland
CIPM	Comité International des Poids et Mesures
CLARA	Compact Light-weight Absolute Radiometer (PMOD/WRC experiment onboard the NORSAT-1 nano-satellite mission)
CMC	Calibration and Measurement Capabilities
CMIP	Coupled Model Intercomparison Project
CNES	Centre National d'Etudes Spatiales, Paris, France
CNRS	Centre National de la Recherche Scientifique, Service d'Aéronomie Paris, France
COCOSIS	Combination of COSI Spectra
COSI	Code for Solar Irradiance (solar atmosphere radiation transport code developed at PMOD/WRC)
COSIR	Code for Solar Irradiance Reconstruction
COSPAR	Commission of Space Application and Research of ICSU, Paris, France
COST	European Cooperation in Science and Technology
CSAR	Cyrogenic Solar Absolute Radiometer (PMOD/WRC research instrument)
CTM	Chemical Transport Model
DARA	Digital Absolute Radiometer (PMOD/WRC experiment onboard the ESA PROBA-3 formation flying mission)
DLR	Deutsche Luft und Raumfahrt, Germany
EIT	Extreme Ultraviolet Imaging Telescope (international experiment onboard the SOHO mission)
EM	Engineering Model
EMRP	European Metrology Research Programme
ESA	European Space Agency
ESF	European Science Foundation
ETHZ	Eidgenössische Technische Hochschule Zurich
EUI	Extreme Ultraviolet Imager (international experiment onboard the Solar Orbiter mission)
EUV	Extreme Ultraviolet region of the light spectrum
FM	Flight Model
FP7	Seventh Framework Programme of the European Commission
FS	Flight Spare
FUPSOL	Future and Past Solar Influence on the Climate, SNF Sinergia Project
FY-3	Feng Yun 3 series of Chinese space missions (FY-3A to E)
GAW	Global Atmosphere Watch, a WMO Research Programme
GCM	General Circulation Model
GHG	Greenhouse Gases
GSFC	Goddard Space Flight Center, Greenbelt, MD, USA
IACETHZ	Institute for Climate Research of the ETHZ, Switzerland
IAMAS	International Association of Meteorology and Atmospheric Sciences of IUGG
IAU	International Astronomical Union of ICSU, Paris, France
ICSU	International Council of Scientific Unions, Paris, France
IPC	International Pyrheliometer Comparisons, held at PMOD/WRC every 5 years
IR	Infrared region of the light spectrum
IRC	International Radiation Commission, Commission of IAMAS
IRIS	Infrared Integrating Sphere Radiometer (PMOD/WRC research instrument)
IRS	International Radiation Symposium of the Radiation Commission of IAMAS
IRRCAM	Infrared Cloud Camera (PMOD/WRC research instrument)
ISO/IEC	International Oranisation for Standardisation/International Electrotechnical Commission
ISS	International Space Station
IWV	Integrated Water Vapour
JTSIM	Joint Total Solar Irradiance Monitor (experiment onboard the Chinese FY-3E mission)
LASP	Laboratory for Atmospheric and Space Physics, Boulder, USA
LATMOS	Laboratoire Atmosphères, Milieux, Observations Spatiales, French research institution
LVPS	Low Voltage Power Supply (PMOD/WRC contribution to the Solar Orbiter mission)
LYRA	Lyman-alpha Radiometer (PMOD/WRC experiment onboard PROBA-2 mission)
MDI	Michelson Doppler Interferometer (experiment onboard SOHO mission)
METAS	Federal Office of Metrology
MIPAS	Michelson Interferometer for Passive Atmospheric Sounding
MITRA	Monitor to Determine the Integrated Transmittance (PMOD/WRC research instrument)
MPS	Max Planck Institute for Solar System Research
MRA	Mutual Recognition Arrangement
MRR	Manufacturing Readiness Review

NASA	National Aeronautics and Space Administration, Washington DC, USA
NEWRAD	New Developments and Applications in Optical Radiometry
NILU	Norwegian Institute for Air Research, Norway
NIR	Near Infrared region of the light spectrum
NIST	National Institute of Standards and Technology, Gaithersburg, MD, USA
NOAA	National Oceanographic and Atmospheric Administration, Washington DC, USA
NORSAT-1	Norwegian Satellite-1
NPL	National Physical Laboratory, Teddington, UK
NRL	Naval Research Laboratory, Washington DC, USA
NREL	National Renewable Energy Laboratory, Golden, CO, USA
PFR	Precision Filter Radiometer (previously manufactured by PMOD/WRC)
PI	Principle Investigator, leader of an experiment/instrument/project
PICARD	French space mission
PMOD	Physikalisch-Meteorologisches Observatorium Davos, Switzerland
PMO6-CC	PMO6-CC type of radiometer (manufactured by PMOD/WRC)
PREMOS	Precision Monitoring of Solar Variability (PMOD/WRC experiment onboard the PICARD mission)
PROBA	ESA Satellite Missions (PROBA-1 to 3)
PRODEX	PROgramme de Développement d'Expériences scientifiques, ESA
PSR	Precision Spectroradiometer (manufactured by PMOD/WRC)
PTB	Physikalisch-Technische Bundesanstalt, Braunschweig and Berlin, Germany
QASUME	Quality Assurance of Spectral Ultraviolet Measurements in Europe
QM	Qualification Model
QMS	Quality Management System
RTM	Radiative Transfer Model
SATIRE-S	Spectral and Total Irradiance Reconstructions for the Satellite era
SCNAT	Swiss Academy of Sciences
SLF	Schnee und Lawinenforschungsinstitut, Davos, Switzerland
SFI	Schweiz. Forschungsinstitut für Hochgebirgsklima und Medizin, Davos, Switzerland
SI	International System of Units
SIM	Spectral Irradiance Monitor (experiment on SORCE mission)
SIAF	Schweiz. Institut für Allergie- und Asthma-Forschung, Davos, Switzerland
SNSF	Swiss National Science Foundation
SOCOL	Combined GCM and CTM Computer Model developed at PMOD/WRC
SOHO	Solar and Heliospheric Observatory (ESA/NASA space mission)
SOLAR	Experiment Platform on the ISS
SOLID	Solar Irradiance Data Exploitation (FP7 EU project)
SORCE	Solar Radiation and Climate Experiment (NASA Space Mission)
SOTERIA	Solar - Terrestrial Investigations and Archives
SOVAC	Solar Variability and Climate Change
SOVIM	Solar Variability and Irradiance Monitoring (PMOD/WRC experiment onboard the ISS)
SPICE	Spectral Imaging of the Coronal Environment (PMOD/WRC contribution to the Solar Orbiter mission)
SSI	Solar Spectral Irradiance
STM	Structural Thermal Model
SUSIM	Solar Ultraviolet Spectral Irradiance Monitor onboard UARS
SZA	Solar Zenith Angle
TIM	Total Irradiance Monitor (experiment on the SORCE mission)
TRF	TSI Radiometer Facility
TSI	Total Solar Irradiance
UARS	Upper Atmosphere Research Satellite (NASA)
UV	Ultraviolet region of the light spectrum
UVA	UV Radiation in the 315 – 400 nm range
UVB	UV Radiation in the 280 – 315 nm range
VIRGO	Variability of Solar Irradiance and Gravity Oscillations (PMOD/WRC experiment onboard the SOHO mission)
VIS	Visible region of the light spectrum
WCRP	World Climate Research Program
WDCA	World Data Centre for Aerosols
WIGOS	WMO Integrated Global Observing System
WIS	WMO Information System
WISG	World Infrared Standard Group of pyrgeometers (maintained by WRC-IRS at PMOD/WRC)
WMO	World Meteorological Organisation, a United Nations Specialised Agency, Geneva, Switzerland
WRC	World Radiation Centre, Davos, Switzerland
WRC-IRS	Infrared Radiometry Section of the WRC
WRC-SRS	Solar Radiometry Section of the WRC
WRC-WORCC	World Optical Depth Research and Calibration Centre of the WRC
WRC-WCC-UV	World Calibration Centre for Ultraviolet of the WRC
WRR	World Radiometric Reference
WSG	World Standard Group of pyrheliometers (realises the WRR; maintained by WRC at PMOD/WRC)

Annual Report 2016

Editors: Werner Schmutz and Stephan Nyeki
Layout by Stephan Nyeki

Publication by PMOD/WRC, Davos, Switzerland
Edition: 600, printed 2017

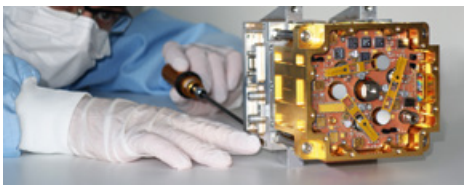

Front cover: The Compact Lightweight Absolute Radiometer (CLARA), a payload onboard the Norwegian NORSAT-1 nano-satellite. CLARA is a new generation of radiometers to measure the Total Solar Irradiance which continues the long-term involvement of the PMOD/WRC in space and solar research.

Dorfstrasse 33, 7260 Davos Dorf, Switzerland
Phone +41 58 467 51 11, Fax +41 58 467 51 00
www.pmodwrc.ch